ABSTRACT

MECHANICAL PROPERTIES OF
SAND-ICE MATERIALS

By

Bernard D. Alkire

Experimental shear strength and creep data obtained for confining pressures up to 1000 psi are presented for sand-ice materials. To investigate factors that affect the strength of the material, constant axial strain rate tests were conducted on samples with various void ratios, strain rates, and ice contents. Uniaxial, confined and step-stress creep tests were conducted to determine the effect of confining pressure on sand-ice materials and to develop an expression that would be descriptive of the creep behavior for confining pressures up to 1000 psi.

The granular part of the samples consisted of Ottawa sand sized between the number 20 (0.84mm) and 30 (0.59mm) U. S. Standard sieve sizes. The ice was prepared from deaired, deionized and distilled water with sample ice contents ranging from 33 to 100 percent of the sand void volume. Samples prepared in a split aluminum mold were 1.13 inches in diameter by 2.26 inches in height. All tests were conducted in a high pressure

triaxial cell with temperature controlled by submersion in a low-temperature bath maintained very close to -12.0° C.

The constant strain rate tests showed that high confining pressure causes a distinctive stress-strain curve. This curve has an initial linear portion, up to approximately two percent strain, followed by a near linear increase in stress up to failure of the sample. Strains at failure increased with confining pressure and were six to seven percent for samples tested with 700 psi confining pressure.

Results from the constant axial strain rate tests are presented in terms of the Mohr-Coulomb theory where the factors that affect the frictional and cohesive components of strength are identified. It is shown that the cohesive component of strength is due to the response of the ice matrix to test conditions. The cohesion is dependent on strain rate and ice content for constant temperature. The frictional component is shown to be dependent on the void ratio and the confining pressure. It is shown that the frictional behavior of the sand-ice material is very similar to the frictional characteristics of unfrozen sand tested at high confining pressure.

Uniaxial creep tests conducted at various levels of constant axial stress were used to obtain the general creep behavior of the sand-ice materials. With these

tests as a basis for comparison, the effects of confining pressure were determined from step-stress and confined triaxial creep tests. The results show that increases in the confining pressure reduce the strain rate. An expression for calculating the strain rate as a function of deviator stress and confining pressure was developed. This expression indicates that creep decreases exponentially with increasing confining pressure. Confining pressure below 200 psi has the greatest effect on the strain rate, and two regions of definition are necessary to totally describe the effects of confining pressures up to 1000 psi.

Results from the creep tests with reduced ice content samples are used to show the influence of relative ice content by a term called the percent of maximum deviator stress. The term, regardless of ice content, is defined as the applied creep deviator stress divided by a peak deviator stress. The peak deviator stress is obtained from a constant axial strain rate test conducted at a confining pressure equal to the confining pressure used in the creep test. All creep tests performed at the same percent of maximum deviator stress produced the same strain rates. Using this fact the equation developed for high ice content samples may be used for the reduced ice content if the deviator stress is modified to include the effect of ice content.

MECHANICAL PROPERTIES OF SAND-ICE MATERIALS

By

Bernard D. Alkire

A THESIS

Submitted to
Michigan State University
in partial fulfillment of the requirements
for the degree of

DOCTOR OF PHILOSOPHY

Department of Civil Engineering

1972

ACKNOWLEDGMENTS

The writer wishes to express his appreciation to his major professor, Dr. O. B. Andersland, Professor of Civil Engineering, for his guidance, assistance and numerous helpful suggestions during the preparation of this thesis. Thanks also to the members of the writer's doctoral committee: Dr. R. R. Goughnour, Professor of Civil Engineering; Dr. W. A. Bradley, Professor of Metallergy, Mechanics, and Material Science; and to Dr. C. C. Ganser, Professor of Mathematics. The writer also owes his appreciation to: Mr. Leo Szafranski of the Division of Engineering Research Machine Shop for his help in modifying and setting up the experimental equipment; Dr. S. S. Kuo for his assistance in the laboratory; and to my wife, Pat, for her help and encouragement.

Thanks are also due to the National Science Foundation and the Division of Engineering Research for their financial assistance which made this research possible.

TABLE OF CONTENTS

LIST OF TABLES

LIST OF FIGURES

NOTATIONS

A_{HI} = Area of ice, high ice content

A_{HS} = Area of sand, high ice content

A_{LI} = Area of ice, low ice content

A_{LS} = Area of sand, low ice content

c = Cohesion

D = $\sigma_1-\sigma_3$ = Axial stress difference = Deviator stress

D_a = Dilatancy component

D_r = Relative density

E = Modulus of elasticity

e = Void ratio

f = Shear force acting on a flow unit

ΔF = Free energy of activation, calories per mole

ΔF_o = Activation energy required to overcome cohesion

g = Particle gradation

h = Planck's constant = 6.624×10^{-27} erg-sec^{-1}

H = Mineral type

I = Interparticle forces

j = Ice content

K = Slope factor

K_f = Frictional constant

k = Boltzmann's constant = 1.38×10^{-16} erg $^{o}K^{-1}$

M = Percent of maximum deviator stress

m, b, C, A, N, G = creep parameters

n = Exponent in creep equation

N_c = Flow value = $\frac{1 + \sin \phi}{1 - \sin \phi}$

p = $(\sigma_1+\sigma_3)/2$

P_s = Particle shape

P_H = Force causing shear, high ice content

P_L = Force causing shear, low ice content

q = $(\sigma_1-\sigma_3)/2$

R = Universal gas constant = 1.98 calories $^{o}K^{-1}$ $mole^{-1}$

t = Time

T = Temperature

v = Frequency of activation, sec^{-1}

X = Parameter, a function of the number of flow units

ε = True axial strain, in/in

$\dot{\varepsilon}$ = True axial strain rate, min^{-1}

$\dot{\varepsilon}_c$ = Arbitrary strain rate in creep

λ = Distance between equilibrium positions of flow units

Σ = Stress factor = $D-\sigma_m$

σ = Uniaxial stress

σ_c = Proof stress in creep equation

σ_m = Mean normal stress

τ = Shear stress

τ_H = Shear stress, high ice content

τ_L = Shear stress, low ice content

ϕ = Angle of internal friction

σ_1 = Major principle stress

σ_3 = Minor principle stress = confining pressure

CHAPTER I

INTRODUCTION

The mechanical properties of sand-ice are studied to determine the strength and creep behavior of the material. Originally the strength of frozen soils was determined as for an undrained clay, with strength being stated in terms of cohesion (Vialov, 1965a). As more elaborate testing equipment became available, and strength was determined to be time dependent (Tystovich, 1960), creep testing was used to study the nature of this time dependency and its relationship to strength. Presently, many testing techniques are used to study the mechanical properties of frozen soils. Tension tests (Vialov, 1965b), shear tests (Vialov, 1965b), uniaxial compression tests (Goughnour and Andersland, 1968), confined compression (Andersland and AlNouri, 1970) and constant axial stress tests (Andersland and AlNouri, 1970; Sayles, 1968) have been conducted on frozen soils. These tests have resulted in various empirical formulations that describe the time dependent mechanical properties of frozen soils.

One of the most common methods used to describe the strength of frozen soil is the Mohr-Coulomb failure

theory. This theory has been used by Vialov (1965b); Tystovich (1960); and Andersland and AlNouri (1970) to describe the time dependent behavior of sand-ice materials. The basic problem in this approach to shear strength is determining the interrelationship of the cohesive and frictional components of strength for given test conditions.

Assuming that the Mohr-Coulomb theory is valid for frozen soils, a portion of this study is concerned with identifying factors that affect the frictional and cohesive components of strength. The basic factors that influence strength of sand-ice materials include temperature, strain rate, ice content and the percent of sand in the system. These factors have been discussed by other investigators of sand-ice materials (Vialov, 1965b; Kaplar, 1971; Goughnour and Andersland, 1968). However, the effect of these factors when the sand-ice is subjected to high confining pressures is not known. One of the main objectives of this study is to use the results of tests conducted at high confining pressures as a means of identifying frictional and cohesive components of strength. By using triaxial testing techniques and confining pressures up to 1000 psi, the effects of strain rate, ice content and void ratio on the strength of sand-ice are determined. In order to eliminate the effect of

temperature on the results, all constant strain rate tests were conducted at a temperature of -12.0° C.

From the results of the experimental portion, the Mohr-Coulomb theory is applied for the entire range of confining pressures and an effective angle of friction is determined. It is shown that the angle of friction is independent of ice content and is related to the angle of friction for unfrozen sands tested at high confining pressures.

The second part of this study describes the effect of confining pressure on the creep of sand-ice materials. Andersland and AlNouri (1970) have indicated that the steady state creep rate can be estimated using the rate process theory. For confining pressures up to 150 psi, the steady state creep was determined to be a function of deviator stress and the mean stress. In order to verify this result and to extend the range of mean stresses used, creep tests were conducted at confining pressures up to 1000 psi. From the results of these tests an expression for creep in terms of deviator stress and confining pressure is developed for the entire range of confining pressures.

A problem in determining the time dependent behavior of sand-ice is the identification of the active component of creep. By using samples with reduced ice content, it can be shown that the ice matrix is the

primary agent of creep. Further, it is noted that there is a relationship between the peak deviator stress as determined in a constant strain rate test, and the creep behavior of a sand-ice sample tested at a deviator stress less than the peak value.

Constant deviator stress testing was used to obtain the creep behavior of the sand-ice material. The effect of confining pressure was obtained using step-stress testing techniques where the deviator stress is held constant and the confining pressure is increased in steps as the tests progress. These tests covered a range of confining pressures from 0 to 1000 psi. Uniaxial creep tests were conducted to obtain the general creep characteristics of the material and to verify the effect of confining pressure on creep. Reduced ice content samples were also tested using uniaxial and step-stress techniques.

CHAPTER II

LITERATURE REVIEW

2.1 Frozen Soil Structure

In order to understand the shear strength and creep characteristics of a sand-ice material, it is useful to describe the various components that make up the system. Frozen soils, in general, can be considered to be multi-phase systems made up of an assemblage of soil particles, unfrozen pore water, polycrystalline ice and entrapped air. The relative proportions of each of these components will have substantial effects on the mechanical behavior of the material. Some of the phases are interrelated, such as the amount of unfrozen pore water and the type of soil particles. Others are directly affected by ambient conditions and testing techniques. Overall, the picture obtained is a complicated system responsive to numerous changes in conditions. The discussion to follow will emphasize sand-ice materials, but other types of frozen soil will be included to give a better idea of the available theories used to determine the strength characteristics of sand-ice materials.

Vialov (1965b), Scott (1969) and Tsytovich (1960) have shown that variations in mechanical properties of frozen soils can be related to the amount of unfrozen pore water in the soil-ice system. There are two phases of unfrozen water in frozen soil: water vapor having a variable composition, and water that is strongly attracted to the soil particles by intermolecular forces.

Water vapor is a gaseous phase found in the void spaces. At temperatures below freezing its properties remain the same until frozen. Water vapor has been found in polar ice at temperatures as low as -40.0° C (Tsytovich, 1960). Water vapor transport may contribute substantially to the formation of ice lenses in soil systems where the freezing front is isolated from the source of the water. In this process, moisture is transported by vapor diffusion from the warmer source to the colder freezing front (Jumikis, 1966). For soils that were saturated before freezing this phenomenon does not occur.

The other type of unfrozen water that may be present in a frozen soil can be explained using the "diffuse double layer" concept. According to this theory the layer of water molecules closest to the soil particles are attracted to the surface molecules and have higher energy states and different characteristics than water which is located at some distance from the particle surface. The

amount of water in the bound layer that will freeze is dependent upon the interaction of the forces of crystallization and the forces of attraction to the particle surface. The forces of attraction are dependent on the mineralogical composition of the particles and will be influenced by the specific surface of the particles while the forces of ice crystallization are dependent to a large degree on the temperature. For any given temperature, the larger the specific surface area of the mineral, the larger the amount of unfrozen water. Tsytovich (1960) showed that unfrozen water was present in clays even at temperatures below -30.0° C. Anderson (1967) verifies this fact and states,

> It seems beyond a doubt that in frozen silicate mineral-water systems, the ice crystals are separated from the substrate surface by an unfrozen fluid-like interfacial zone of water.

Some of the differences in behavior between frozen sands and clays can be explained when it is known that the sands with their round large sized particles have low specific area as compared to clay particles. Because sands have low specific surface, and unfrozen water contents are directly related to these surface areas, nearly all available water in sand is frozen at temperatures slightly below 0.0° C (Scott, 1969).

2.2 Freezing Process

Since all frozen soils are at some time unfrozen, it is necessary to understand the mechanism of freezing.

Basically, freezing is a thermodynamic process. By sufficiently lowering the temperature, molecules in a higher state of energy--the liquid state--change to molecules in a lower state of energy--the solid state. It is possible (Scott, 1969) to visualize the liquid state as consisting of aggregates of liquid molecules, which for a given temperature will have an equilibrium size that is determined by the ambient conditions. From quantum mechanics it is known that other aggregates of molecules will exist that are both larger and smaller than the equilibrium size. The larger aggregates will grow to form 'nuclei' of solidification. The formation of ice crystals depends upon the existence of these nuclei in the water as distinct starting points for crystallization of ice (Jumikis, 1966). The actual temperature at which crystallization will take place is a function of the grain size.

When a soil freezes, the soil structure may be considerably altered by the formation of ice lenses. In addition, the soil may be consolidated by the development of negative pore pressures developed below or adjacent to the ice/water interface. The degree of this alteration depends primarily on the mineralogical composition of the soil, grain size, freezing history and saturation. For large grained sand or gravel the soil structure is unaltered

(Vialov, 1965b) as freezing occurs with void spaces being filled with randomly oriented crystals of ice.

It was noted that the unfrozen water may have two different phases: water vapor and water attached to or adsorbed on the soil particles. For sand-ice materials these types of water are not present in any great amount. At temperatures slightly below 0^{o} C all water freezes directly in the pore spaces forming a massive structure (Vialov, 1965b) with little sensitivity to freezing history (Scott, 1969; Sayles, 1968).

Another factor in the freezing of a soil is the change in volume of water as freezing takes place. This factor may have considerable importance in the laboratory if samples of constant void ratio are to be prepared. The amount of soil volume increase (frost heave) is dependent upon the amount of water available and the grain size of the material. When water freezes there is an increase in volume of approximately nine percent. The change in volume may or may not affect the soil structure depending on the drainage conditions. Tsytovich (1960), states that under the conditions of free drainage, no changes in soil volume for sand will occur because the excess water resulting from freezing will be squeezed out. This will not be the case for fine grained soils since their low permeability will inhibit drainage of the excess

water resulting in expansion of the soil system as volume change occurs during freezing.

2.3 Cohesion

Unfrozen sand has no unconfined shear strength. When sand is saturated and frozen, there will be a substantial unconfined strength. The increase in strength due to the confinement of the ice matrix is called cohesion. In general, cohesion may result from three causes (Vialov, 1965b): (1) intermolecular cohesion due to forces of attraction between particles, (2) structural cohesion resulting from the process of formation and (3) cohesion due to confinement of the ice matrix (ice cementation). Depending on the type of soil, any or all of these components may be present. For sand-ice materials it is reasonable to assume that the first two components of cohesion are negligible and consider only the cohesion due to confinement of the ice matrix.

Cohesion due to the ice matrix is very responsive to temperature change and is a function of time, moisture content, plastic strain, load, and strain energy. One theory used to explain cohesion is based on variations and movement of unfrozen water in the soil-ice structure (Scott, 1969; Vialov, 1965a; Tsytovich, 1960). This theory states that upon application of some stress, high pressures are caused near the points of contact of the grains, resulting

in the melting of the ice in these regions. The melted ice flows to zones of lower stress where it refreezes. On the macro-scale this may be considered a weakening process followed by a strengthening process. Goughnour (1967), used this basic idea to explain creep characteristics of ice and identified the weakening and strengthening mechanisms.

Vialov (1965a), using rigid ball penetration test techniques, has obtained extensive data for the cohesion of frozen soils. His basic observations are: (1) sandy soils have small rheological response compared to clays; (2) cohesive properties increase up to some maximum as ice content increases; (3) temperature changes are one of the main causes of variations in the cohesive component in frozen soils; and (4) long term cohesion may be significantly less than the instantaneous cohesion (three to nine times). Vialov's tests are the most extensive long term investigations available into the cohesive properties of soils. However, the resulting mathematical formulations may be in question due to the testing technique (Scott, 1969).

2.4 Mechanical Properties of Ice

The properties of the pore ice may affect the mechanical behavior of frozen soil. It is know that the direction of the applied loads in relation to the direction of the ice crystal's axis has a definite effect on the

mechanical behavior of the ice (Gold, 1963). However, it is generally assumed that when ice freezes in the pore spaces of a soil-ice material, a polycrystalline structure is formed and there exists no oriented planes of weakness (Goughnour, 1967). It is for this reason that the discussion of the mechanical properties of ice, as they affect sand-ice systems, is limited to polycrystalline ice.

In addition to the orientation of the crystals, the mechanical properties of ice are affected by a substantial number of variables. Among the most important of these are strain rate and temperature. Leonards and Andersland (1960) have shown that unconfined compressive strength increases approximately 15 psi per degree centigrade from 370 psi at -4^{o} C. Their tests were conducted at a strain rate of $2 \times 10^{-2} min^{-1}$; and results showed considerable scatter due to the random nature of the freezing process. The strain rate also affects the strength of polycrystalline ice. Halbrook (1963) noted both an increase in Young's modulus and ultimate strength with an increase in rate of strain. However, Sanger (1971) in his review of available test results, indicates a decrease in strength of fresh water ice with an increase in strain rate.

Concerning the creep of polycrystalline ice, Gold (1963) noted that slip takes place only along basal planes and the deformation mechanism must be described in ways

which ice grains respond to this constraint. Gold (1963) has identified seven mechanisms which may take part in the response to applied loads. In the central part of the ice grains, slip bands and kink bands develop to conform to imposed deformations. However, for the grain boundary regions; boundary migration, crack formation, and distortion of the boundaries may take place as the grains respond to the applied loads. As a final response, recrystallization may take place, which is usually an indication of tertiary creep. The rate of loads application has a definite effect on which mechanisms predominate. For high loading rates, accommodation cracking and grain boundary migration are the controlling mechanisms.

2.5 Shearing Resistance

The shear resistance of sand-ice materials is dependent on a complex interaction of the ice matrix and the granular portion of the system. The Mohr-Coulomb theory is most frequently used to describe the shear strength of soils. It is a summation of the cohesive component and a frictional component. The cohesive component of frozen soils was discussed in section 2.3. The frictional component is best understood by examining the frictional characteristics of unfrozen sands.

2.5.1 Sand (Unfrozen)

In a sand-ice system it is apparent that for some conditions the frictional characteristics of the sand will contribute to the shear strength of the sand-ice material. The frictional properties of sands are well known and have been the subject of many articles. A good basic discussion of the many factors that affect the frictional behavior of single mineral sand was prepared by Koerner (1970). More important in relation to frozen sand is the frictional behavior of sand at high confining pressure. Several investigators have considered this problem (Hirschfeld and Poulous, 1963; Hall and Gordon, 1963; Vesic and Clough, 1968; Lee and Seed, 1967). The basic conclusions from their work that may be applied to sand-ice materials are:

1. Shearing resistance is made up of three components; sliding friction, dilatancy, and particle crushing and rearranging.
2. The dilatancy component of strength becomes small at high confining pressures.
3. The angle of friction decreases as confining pressure increases.
4. The strain at failure increases with increased confining pressure.
5. At high confining pressure sands exhibit a plastic stress-strain relationship.

2.5.2 Sand-Ice Materials

Shear strength of soil has traditionally been determined by the Coulomb equation which divides the shear strength into a frictional and cohesive component. The equation,

$$\tau = c + \sigma_n \tan \phi \qquad (2\text{-}1)$$

may be used for soil-ice materials if the coefficients are adequately descriptive of the behavior of the frozen soil system. It is known that shear strength in frozen soils is time dependent (Vialov, 1965a) making it necessary to include the time factor in the defining equation.

Considering the Coulomb equation term by term, the frictional component may be expressed as:

$$\tau_f = \sigma_n \tan \phi = \sigma_n K_f$$

and (2-2)

$$K_f = f(\sigma_3, I, e, \dot{\varepsilon}, P_s, g, H)$$

where σ_3 = confining pressure
I = interparticle attractive or repulsive forces
e = void ratio
$\dot{\varepsilon}$ = strain rate
P_s = particle shape
g = particle gradation
H = mineral type

It is usually assumed that the interparticle forces are insignificant for sand, and for a given type of sand the particle shape, gradation and mineral type can be held constant. Then for a given soil:

$$\tau_f = f(\sigma_3, e, \dot{\varepsilon}) \qquad (2\text{-}3)$$

The strain rate dependency is small for granular soils and for tests of short duration may be considered constant (Whitman, 1957). Thus, the functional relationship is usually interpreted as being related to initial void ratio and the applied confining pressure. Then, $K_f = f(\sigma_3, e) = \tan \phi$ where $\tan \phi$ may be defined at failure or at intermediate points along the stress path (Schmertmann and Osterberg, 1960).

The cohesive component in equation 2-1 representing a frozen soil is a function of three components (Vialov, 1965a). For sand-ice materials the interparticle and structural cohesion are negligible in magnitude and it is the confinement due to the ice matrix which controls cohesion. The component of shear strength contributed by the ice may be defined as:

$$c_i = f(\varepsilon, T, \dot{\varepsilon}, j, t) \qquad (2\text{-}4)$$

where ε = strain

$\dot{\varepsilon}$ = strain rate

T = temperature

j = ice content

t = time

The composite soil shear strength is:

$$\tau = c_i + \sigma_n K_f \qquad (2\text{-}5)$$

Although the equation indicates a summation, it is possible that c_i and K_f do not reach their maximum at the same time. In fact, experimental evidence for clays (Schmertmann and Osterberg, 1960) indicates they do not. Further, if the cohesive component due to the ice is time dependent, eventually reducing to zero, then the shear strength will be a purely frictional phenomenon. It is doubtful that this is ever completely true; however, the contribution to shear strength due to the ice may approach a constant as this component is fully mobilized.

Other attempts have been made at defining the shear strength of frozen soils using the Mohr-Coulomb failure theory (Tsytovich, 1960; Vialov, 1965b). However, the fact that the strength of frozen soils is time dependent requires the modification of the usual form of equations to include the time factor. Tsytovich (1960) indicated that the shear strength of frozen soil is a function of at least three factors:

$$\tau = f(T, \sigma_3, t) \qquad (2\text{-}6)$$

T = temperature of the soil below freezing

σ_3 = confining pressure

t = time of action of the load

Thus, the shear strength for frozen soils can be determined by the equation

$$\tau = c_T + P \tan \phi_T \qquad (2\text{-}7)$$

where both c_T and ϕ_T are functions of temperature and time. For a given time and stress the angle of friction increases as the temperature increases until at 0° C the value is equal to the value for unfrozen soils. The above relationship does not necessarily hold for all types of soils. Vialov (1965b) showed that the frictional component $\tan \phi_T$, is not time dependent for frozen sands, sandy loams and dense clays. Other tests from the same study showed that for sands, the angle of friction at failure was constant for times to failure of 1 to 24 hours. The difference in the time factor, as it affects the friction term for various types of soil makes it very difficult to express the strength characteristics of clays and sands with one all inclusive equation.

Andersland and AlNouri (1970) have also used the Coulomb expression to evaluate the time dependent strength characteristics of frozen sands. They obtained a constant value of C and tan ϕ when the factors affecting the cohesive component were held constant. In their study the

cohesion and angle of friction were determined from both constant strain rate and differential creep tests.

Another approach to the determination of the shear strength of sand-ice is to relate the strength of the sand-ice material to the strength of ice by a stress factor (Goughnour and Andersland, 1968). In this procedure the strength of a sand-ice material is obtained by multiplying the strength of ice at various strains by a stress factor. The stress factor is the ratio of sand-ice strength to the strength of ice obtained from samples tested at similar conditions. For this type of presentation it was noted that for strains less than approximately two percent, the stress factor is constant. Above this amount the stress factor is no longer constant, but increases in a linear manner up to a maximum value. After the peak strength of the sand-ice is reached the stress factor is again constant. Using the results from stress factor versus strain graphs, Goughnour (1967), identified the three stages of strengthening in a sand-ice system as follows:

1. The initial strengthening occurs at low values of strain where the characteristics of the ice predominate. In this stage the strength of sand-ice materials is a linear function of the strength of ice.

2. The second stage occurs where solid to solid contact becomes apparent. This effect may be mobilized throughout deformation when the volume of sand is greater than 42 percent.
3. The third stage, related to dilatancy of the sand occurs as the particles act against the confinement of the ice matrix.

2.6 Creep Behavior

Since the strength of frozen soils has a strong time dependence, it is necessary to understand the rheologic behavior of the soil-ice system. One of the manifestations of the rheological characteristics of soil-ice is creep.

It has been demonstrated by several investigators (Vialov, 1965b; Sayles, 1968; Goughnour and Andersland, 1968) that soil-ice systems when subject to constant stress will develop what is considered to be a "classic" creep curve. Figure 2-1 shows this curve as a strain-time relationship for damped and undamped creep. Damped creep is defined as creep in which the strain approaches a limit as time increases. It is characterized by an instantaneous elastic strain and a region of decreasing strain rate approaching a constant strain. The undamped creep does not approach a constant strain and is typically divided into four sections: (1) instantaneous elastic strain resulting

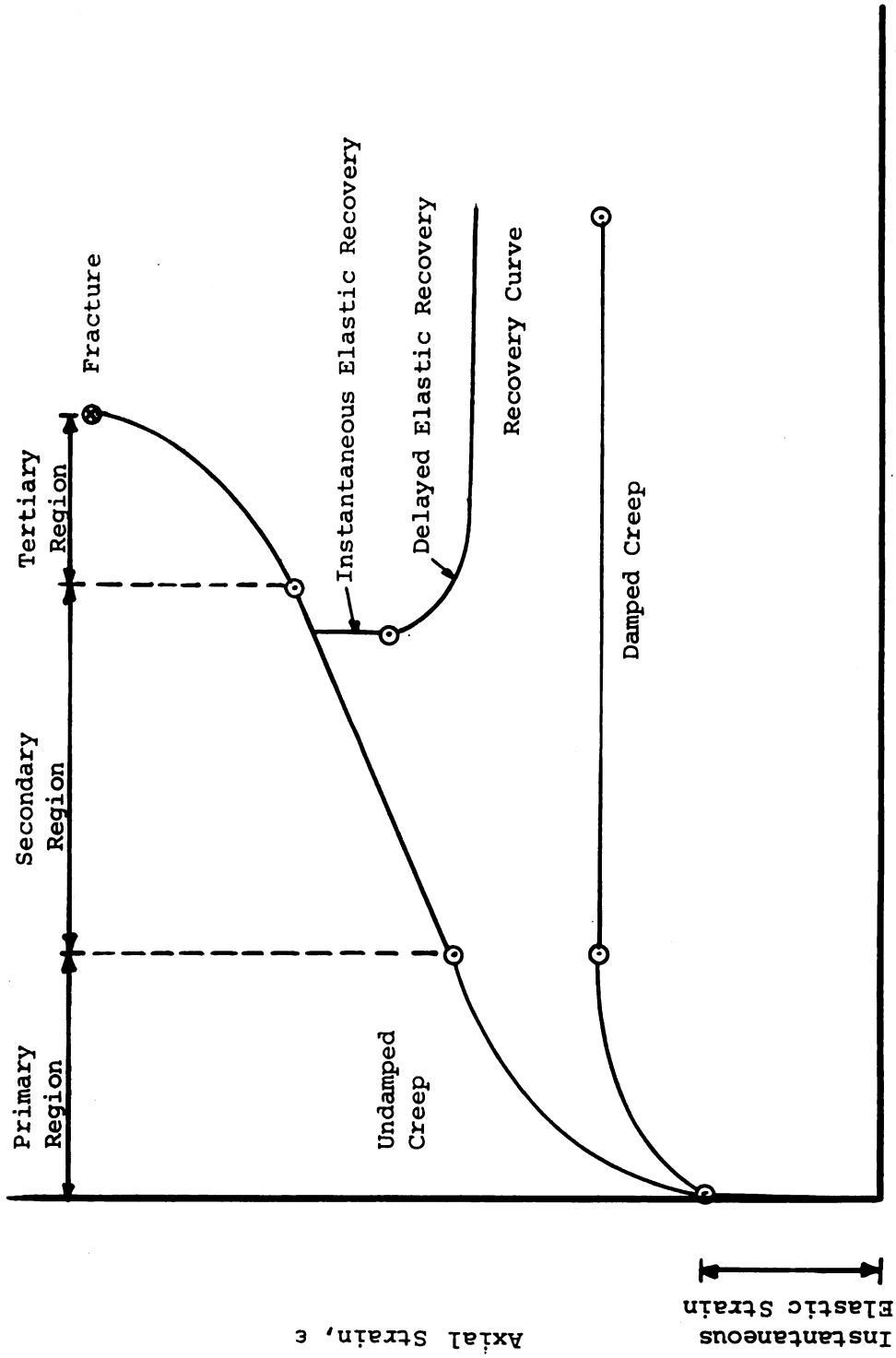

Figure 2-1.--Typical constant axial stress creep curves.

from the application of the load, (2) primary creep with a decreasing rate of strain, (3) a secondary region of constant or minimum strain rate and (4) the tertiary region in which strain rates increase to failure. Vialov (1965b), identifies these regions in terms of deformation processes. The region of instantaneous deformation is termed elasto-plastic since not all of the deformation is recoverable. The primary region is the region of plastic deformation if irreversible deformation takes place. The secondary region is termed plastic-viscous since the constant deformation with time is comparable to the flow of a viscous fluid. Finally, the tertiary region is the region of progressive flow leading to a viscous failure. The division between damped and undamped creep is somewhat arbitrary since what at first glance is considered to be damped creep could be the secondary region of creep leading to failure if long term readings were obtained. It has been suggested (Scott, 1969) that the maximum load that can be applied and still produce damped creep is related to the unfrozen strength of the soil system. Any load which exceeds the ultimate strength of the soil structure alone will eventually lead to a creep failure.

If the undamped sample had been unloaded during the test a recovery curve similar to the one shown in Figure 2-1 would have resulted. Recovery is broken into two sections:

the instantaneous elastic recovery and the delayed elastic recovery. Not all of the strain that accumulated up to the time of removal of the load will be recovered, and most of the deformation remains permanently (Scott, 1969).

2.6.1 Theory

Various methods have been used to describe the behavior of a material as it deforms under a constant load. The most common methods include power law relationships, hyperbolic relationships and the hereditary creep theory as proposed by Vialov (1965a).

The hereditary creep theory is based on the assumption that the deformation at any time depends not only on the level of stress applied, but also on the history of prior deformations (Vialov, 1965b). The theory is straight forward mathematically and reduces to an equation for strain as a function of time as follows:

$$\varepsilon(t) = \frac{\sigma(t)}{E_o} + [K(t-t_o)\sigma(t_o)\Delta t] \qquad (2\text{-}8)$$

where the various components may be identified. The first term on the right, $\frac{\sigma(t)}{E_o}$, is the instantaneous deformation which takes place after the application of the load $\sigma(t)$ at the present time t. E_o is the instantaneous modulus of elasticity. The second term is the result of previous loading and is the history dependent term. $K(t-t_o)$ is a relaxation term, where K is a coefficient and $(t-t_o)$ is the

time of relaxation. $\sigma(t_o)$ is the previous load applied to the system at time t_o and Δt is the duration of the previous loads. Using this equation and the principle of superposition, all possible loading histories may be considered. In this equation the temperature dependency appears in the evaluation of the coefficient K and has a very strong influence on the developed strains. The hereditary creep theory has been used extensively by various Russian investigators to describe the rheological properties of both frozen and unfrozen soils (Vialov, 1965b).

The most recent theory to be used extensively to explain the creep characteristics of frozen soil is the rate process theory. This theory, as proposed by Gladstone, Laidler, and Eyring (1941), has its basis in statistical and quantum mechanics, and its application has been discussed by a number of investigators (Abdel-Hady, 1964; Dillon and Andersland, 1967; Mitchell, 1964) for various types of materials.

The rate process theory treats creep as a thermally activated process in which flow units of atoms, molecules or groups of molecules move across an energy barrier from one equilibrium position to another. The movement across the energy barrier is determined on a statistical basis and requires a flow unit to obtain sufficient energy ΔF,

termed the free energy of activation to surmount the barrier. For equilibrium conditions the movement is entirely random and the flow units cross the energy barrier equally in all directions resulting in no net flow of the material. If a directed potential is applied to the system, such as an axial stress, then the energy barrier becomes distorted in the direction of the applied potential and more flow units have sufficient energy to move in the direction of the potential than in the direction opposing the potential. The result is a net flow in the direction of the applied potential. Expressed in mathematical terms; the division of thermal energy among flow units is given by the Boltzmann distribution (Mitchell, 1964) and the frequency of activation v may be expressed as:

$$v = \frac{kT}{h} \exp\left[-\Delta F/RT\right] \qquad (2\text{-}9)$$

where k = Boltzmann's constant (1.38×10^{-16} erg $^{o}K^{-1}$)

T = absolute temperature, degrees Kelvin

h = Planck' constant (6.624×10^{-27} erg-sec^{-1})

R = universal gas constant (1.98 cal$^{o}K^{-1}$ mole^{-1})

ΔF = free energy of activation, Cal/mole

With application of the directed potential the energy barrier becomes distorted by an amount $\frac{f\lambda}{2}$, where f is the

applied potential and λ is the distance between equilibrium positions. The result is that the energy barrier has a height of $(\Delta F + \frac{f\lambda}{2})$ in the direction opposing the potential and $(\Delta F - \frac{f\lambda}{2})$ in the direction of the potential. Substituting these values into equation 2-9 and subtracting, results in an expression for the net increase in frequency of movement in the direction of the applied potential. If both sides of the expression are then multiplied by a parameter X, a function of the number of flow units, an expression for strain rate is obtained as:

$$\dot{\varepsilon} = \frac{2XkT}{h} \exp[-\Delta F/RT] \sinh [f\lambda/2kT] \qquad (2\text{-}10)$$

If the applied stress is large enough, the expression reduces to

$$\dot{\varepsilon} = \frac{XkT}{h} \exp [-\Delta F/RT] \exp [f\lambda/2kT] \qquad (2\text{-}11)$$

This is the form of the equation that is most frequently used in describing creep.

Using equation 2-11, some insight into factors that affect the frictional component of a sand-ice material can be shown. Mitchell (1964) proposed that

$$\Delta F = \Delta F_o + P(\phi + D_a) \qquad (2\text{-}12)$$

in which ΔF_o is the activation energy required to overcome the cohesive component of strength and P is the interparticle

component of activation energy composed of a frictional part ϕ and a dilatancy part D_a. Then, substituting into equation 2-11

$$\dot{\varepsilon} = \frac{XkT}{h} \exp\left[\frac{-\Delta F_o - P(\phi+D_a)}{kT}\right] \exp\left[\frac{f\lambda}{2kT}\right] \qquad (2\text{-}13)$$

If logarithms of both sides are taken, the result is

$$\ell n\dot{\varepsilon} = \ell n \frac{XkT}{h} - \frac{\Delta F_o}{kT} - \frac{P(\phi+D_a)}{kT} + \frac{f\lambda}{2kT} \qquad (2\text{-}14)$$

The shear force f is equal to the applied stress difference $(\sigma_1-\sigma_3)$ divided by a structural factor S, and solving for the stress difference:

$$(\sigma_1-\sigma_3) = \text{constant} + \text{constant} + \text{constant} + P\ (\phi+D_a) \qquad (2\text{-}15)$$

This equation separates the deviator stress into various components and can be used to study the factors that affect these components. For example, the frictional component is shown to be independent of both temperature and strain rate. In addition, the equation can be related to the Mohr-Coulomb equation if it is assumed that the test results were obtained at constant strain rate, temperature and structure. This result is particularly interesting since constant strain rate tests can be used to define an effective angle of friction that is independent of the ice properties.

Ladanyi (1972) has discussed the creep characteristics of frozen soils using a power law relationship. In this discussion of creep behavior the steady state strain rate is determined to be some power of the applied uniaxial stress.

$$\dot{\varepsilon} = \dot{\varepsilon}_c \left[\frac{\sigma}{\sigma_c(T)}\right]^n \qquad T = \text{Constant} \tag{2-16}$$

In this equation, $\dot{\varepsilon}_c$ is a small normalizing strain rate, $\sigma_c(T)$ is the uniaxial stress that causes $\dot{\varepsilon}_c$, and n is an experimentally determined power.

Using the basic power law formulation in equation 2-16, it is possible to obtain a relationship between the strain rate equation and the constant strain rate test results predicted by the Mohr-Coulomb equation. Starting with the expression:

$$\tau = C(t,T) + \sigma \tan \phi \tag{2-17}$$

the equation can be rewritten in terms of the maximum stress difference as:

$$(\sigma_1-\sigma_3)_f = \sigma_{fu}(t,T) + \sigma_3(N_c-1) \tag{2-18}$$

where $(\sigma_1-\sigma_3)_f$ = deviator stress at failure

σ_{fu} = unconfined compressive strength at time t and temperature T

N_c = flow value = $(1+\sin \phi)/(1-\sin \phi)$

solving equation 2-16 in terms of the unconfined strength and substituting into equation 2-18 results in an expression for the deviator stress in terms of the confining pressure.

$$\sigma_1-\sigma_3 = \sigma_{cuo}[\frac{\dot{\varepsilon}^c}{\dot{\varepsilon}_c}]^{1/n} f(T)+\sigma_3(N_c-1) \qquad (2\text{-}19)$$

where σ_{cuo} = unconfined compression strength for temperatures near 0^o C.

$\dot{\varepsilon}^c$ = constant strain rate of the test

$\dot{\varepsilon}_c$ = normalizing strain rate

$f(T)$ = temperature term

This equation shows the shear strength as being dependent upon a cohesive term and a frictional term. The frictional term is dependent only on the angle of friction of the material and the confining pressures.

It is interesting to note that both the power law relationships and the rate process equations can be reduced to the form of the Mohr-Coulomb equation. In this form both contain a frictional component that is independent of strain rate and temperature.

2.6.2 Application of the Rate Process Theory

The most extensive investigation into the creep behavior of sand-ice using ideas from the rate process theory was reported by Andersland and AlNouri (1970). In determining the effect of mean stress, the logarithm of

the secondary creep rate was plotted against a stress factor Σ which is a function of the deviator stress and the mean stress. The resulting curve was linear and could be expressed as:

$$\dot{\varepsilon} = b \exp (m\Sigma) \tag{2-20}$$

where b and m are experimentally determined parameters. The b term was found to be an exponential function of the deviator stress and the resulting equation took the form:

$$\dot{\varepsilon} = C \exp (ND) \exp (-m \sigma_m) \tag{2-21}$$

where C and N are constants, D is equal to the deviator stress and σ_m is equal to the mean stress. This equation is in the form of the equations from rate process theory at large stresses and indicates an exponential increase in strain rate with increasing stress difference and an exponential decrease in strain rate with increasing mean stress.

In the same investigation (Andersland and AlNouri, 1970) the effect of temperature on the creep of sand-ice was determined using differential creep testing techniques and was found to be in the form

$$\dot{\varepsilon} = A \exp \left(\frac{-L}{T}\right) \tag{2-22}$$

where A is an experimentally determined parameter that includes the effects of the applied stress. This equation predicts creep to be an exponential function of the temperature. Ladanyi (1972) has noted that this is not descriptive of experimental work conducted over a wide range of temperatures, and suggests that there is evidence of a near linear temperature dependence for sand-ice down to -20.0° C.

CHAPTER III

MATERIALS AND SAMPLE PREPARATION

To eliminate the variables caused by particle composition and gradation, standard Ottawa sand, obtained from Soiltest Incorporated, was used in all sand-ice samples. The sand was composed of uniform sub-angular quartz particles with a specific gravity of 2.65. To insure uniform gradation only particles between the number 20 (0.84mm) and 30 (0.59mm) U. S. Standard sieve sizes were used. A sand volume of 64 percent was selected to obtain a dense soil structure. This volume of sand was well above the critical volume of 42 percent determined by Goughnour (1968) to be the point where intergranular friction is a major factor in the development of strength in sand-ice materials. Actual values of the percent of sand varied between 61.6 and 64.3 as noted in the test data shown in the Appendix. A sand volume of 64 percent produces a sample with a void ratio of 0.562.

The ice matrix was formed from deaired, deionized, distilled water. Using techniques outlined below, polycrystalline ice with densities of 0.918 to 0.854 gm/cm^3

were obtained. The density of ice at -12.0° C is 0.91848 gm/cm^3 (Pounder, 1967). The difference between the actual and the test ice densities was due to small air bubbles trapped in the sample voids as the sample was saturated. If the voids had been completely saturated with ice, an ice content of 100 percent would have been obtained. Actual ice content for the high ice content samples ranges from 92.5 to 99.0 percent. Some special tests were made with ice contents of approximately 55 and 35 percent. These tests are noted in later sections.

Sample size and sample preparation were essentially the same as that used by Goughnour (1967) and AlNouri (1969). The sample size, 1.13 inches in diameter by 2.26 inches in height, was selected to yield a one square inch end area and a volume of 2.26 cubic inches. Knowing the specific gravity of the sand and the percent sand by volume the correct amount of oven dried sand could be predetermined.

The samples were prepared by pouring the predetermined amount of sand into a split aluminum mold that had been lightly greased with silicone vacuum grease to reduce adhesion between the mold and the sample. The mold was filled half full of sand and tamped 25 times with a rubber hammer. The remaining portion of the sand was poured into the mold and tamped just enough to bring the level of sand to the top of the mold.

Initial tests exhibited a tendency to flare at the top of the sample. It was believed that this was caused by local variations in density near the top of the sample. To eliminate this tendency, the mold was built up 0.3 inches and the top part of the sample was trimmed off to the correct height of 2.26 inches. This method eliminated the problem with flaring and the samples exhibited a more uniform cross section after testing.

After the sand had been poured into the mold, deaired, deionized, and precooled water was added to the sample until it appeared at the top of the mold. The mold was then tapped lightly to remove air bubbles that may have been trapped in the sample. This procedure was only partially successful since all samples contained less than 100 percent ice content. The sample was then placed in a cold box maintained at -18.0° C, and allowed to freeze for approximately 24 hours. After this period of time essentially all water was frozen and additional freezing time would not affect the strength of the sample (Sayles, 1968). Prior to mounting the sample in the triaxial cell, one sample end was trimmed with a sharpened paint scrapper to permit uniform seating with the loading cap.

The sample was then removed from the mold and transferred to another cold box for future mounting on the triaxial cell's pedestal. Here, the sample was

weighed both in air and immersed in fuel oil having a specific gravity of 0.832. The sample weight, volume, and ice content were obtained from these measurements.

To reduce end effects, friction reducers made of a sandwich of two layers of polyethelene and a greased aluminum disk were placed on each end of the sample. Next the sample was placed on top of the pedestal and capped with a lucite cap. A protective membrane was placed over the sample and fastened with rubber bands. The sample was then transferred to another cold box where it was mounted on the triaxial cell base plate. Three additional light membranes and one heavy membrane were placed over the sample. The triaxial cell's cover was placed over the sample and bolted to the base plate. The loading ram was brought into contact with the sample and the entire cell assembly was transferred to a work bench and the confining pressure gauge was attached. Finally, the cell and appurtenances were transferred to the cold bath and the cell was filled with coolant. Before testing, the triaxial cell and sample were allowed to stabilize in the cold bath for 12 hours at -12.0° C. This complicated mounting procedure was necessary to insure that the sample was never exposed to an environment that had any contact with the ethylene glycol coolant used in the cold bath since this could cause disintegration of the ice. This procedure took about 20 minutes and resulted

in an unusual temperature history for the samples. However, the samples were exposed to temperatures greater than -10.0° C for only a few seconds, and for sand-ice materials at temperatures less than -10.0° C, history has little effect on the strength of the materials (Scott, 1969).

After the sample had been tested the triaxial cell was removed from the cold bath and disassembled. The sample was inspected for membrane leaks and for indications of failure planes. The sample was weighed and the final volume obtained using the procedure described above. The entire sample was placed in a drying oven and the dry weight of sand and moisture content were obtained.

The sample preparation for the reduced ice content samples was the same, except a known volume of water was added to the sand instead of completely saturating the sample. The amounts of water used were 10, 8, and 4.5 ml, which resulted in ice contents of approximately 75, 55 and 35 percent, respectively.

In preparing reduced ice content samples there was some question as to the actual distribution of ice in the pore spaces. It is doubtful that the procedure described will result in a completely uniform distribution of water, and the ice contents indicated are nominal, based on the moisture content of the entire sample. The actual ice content distribution was higher

than the nominal at the bottom of the sample and lower than the nominal at the top. Use of snow or fine ice particles mixed with the sand was not attempted because of anticipated compaction problems for the desired high sand density. The results from reduced ice content samples did give a fairly reasonable indication of general magnitudes of strength.

CHAPTER IV

EQUIPMENT AND TEST PROCEDURES

Since triaxial tests covering a range of confining pressures from 0 psi to 1000 psi were conducted, the triaxial cell had to be constructed of a material that would withstand this range of pressures. The type of cell used was a special high pressure triaxial cell. The cell was a stainless steel Wykeham-Farrance triaxial cell constructed for a maximum working pressure of 1500 psi and tested to 2250 psi. The cell had a stainless steel hardened ram and adequate valves to provide for drainage and pressure control. Two base plates for the cell were specially designed and constructed at Michigan State University to provide for a 15,000 pound or a 5,000 pound capacity stud transducer. For the constant strain rate tests the base plate with the 15,000 pound capacity transducer was used. The creep and step-stress tests were performed using the base plate with the 5,000 pound capacity transducer.

In order to conduct the triaxial tests at pressures up to 1000 psi a pressure transmitting system was used similar to that described by Warder (1969). This system used pressurized nitrogen gas as the activating

source. The gas was transmitted from the nitrogen tanks through a regulating valve to a high pressure cell. In this cell the gas was brought into contact with the coolant liquid which transmitted the pressure to the triaxial cell. The high pressure cell also kept the coolant from backing up the line into the nitrogen tank during depressurizing. Gages were placed at various locations to monitor the pressure. A master gage attached to the triaxial cell was used to read the confining pressure in the triaxial cell. This gage had a 5 psi increment with an accuracy of 1/2 percent. The constant pressure regulator and the system described held the pressure constant during the tests with very little variation.

The other part of the system consisted of the refrigerator unit and its appurtenances which controlled the test temperature of the coolant. A micro-regulated portable refrigerating unit was used to control the temperature of the coolant. The coolant was circulated from the refrigerating unit to a cold bath in which the triaxial cell was immersed. This system provided very good temperature control. Goughnour (1967) using a similar system determined, by using a thermocouple attached inside the triaxial cell, that temperature varied by not more than 0.05° C from the temperature of the coolant liquid in the cold bath. Temperature at the cold bath was monitored using a thermometer with scale divisions

of 0.1° C from which the temperature could be estimated to ± 0.01° C. The coolant used in the refrigerating unit was a mixture of about 1/2 ethylene glycol and 1/2 water. Figure 4-1 shows a schematic layout of the testing equipment.

Various types of transducers were used to measure the axial force and displacements during a test. The transducer used to measure the loads during the constant axial strain rate tests was a Strainsert model Q-1096 stud transducer with a 15,000 pound capacity. Loads measured with this transducer were accurate to ± 10 pounds. This unit had no provision for pressure equalization, and when the confining pressure was applied the transducer would indicate a negative load. The value for the negative load was set equal to zero and increases in load were measured from this value.

For the constant strain rate tests (samples 77-89) and the creep tests a Strainsert flat load cell type FL5U-2SP with 5,000 psi capacity was used. This load cell had an accuracy of ± 5 pounds.

To measure the axial displacement, a Sanborn Linearsyn differential transformer was used. The transformer was attached to the triaxial cell with the core element bearing on a collar plate fixed to the cell's loading ram. This allowed measurement of axial displacement within the cell and eliminated all other

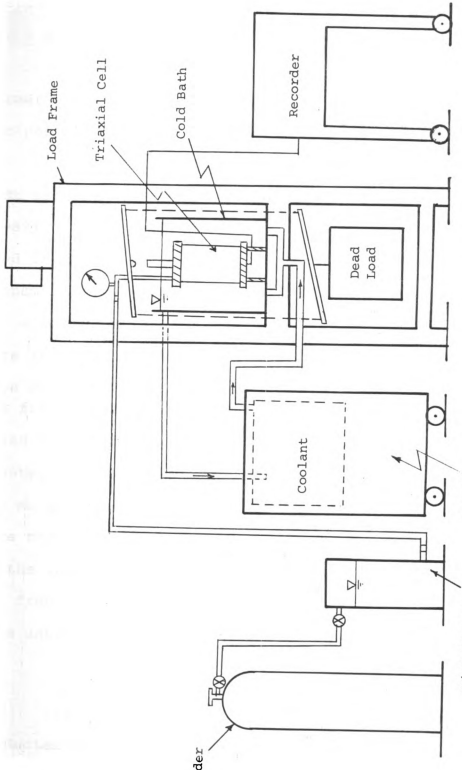

Figure 4-1.--Layout showing test equipment.

displacement measurements. The accuracy of measurements was $\pm$ 0.0004 inches.

The force transducer and the differential transformer were connected to a Sanborn 150 4-channel recorder for permanent display of the results.

Two different load frames were used for the test series. The constant strain rate tests (samples 77-89) and the creep tests were performed on a Soiltest load frame Model T-118-X with a Graham variable speed transmission. The transmission was of the screw type and allowed displacement rates to be changed while tests were in progress. All other constant strain rate tests were conducted on a Wykeham-Farrance variable speed loading frame. This frame had a 30 speed gear box with speed selections from 0.225 to 0.000024 inches per minute. The machine performed satisfactorily, but there was no provision for changing the rate of displacement once the machine had started. The results indicate that as the load was applied, the displacement rate dropped off from the selected rate and did not return to this rate until after the peak load had been reached.

4.1 Triaxial Tests

Triaxial tests with constant strain rates were conducted on both confined and unconfined sand-ice samples. After the sample and triaxial cell had been

in the cold bath for about 12 hours, the test procedure outlined below was followed:

1. The temperature of the cold bath was observed and recorded.
2. The force transducer and the displacement transformer were connected to the Sanborn recorder which was allowed to warm up. After an adequate warm up period both transducers were brought to a zero reading.
3. The load frame ram was lowered until it was just in contact with the triaxial cell's ram, with no load applied.
4. If the test was to be confined, the appropriate level of pressure was applied to the triaxial cell. If the test was unconfined, this step was omitted.
5. The drive mechanism was set at the desired speed (usually 0.006 in/min) and the loading ram was activated.
6. The trace of the load and deflection readings were observed on the recorder output charts. As the trace approached the top of the graph, the stylus was turned back using the zero suppression capability of the recorder.
7. After the peak load was observed on the recorder the driving mechanism was stopped

and the confining pressure, if any, was removed.

8. The temperature of the cold bath was recorded and the triaxial cell was removed from the cold bath.

Most of the constant strain rate triaxial tests were conducted on the Wykeham-Farrance load frame. However, 15 tests were conducted using the Soiltest apparatus. In these tests the procedure was as noted above with the exception of step six in which the trace of the displacement curve was observed and adjustments of the strain rate were made as the test progressed.

4.2 Creep Tests

All creep tests were conducted on the Soiltest load frame. Loads were applied by a loading yoke supporting a dead weight of lead bricks. The yoke was lowered by the drive motor of the load frame. When loads were applied to the sample, the drive was lowered at the fastest rate possible. Loading time was approximately five seconds.

4.2.1 Uniaxial

The procedure for conducting a uniaxial creep test was basically the same as the triaxial tests. The preliminary steps were the same as steps 1-4 listed in section 4.1. After the load was applied the trace of the

deflection curve was observed and at predetermined intervals small increments of weight were added to the sample to compensate for the increase in cross sectional area and to maintain a constant stress. The increments of weight were noted and used to check the load readings obtained from the recorder. The tests were allowed to run for approximately six hours before the load was removed. The samples were allowed to recover for one hour, then the triaxial cell was removed from the cold bath and disassembled.

4.2.2 Step-Stress

In step-stress testing the deviator stress was held constant and the confining pressure applied to a sample was changed by increments or steps. Except for the loading stage, the step-stress tests were conducted in the same manner as the uniaxial creep tests. During loading the selected level of stress was applied to the sample which was permitted to deform in the uniaxial state of stress for 60 minutes. At the end of this time an initial increment of confining pressure of 100 psi was applied to the sample. After the confining pressure was applied it was necessary to add weight to the dead load to retain the selected level of deviator stress. This was accomplished by observing the load trace on the recorder and adding weight until it returned to the

initial value. Additional increments of confining pressure were added at 120, 180, 240, 300 and 360 minutes. The total confining pressure after each of these increments was 200, 400, 600, 800 and 1000 psi, respectively. When operating at elevated confining pressure, the membranes were easily ruptured causing several of the step-stress tests to be terminated.

CHAPTER V

EXPERIMENTAL RESULTS

5.1 Constant Axial Strain Rate Tests

The mechanical properties of soils are usually measured using triaxial compression tests. More recently the effect of strain rate has been recognized as one of the many variables that affect the stress-strain relationships. As a consequence, constant axial strain rate testing was used to eliminate this potential variable. This section presents the results from constant axial strain rate tests on unfrozen sands, sand-ice with high ice content and sand-ice with reduced ice content.

5.1.1 Drained Tests

To provide a correlation between the frictional characteristics of frozen and unfrozen sands, the frictional behavior of the unfrozen sand was obtained for the same test conditions as the frozen sands. A series of drained triaxial tests were conducted on unfrozen Ottawa sand at a strain rate of $2.66 \times 10^{-3} min^{-1}$ and a void ratio of 0.58. These tests were conducted in a standard perspex triaxial cell and were limited to 110 psi confining pressure. The frictional

characteristics for unfrozen sand at higher confining pressures were obtained from data presented by Lee and Seed (1967) and Vesic and Clough (1968).

Typical results of drained triaxial tests on unfrozen sand are shown in Figures 5-1 and 5-2. An angle of internal friction equal to 37° was obtained from the Mohr diagram shown in Figure 5-2. This value is typical for Ottawa sand with a void ratio of 0.58. Figure 5-1 shows the stress-strain and volume changes characteristic of the Ottawa sand. The curves indicate: (1) Volume change is negative (increases) for all tests with little variation between the tests at different confining pressures. At higher confining pressures the amount of volumetric strain decreases but will remain negative for pressures through 1000 psi (Lee and Seed, 1967); (2) Strain at failure ranges from four to six percent for all tests and (3) The peak strength increases as confining pressure increases. These results are in agreement with expected behavior.

5.1.2 High Ice Content

The effect of confining pressure on the strength of sand-ice materials tested at confining pressures from 0 to 1000 psi and a strain rate of $2.66 \times 10^{-3} min^{-1}$ are shown in Figure 5.3. This rate of strain is fairly fast and resulted in failure times of 10-30 minutes, depending

on the confining pressures. In this figure it is apparent that strains at failure and peak strength of the sand-ice samples increase with confining pressures. This is also typical of results for unfrozen sand at high confining pressures (Lee and Seed, 1967). However, the curves for sand-ice materials show two yield points depending on the amount of confining pressure. For confining pressures in excess of 100 psi the curves have an initial yield point followed by a fairly linear increase in strength up to a second yield point that progresses to failure. This behavior is typical of all the samples tested at higher confining pressures. There is no indication that confining pressure greatly alters the value of the Young's modulus for the initial portion of the curves and except for the sample 44, there was little variation in the value of the initial yield point.

Figure 5-3 includes a plot of strain versus time for the various tests. The fact that this curve has a slight curvature indicates that the actual strain rate varies only slightly from the nominal strain rate of $2.66 \times 10^{-3} min^{-1}$. The variation is due to the test apparatus and appears to be typical of all the tests conducted on the Wykeham-Farrance loading frame.

Volume of sand, or void ratio is an important factor in determining the strength of sand-ice materials. To obtain the effect of confining pressure on this

variable, tests were conducted at various void ratios and confining pressures. Figure 5-4 and 5-5 show that void ratio affects strength through the entire range of confining pressures tested.

The initial yield for these tests is approximately 1200 psi and appears to be independent of the volume of sand. This value is greater than the maximum shear strength of ice tested under similar conditions, indicating some reinforcing effect due to the sand. The spread of the curves above the initial yield is the result of variations in the development of the frictional component resulting from the different volumes of sand. These figures show that the ice matrix does not appear to affect the basic frictional mechanism of a sand.

An additional factor which may affect the strength of a sand-ice sample is the strain rate. It is generally considered that increasing the strain rate will increase the strength of frozen soils (Kaplar, 1970). The results of uniaxial constant strain rate tests performed at three different strain rates are shown in Figure 5-6. These tests show an increase in peak strength as strain rate increases; however, the magnitude of the increase is only 250 psi for a ten-fold increase in the strain rate. What is more interesting is the trace of the curves. For the slowest strain rate there is a low initial yield followed by a non-linear increase of stress progressing to failure.

The faster strain rates have higher values for the initial yield point, and then progress much more rapidly to failure. Since the soil structure and volume of sand for the samples are constant, this indicates that the strain rate primarily affects the ice matrix. The difference in peak strength noted is approximately equal to the difference in the initial yield values.

To investigate the effect strain rate has on confined samples, a series of tests were conducted at 700 psi confining pressure for various strain rates. The strain rates varied from $7.07 \times 10^{-5} min^{-1}$ to $5.3 \times 10^{-3} min^{-1}$ or a factor of 75 when compared to the lower rate. Figure 5-7 shows the results of this test series. As is typical for confined samples, there is an initial yield followed by a linear increase of stress leading ultimately to failure. The initial yield is shown to be dependent upon strain rate, although the peak stresses for the samples varies by only a small amount. If the samples with constant strain rates are corrected for variations in percent of sand to a constant 63 percent, the peak strengths are as follows: sample 50, 2750 psi; sample 38, 2745 psi; and sample 48, 2450 psi. The differences noted are of the same magnitude as noted for the unconfined tests and are only a small percent of the peak stress.

Of particular interest in this test series are the results for sample 19 where three values of

strain-rate were used. For each increase in strain rate there is a corresponding linear increase in the stress followed by another yield point. As the strain rates increase, Young's modulus also increases. This implies that the ice matrix is responsive to the strain rate, and any change in test conditions will interrupt the existing equilibrium relationship and cause a new relationship to form.

The results of the constant axial strain rate tests on high ice content samples are summarized in Table 5-1.

5.1.3 Reduced Ice Content

To determine the effects of ice content and confining pressure, a series of tests were conducted on samples with ice contents of approximately 55 percent. The confining pressures were the same as used for the samples with high ice contents. The results for this test series are shown in Figure 5-8. The stress-strain behavior for samples with reduced ice contents was about the same as for the high ice contents, except that the peak strength was lower for all confining pressures. These curves also show that confining pressure does not increase the Young's modulus to any great extent, but the initial yield value does increase with increasing confining pressure. For the reduced ice content sample,

the initial yield that was so prominent for the high ice content samples was almost completely obscured until a confining pressure of 700 psi was applied. This suggests that the initial yield is related to the ice matrix and as the ice content is reduced, the behavior becomes more frictional in nature.

A better indication of the effect of reduced ice content on the stress-strain characteristics is shown in Figure 5-9. In this figure the results of both high and low ice content tests for typical unconfined and confined conditions are shown. It can be seen that for reduced ice content: (1) the strains at failure are slightly less than for the high ice content and (2) the difference in peak strength between high and low ice content is greatest for the unconfined samples.

To obtain a wider range of reduced ice contents, additional tests were conducted with an ice content of approximately 35 percent. Figure 5-10 shows that results of samples with four different ice contents and 100 psi confining pressure. These curves clearly show a small increase in Young's modulus as the ice content increases. One anomaly in the results of these tests is the strain at failure. As the ice content decreases, the strains at failure decrease. However, for the sample with zero ice content the strain at peak strength was larger than for any of the other tests.

The results obtained for all samples with reduced ice content emphasize the nonfrictional behavior of the initial portion of the stress-strain curve and the dominance of the frictional components as soon as adequate yielding has taken place. The results for the reduced ice content tests are summarized in Table 5-2.

Two samples of polycrystalline ice were prepared (as suggested by Goughnour (1967)), and tested at 0 and 685 psi confining pressure to verify the fact that ice is not appreciably affected by confining pressure. The results from these tests are shown in Figure 5-11 and indicate the effect of confining pressure is not very great. The small increases in strength may be due to confining pressures tending to prevent cracking of the ice as failure is approached. However, these tests may be inconclusive since only two samples were tested.

5.2 Creep Tests

It is known that the strength of frozen materials are highly dependent upon the time of load application and their behavior can be studied using creep testing techniques. In the following section the results of creep tests on sand-ice materials will be presented.

5.2.1 High Ice Content

The creep behavior of sand-ice materials and relationships that are descriptive of their behavior

were studied using creep tests conducted in three different ways: uniaxial, confined and step-stress. Temperature was held constant at -12.0° C for all tests and selected constant deviator stresses of 400, 640, 750 and 1070 psi were used to give a wide range of creep behavior.

5.2.1.1 Uniaxial.--The main objective of the uniaxial tests on the sand-ice was to obtain the general creep behavior of the material and the magnitude of strains that result for a test time of approximately six hours. Typical results for the selected levels of stress are shown in Figure 5-12. Each of the curves show an instantaneous strain immediately after the application of the load followed by a region of decreasing strain rate. In sample 90 the region of noticeable decreasing strain rate was up to 200 minutes. Beyond this time the curves approach linearity.

The initial instantaneous deformation does not exhibit any clear trend because of slight variations in friction reducers and sample seating. To eliminate these variables, the strains for all the tests have been corrected by subtracting the strain at one minute. Figure 5-13 shows the corrected results for the four levels of axial stress. This curve gives a much clearer picture of the variations in strain between the stress levels.

5.2.1.2 Confined.--Before conducting step-stress creep tests where the confining pressure was varied at selected time intervals, it was necessary to observe the creep response of sand-ice under continuous confining pressure. The results of two tests conducted at a constant deviator stress and constant confining pressure are plotted in Figure 5-14. Shown for comparison are the results of a uniaxial test at the same stress level. If the test results are corrected as described in section 5.2.1.1, and replotted as in Figure 5-15, the effect of confining pressure is more apparent. As the confining pressures increase, the strains and strain rates decrease for any selected time. It is noted that the effect of confining pressure is greatest at low values since the original 200 psi increase in confining pressure had more than twice the effect of the 390 psi increment between the 210 psi and 600 psi level.

5.2.1.3 Step-Stress.--The effect of confining pressure on creep rate is shown by step-stress creep tests conducted at 400, 640 and 750 psi levels of constant deviator stress. Test results are shown in Figure 5-16 for confining pressures added at one hour intervals in the sequence 100, 200, 400, 600, 800 and 1000 psi. As each increment of confining pressure was applied, a rapid increase in strain took place due primarily to expansion

of the triaxial cell. Following this increase in strain due to cell expansion there was a region of fairly rapid increase in strain with time which quickly decreased, resulting in a strain rate less than the minimum for the preceding increment.

One additional test conducted to observe the step-stress characteristics at a constant deviator stress of 1070 psi is shown in Figure 5-17. A uniaxial creep test at the same level of stress has been shown for comparison. The increase in strain due to cell expansion followed by the region of decreasing strain with time, demonstrates that there was no basic difference between the step-stress test shown here and those discussed above. The region of decreasing strain and dampening effect of the confining pressure are more noticeable here than for the samples tested at lower levels of deviator stress.

Table 5.3 contains a summary of the experimental results for the creep tests on high ice content samples.

5.2.2 Reduced Ice Content

The creep behavior of frozen sand at reduced ice contents was studied by using constant deviator stresses of 400, 640 and 750 psi. These constant stresses were the same as for the high ice content samples. Sand volume and temperature (-12.0° C) were held as constant as possible. It was expected that reduced ice contents

would increase the frictional characteristics of creep and lead to a better identification of the processes involved in sand-ice materials.

5.2.2.1 Uniaxial.--The results of uniaxial creep tests on reduced ice samples are shown in Figure 5-18. The curves illustrate the changes in creep behavior as axial stress increases. The curves all have the characteristic chape of "classical" creep curves, and one has progressed into the tertiary region and is in the process of failing. When compared to the high ice content samples with equal axial stresses, shown in Figure 5-12, the reduced ice content greatly accelerates the strain rates for any given axial stress.

The change in creep behavior for reduced ice content is shown by samples with three ice contents and a constant axial stress of 750 psi in Figure 5-19. As the ice content decreases, the strains at a constant time increase substantially, indicating a close relationship between the ice matrix and the creep behavior.

5.2.2.2 Confined.--The results of a uniaxial creep test and a constant deviator stress creep test with continuous confining pressure on reduced ice content samples are plotted in Figure 5-20. When compared to the uniaxial test, the effect of the confining pressure is to dampen the response of the sample to the applied

stress. The same effect was noted for the high ice content samples, but the magnitude of the change of strain rates was not nearly as great.

5.2.2.3 Step-Stress.--Step-stress tests for the reduced ice content samples illustrated in Figure 5-21 include two levels of constant deviator stress. The sample tested at 640 psi developed a leak after the third increment of confining pressure was applied and the test was terminated after 180 minutes. The effect of confining pressure and development of the strain versus time curves are similar to the high ice content samples presented in section 5.2.1.3.

Uniaxial tests showed that a reduced ice content sample tested at an axial stress of 750 psi would progress to failure within one hour. Therefore, the time increments for applying confining pressure in the step-stress tests were decreased. The results of a step-stress test at a constant deviator stress of 750 psi is shown in Figure 5-22. For this test the confining pressure decreased strain rates significantly. Even at 90 minutes, the test did not progress into the tertiary region and strain rates were still decreasing. This test indicated that creep of a sand-ice material will be greatly decreased or prevented as confining pressures are increased.

TABLE 5-1.--Experimental results for constant axial strain rate tests, high ice content.

Sample No.	Percent Sand	Strain Rate	Strain at Failure	Peak Strength	Confining Pressure	Percent Ice	Total Volume Change	Remarks
	%	min^{-1}	in/in	psi	psi	%	cm^3	
1	61.6	$2.66x10^{-3}$	.018	1365	0	99.8	NA	
2	62.1	"	.020	1460	0	92.8	NA	
4	63.5	"	.023	1364	0	97.4	NA	
5	62.5	"	.039	1486	0	94.5	NA	
7	62.9	"	.018	1331	0	94.5	NA	
8	62.9	$1.33x10^{-3}$	.051	1473	0	96.0	NA	
10	63.0	$2.66x10^{-3}$	.052	1906	355	95.0	NA	
11	62.9	"	.059	1649	100	95.0	NA	
13	62.8	"	.050	1546	350	97.5	NA	
14	62.3	"	.082	2502	700	95.0	NA	
18	62.5	$266x10^{-2}$	.016	2093	700	97.0	+0.193	
19	62.4	varies	.072	2764	700	97.5	+0.332	
21	63.0	$2.66x10^{-3}$	.072	1840	350	97.0	+0.662	
22	62.8	"	.055	1783	350	96.0	NA	
24	63.0est	"	.064	2136	350	96.0est	NA	Recorder mistake
26	62.0	"	.027	1436	0	97.5	+0.656	Possible leak
27	63.5	"	.049	1974	350	96.5	+0.403	
28	62.7	"	.075	2668	700	96.5	+0.484	
33	62.4	"	.057	1516	0	NA	NA	
34	62.9	"	.043	1642	0	NA	+0.282	
35	62.6est	"	.074	2619	700	NA	NA	
36	63.0est	"	.083	2744	700	NA	NA	
38	63.0	"	.069	2734	700	97.0	+0.559	
39	63.2	"	.052	2243	360	97.0	+0.696	
40	63.0	"	.036	1720	100	NA	NA	
41	62.9	"	.036	1701	100	96.0	+0.246	

42	62.8	2.66×10^{-3}	.028	1439	0	96.0	+0.240
43	63.6	"	.027	1610	0	96.5	+0.426
44	63.5	"	.055	2878	700	96.0	+0.450
47	63.5	5.33×10^{-3}	.059	2851	700	96.5	+0.100
48	63.7	2.66×10^{-4}	.068	2849	700	96.0	+0.493
50	63.2	5.33×10^{-3}	.067	2918	690	96.0	+0.745
51	62.8est	2.66×10^{-3}	.043	2473	660	NA	NA
52	63.2	"	.063	2649	640	96.5	+0.601
77	62.3	"	.067	2833	1000	95.0	+0.890
80	63.4	"	.020	1810	200	95.5	+1.184
81	62.6	"	.070	2901	1000	96.0	1.178
82	62.8	"	.032	1956	200	97.0	NA
83	63.5	"	.019	1562	0	96.0	NA
84	63.7	"	.016	1648	100	95.5	NA
88	64.3	"	.014	1612	100	98.0	NA
89	63.0	2.66×10^{-3}	.016	1505	100	97.0	NA

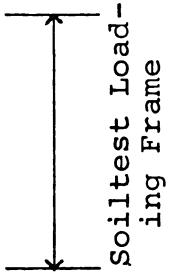

Ice Samples

20	0	2.66×10^{-3}	,030	735	685	98.0	-0.403
45	0	"	.022	668	0	98.0	+0.294

All tests:

-12.0° C
Wykcham-Farrance Loading Frame unless noted

NA = Not Available

TABLE 5-2.--Experimental results for constant axial strain rate tests, reduced ice content.

Sample	Percent Sand	Strain Rate	Strain at Failure	Peak Strength	Confining Pressure	Percent Ice	Remarks
	%	min^{-1}	in/in	psi	psi	%	
72	62.7	$4.42x10^{-3}$	.023	885	0	57.0	
73	63.0	$2.66x10^{-3}$	.040	1636	350	53.6	
74	62.5	"	.057	2584	1000	55.8	
76	63.4	"	.052	2325	700	58.2	
78	62.9	"	.026	1029	100	55.0	
79	63.7	"	.022	834	0	59.4	
87	63.2	$2.66x10^{-3}$	.022	817	100	32.9	

All tests:

-12.0° C

Soiltest Loading Frame

TABLE 5-3.--Experimental results for creep tests, high ice content.

Sample No.	Applied Deviator Stress	Maximum Deviator Stress Fig. 6-3	Percent of Maximum Deviator Stress	Confining Pressure	Total Volume Change	Total Test Time	Minimum Strain Rate	Percent Ice	Percent Sand
	psi	psi	%	psi	cm^3	min	min^{-1}	%	%
90	1070	1520	70.5	0	+0.228	320	3.0×10^{-5}	94.7	63.3
96	400	1540	26.0	0	-0.078	320	4.5×10^{-6}	95.2	63.8
99	640	1550	41.0	0	-0.078	240	1.0×10^{-5}	95.1	63.9
101	640	1500	42.5	0	-0.012	350	0.9×10^{-5}	95.7	62.9
102	1070	1520	70.5	0	+0.144	290	2.5×10^{-5}	95.8	63.3
108	750	1540	49.0	0	-0.054	290	1.0×10^{-5}	95.2	63.7
115	750	1994	38.0	205	-0.012	300	1.2×10^{-5}	95.9	63.2
118	750	2465	30.5	600	-0.216	270	1.2×10^{-5}	94.7	62.7

91	1070	1540	69.5	0	+0.108	180	4.3×10^{-5}	95.1	63.6
			45.5	350		370	1.8×10^{-5}		
100	640	1540	41.5	0	-0.078	60	4.0×10^{-5}	95.5	63.8
		1770	36.0	100		120	2.5×10^{-5}		
		2030	31.5	200		180	1.9×10^{-5}		
		2500	25.5	400		240	1.3×10^{-5}		
		2840	22.5	600		300	1.2×10^{-5}		
		3120	20.5	800		360	1.1×10^{-5}		
		3350	19.0	1000		400	0.9×10^{-5}		
109	400	1510	26.5	0	-0.072	60	1.5×10^{-5}	95.5	63.1
		1720	23.0	100		120	1.2×10^{-5}		
		1900	21.0	200		180	1.0×10^{-5}		
		2270	17.5	400		240	7.8×10^{-6}		
		2600	15.5	600		300	8.0×10^{-6}		
		2880	14.0	800		360	8.0×10^{-5}		
		3100	13.0	1000		400	1.0×10^{-5}		
121	750	1470	51.0	0	-0.048	60	4.4×10^{-5}	95.5	62.3
		1660	45.0	100		120	2.7×10^{-5}		
		1760	42.5	200		180	1.8×10^{-5}		
		1990	37.5	400		240	1.5×10^{-5}		
		2340	32.0	600		300	1.2×10^{-5}		
		2600	29.0	800		360	1.1×10^{-5}		

All tests: -12.0° C

TABLE 5-4.--Experimental results for creep tests, reduced ice content.

Sample No.	Applied Deviator Stress	Maximum Deviator Stress Fig. 6-3 x % Ice	Percent of Maximum Deviator Stress	Confining Pressure	Total Test Time	Minimum Strain Rate	Percent Ice	Percent Sand	Remarks
	psi	psi	%	psi	min	min^{-1}	%	%	
93	400	937	42.5	0	350	9.0×10^{-6}	60.8	63.8	
97	640	895	71.5	0	365	3.7×10^{-5}	58.8	63.3	
107	750	895	83.5	0	46	5.0×10^{-4}	59.6	63.5	
111	750	1060	70.5	0	510	1.1×10^{-5}	69.5	63.4	
114	750	1100	68.5	0	240	4.1×10^{-5}	70.7	64.2	
119	640	1210	52.4	205	150	NA	62.5	63.6	Leak@30 min
120	640	1860	34.5	600	260	0.9×10^{-5}	64.6	63.9	
94	400	915	43.5	0	60	4.5×10^{-5}	59.4	63.8	
		1050	38.0	100	120	2.5×10^{-5}			

		1210	33.0	200	180	1.8×10^{-5}			
		1480	27.0	400	240	1.5×10^{-5}			
		1690	23.7	600	300	1.3×10^{-5}			
		1860	21.5	800	360	1.2×10^{-5}			
		1990	20.0	1000	400	0.9×10^{-5}			
98	640	920	70.0	0	60	9.0×10^{-5}	60.0est	63.6	Leak@180 min
		1060	60.5	100	120	5.4×10^{-5}			
		1200	53.5	200	180	2.7×10^{-5}			
104	750	930	81.0	0	5	1.1×10^{-3}	60.0est	64.0	Leak@ 28 min
		1240	60.5	200	13	3.0×10^{-4}			
		1540	49.0	400	28	3.0×10^{-4}			
112	640	930	69.0	0	60	8.0×10^{-5}	60.0est	64.0	Leak@180 min
		1070	60.0	100	120	4.0×10^{-5}			
		1240	51.5	200	180	1.8×10^{-5}			
113	400	905	44.5	0	60	6.5×10^{-5}	60.0est	63.1	Leak@120 min
		1030	39.0	100	120	2.5×10^{-5}			
117	750	925	81.0	0	9	6.4×10^{-4}	60.5	63.6	
		1070	70.0	100	15	3.2×10^{-4}			
		1210	62.0	200	26	1.4×10^{-4}			
		1470	51.0	400	40	9.0×10^{-5}			
		1670	45.0	600	60	5.0×10^{-5}			
		1850	40.5	800	95	2.0×10^{-5}			

All tests: -12.0° C

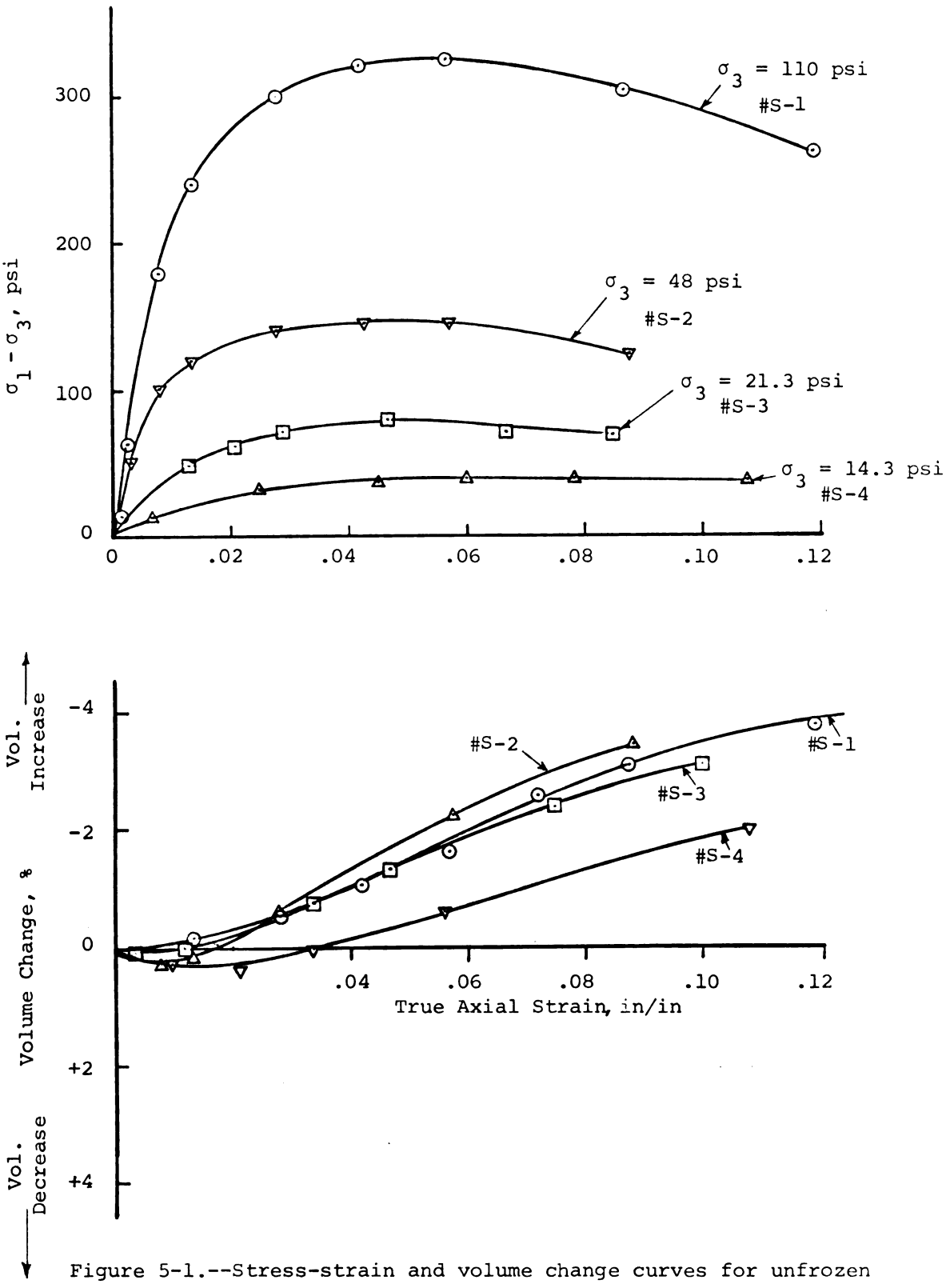

Figure 5-1.--Stress-strain and volume change curves for unfrozen Ottawa sand.

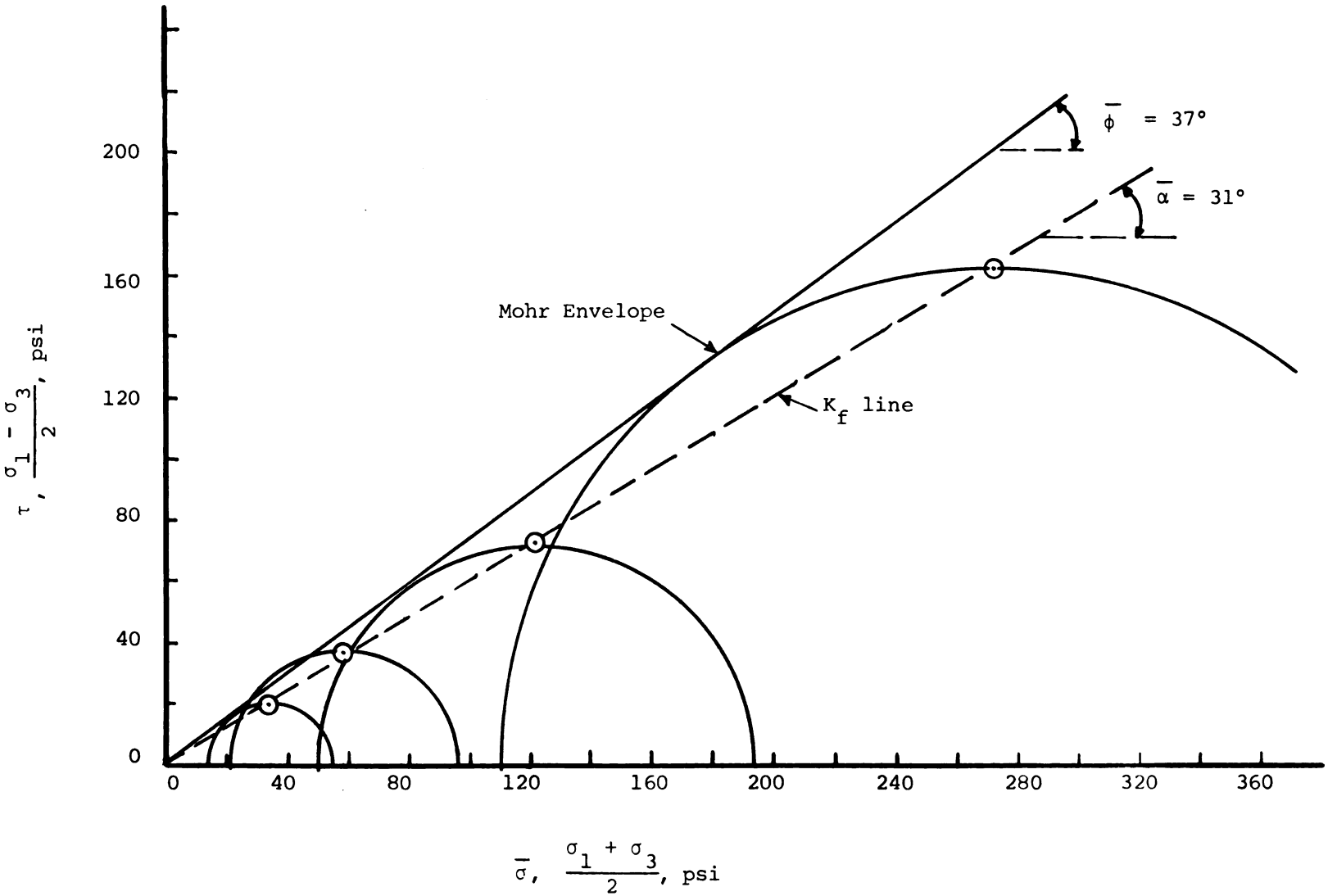

Figure 5-2.--Drained test results on unfrozen Ottawa sand.

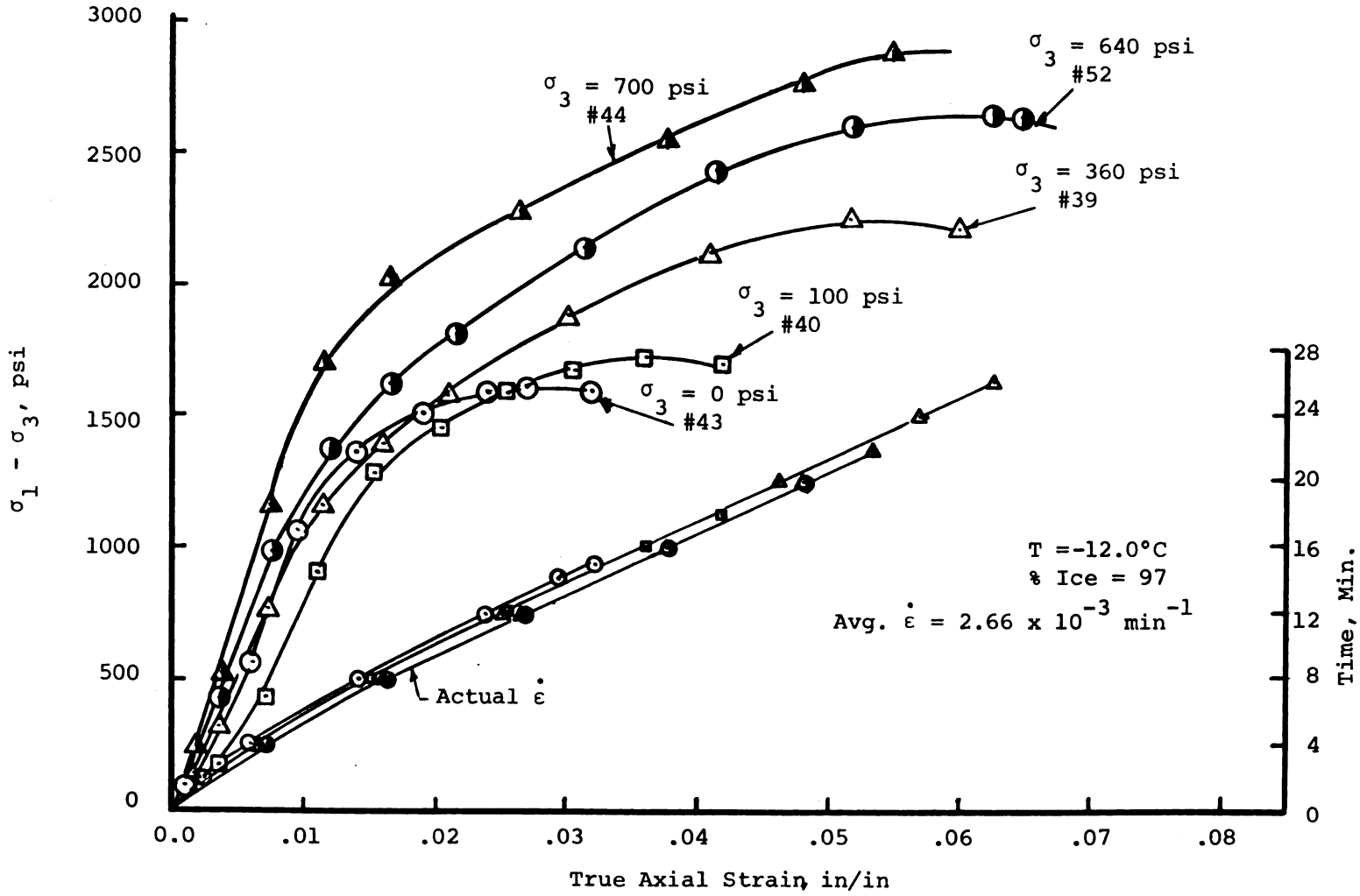

Figure 5-3.--Effect of confining pressure on the stress-strain behavior of sand ice materials.

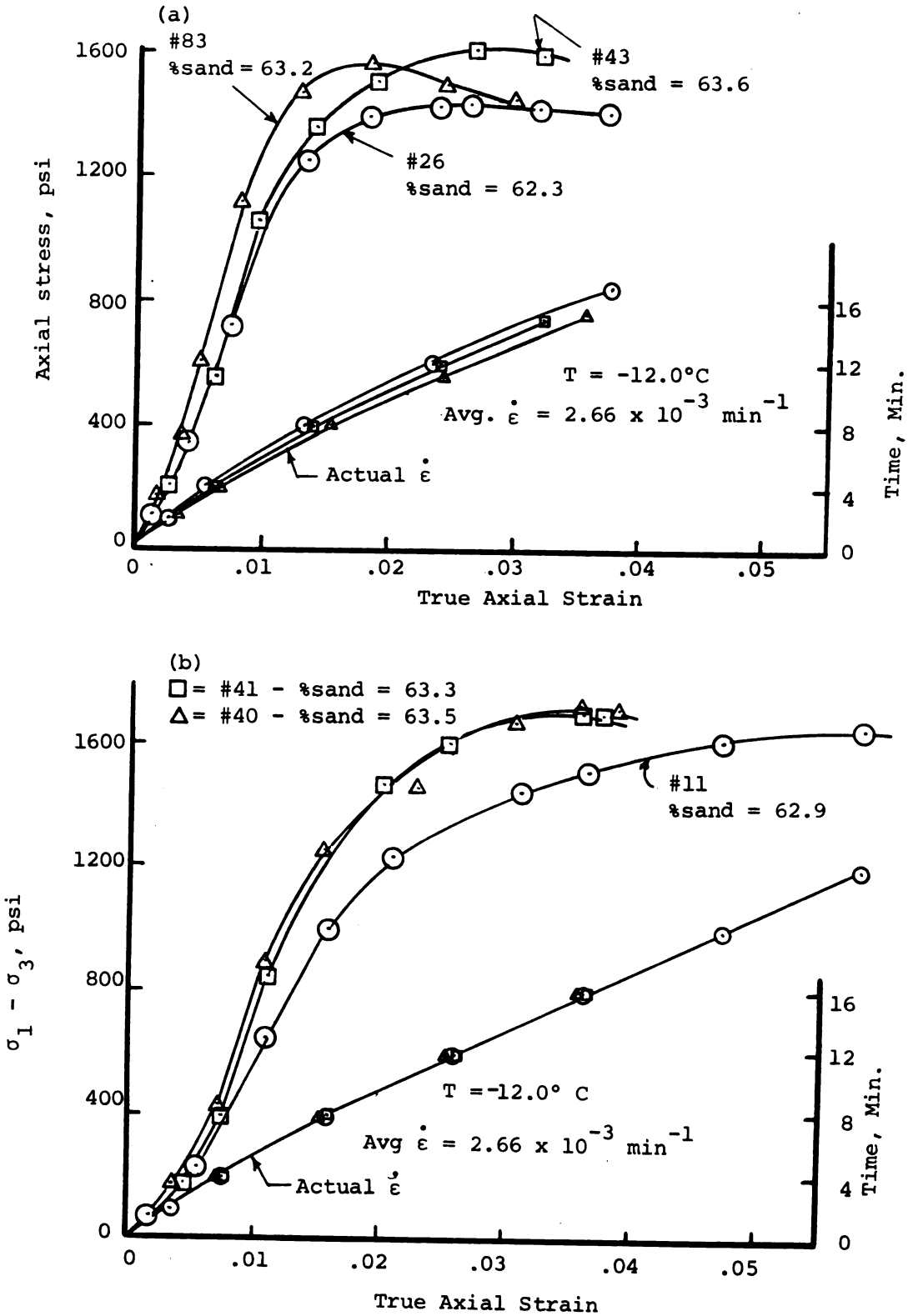

Figure 5-4.--Effect of volume of sand on strength.
(a) Unconfined
(b) Confining pressure 100 psi.

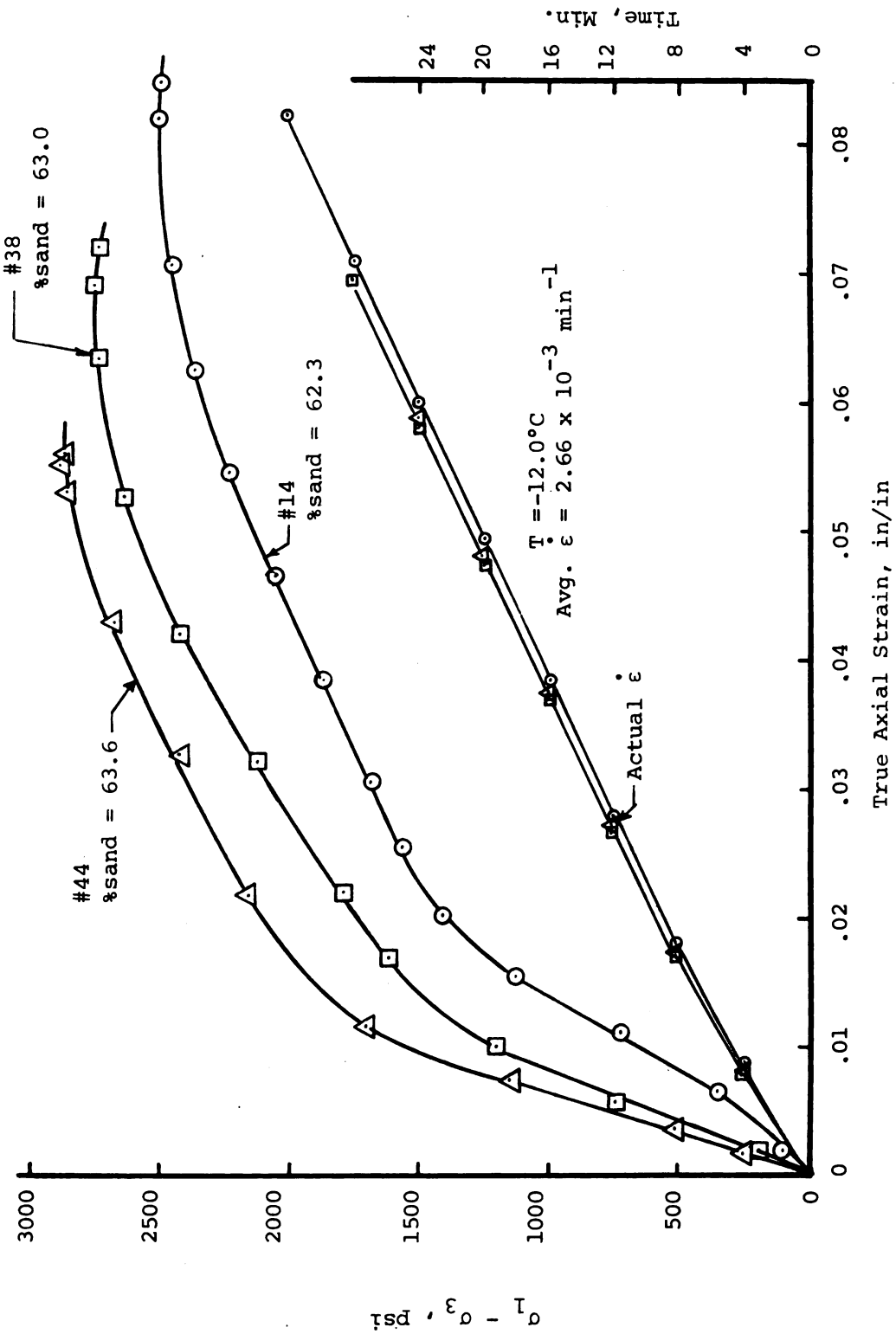

Figure 5-5.--Effect of volume of sand on strength for a confining pressure of 700 psi.

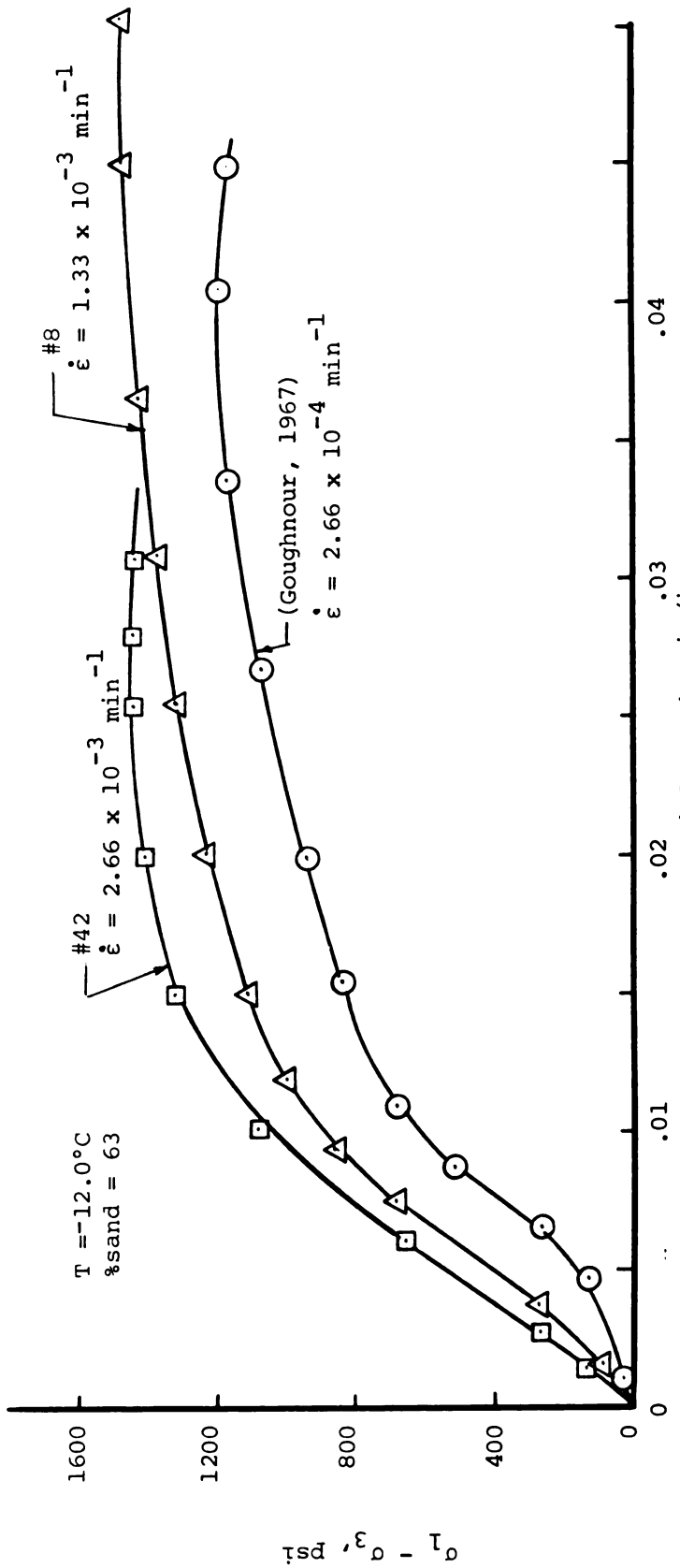

Figure 5-6.--Effect of strain rate on strength for unconfined tests.

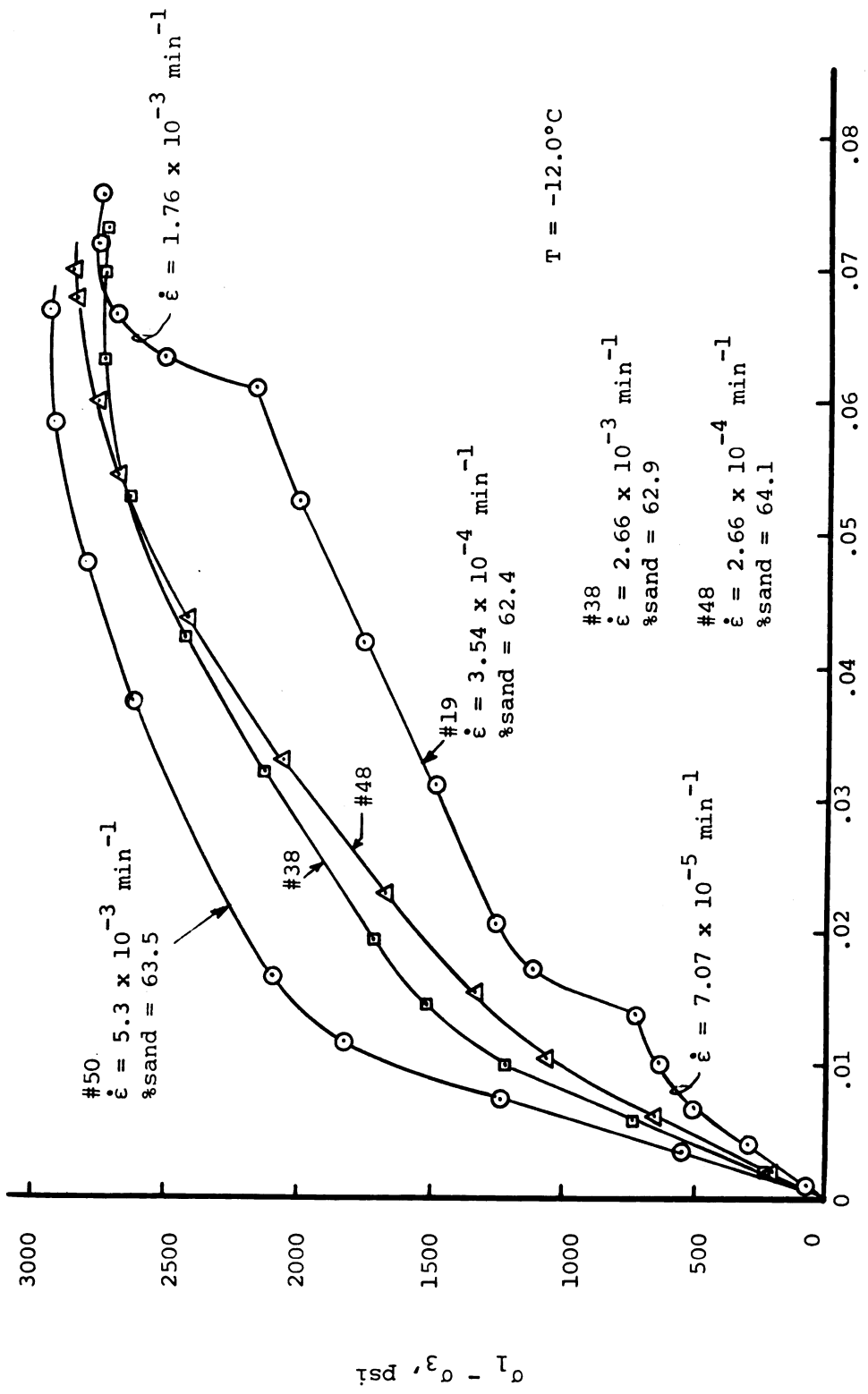

Figure 5-7.--Effect of strain rate on strength for confining pressure equal to 700 psi.

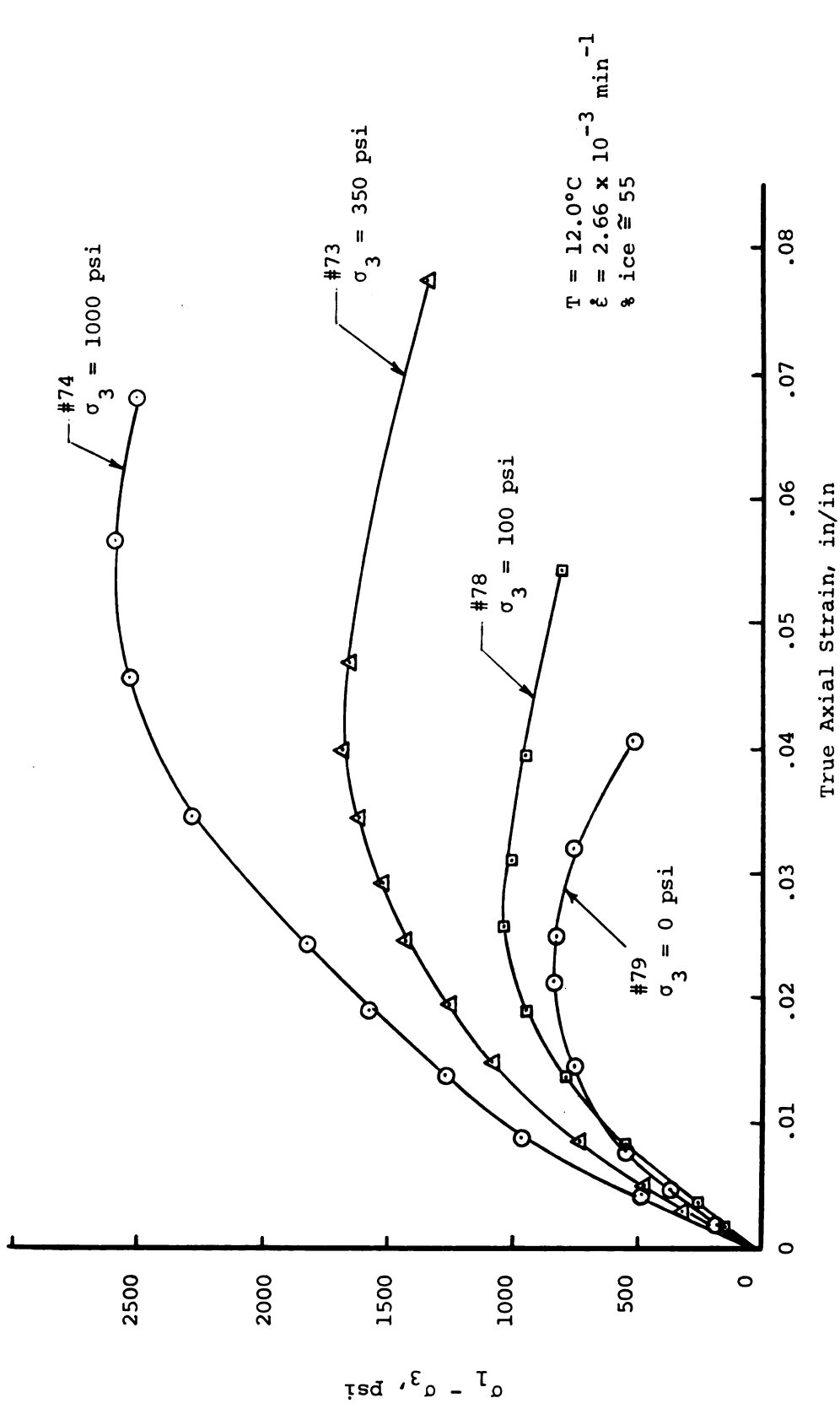

Figure 5-8.--Effect of confining pressure on strength for reduced ice contents.

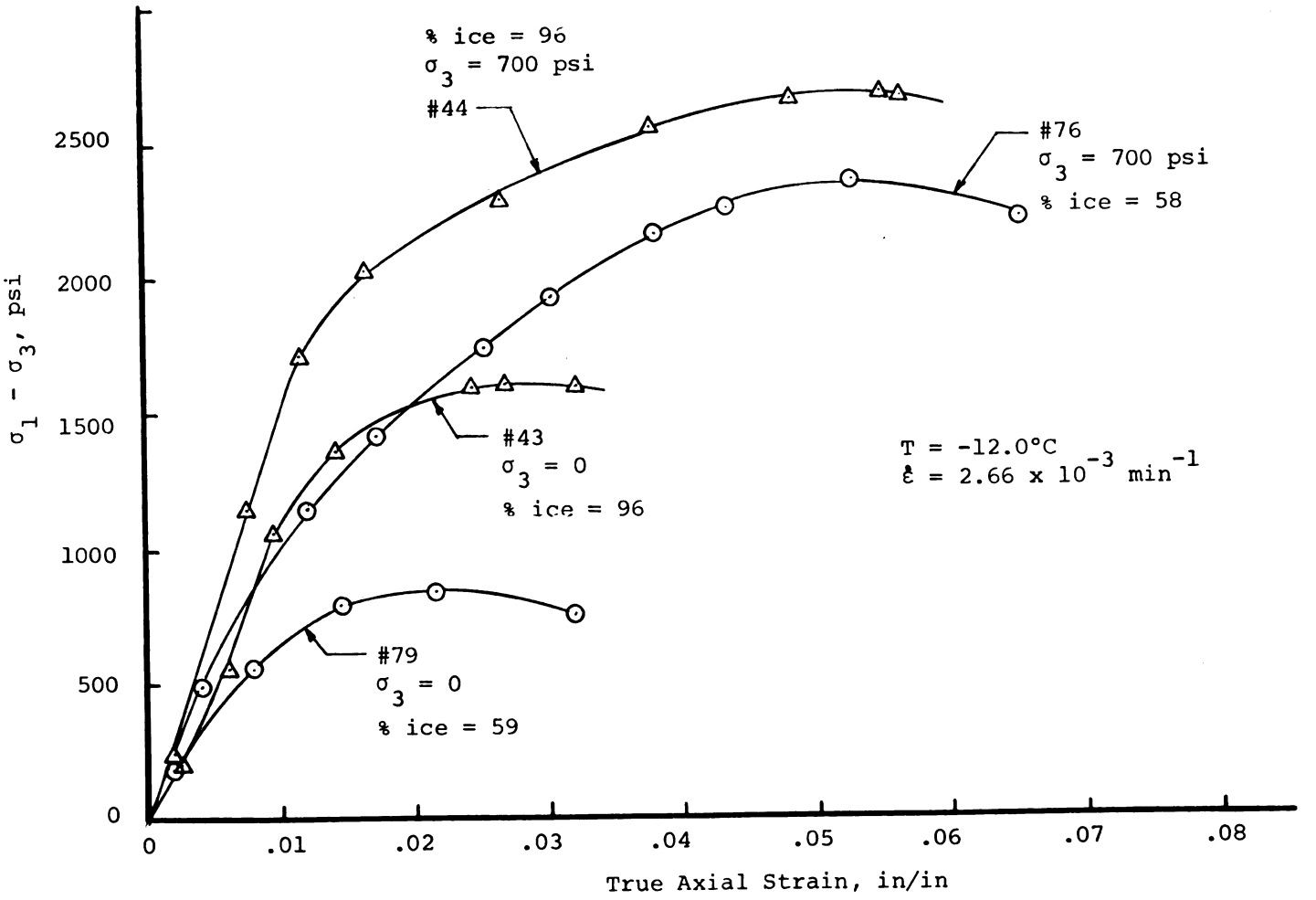

Figure 5-9.--Stress-strain curves for high and reduced ice contents.

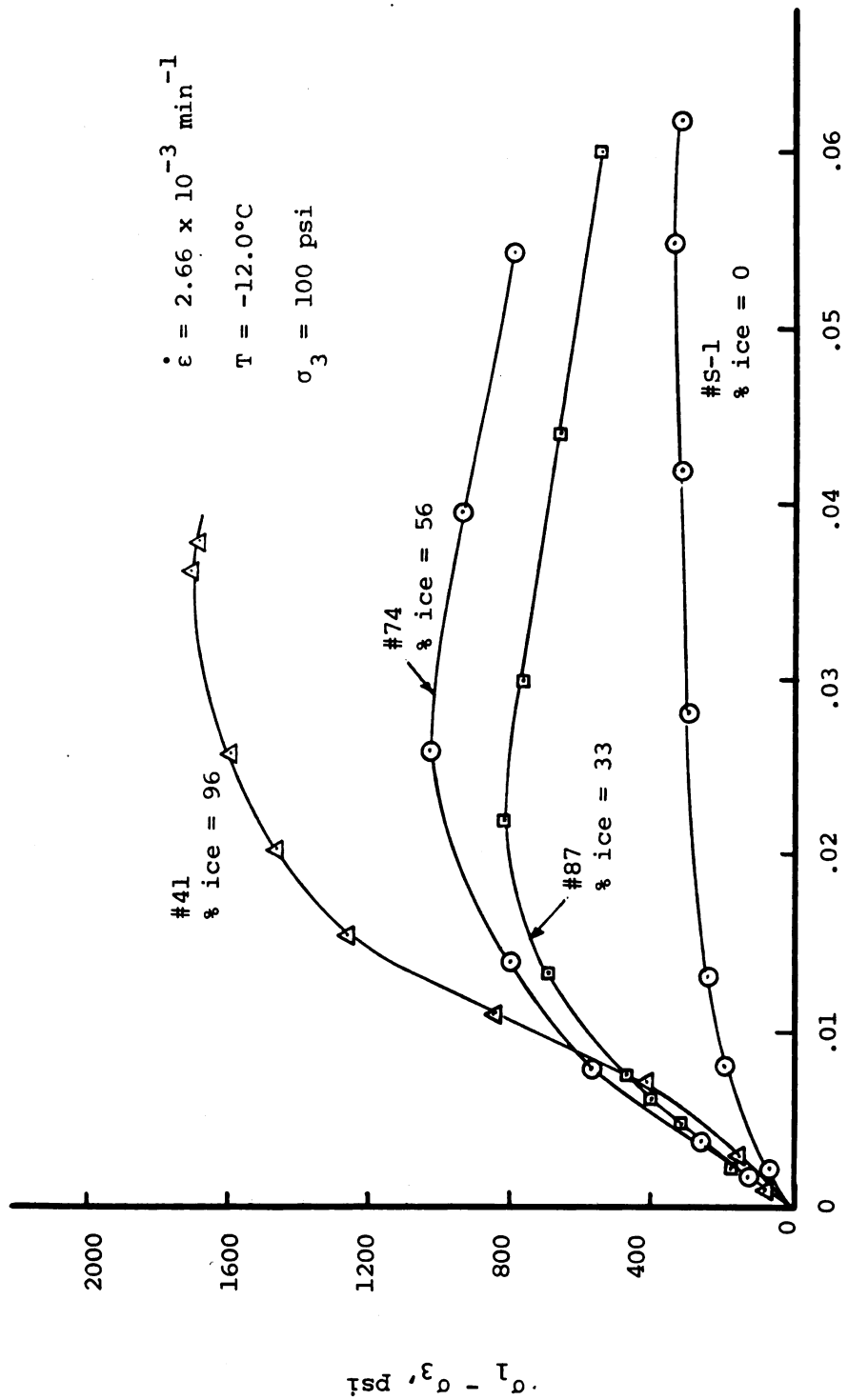

Figure 5-10.--Stress-strain curves for various ice contents.

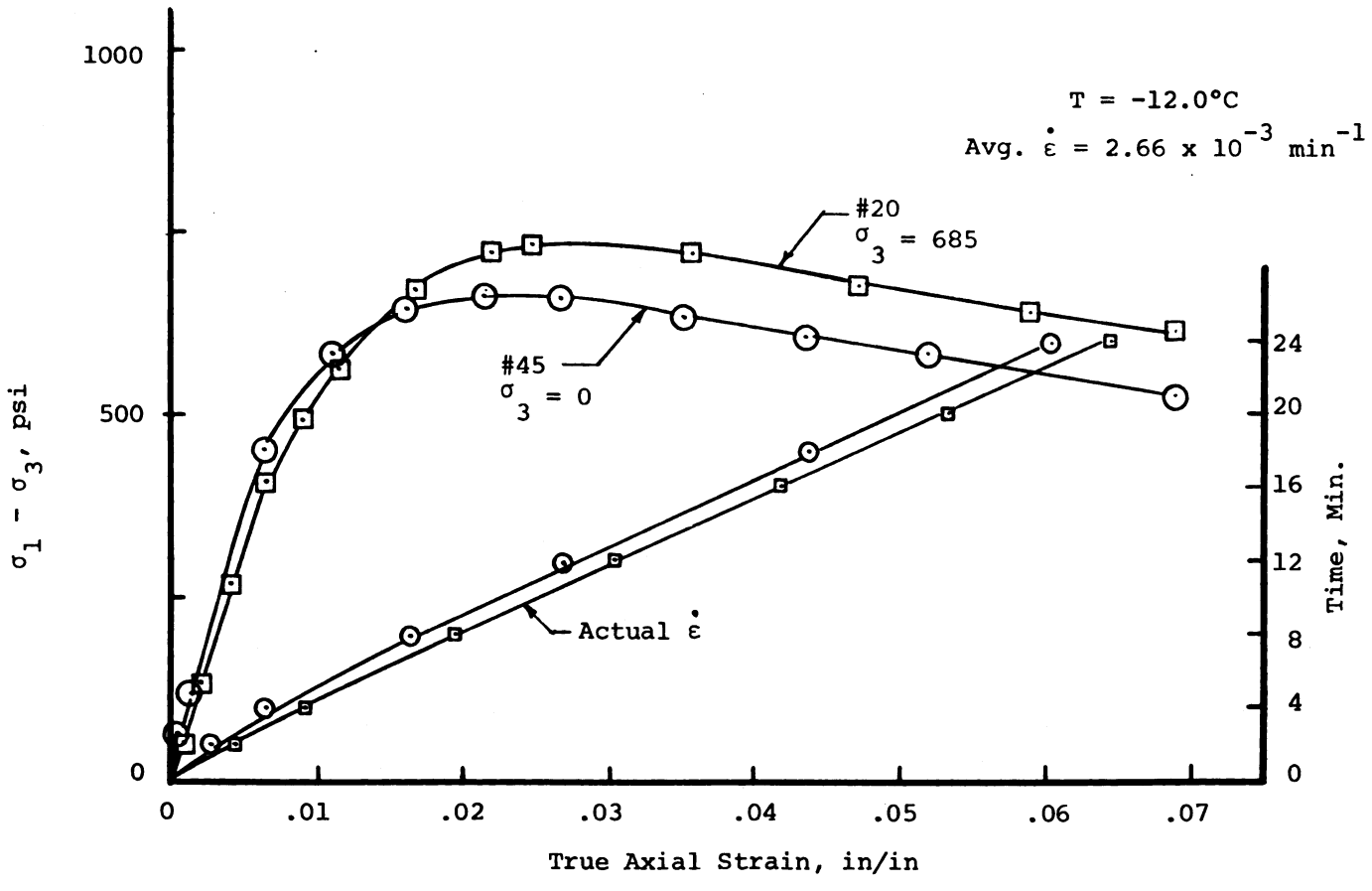

Figure 5-11.--Stress-strain curves for polycrystalline ice samples.

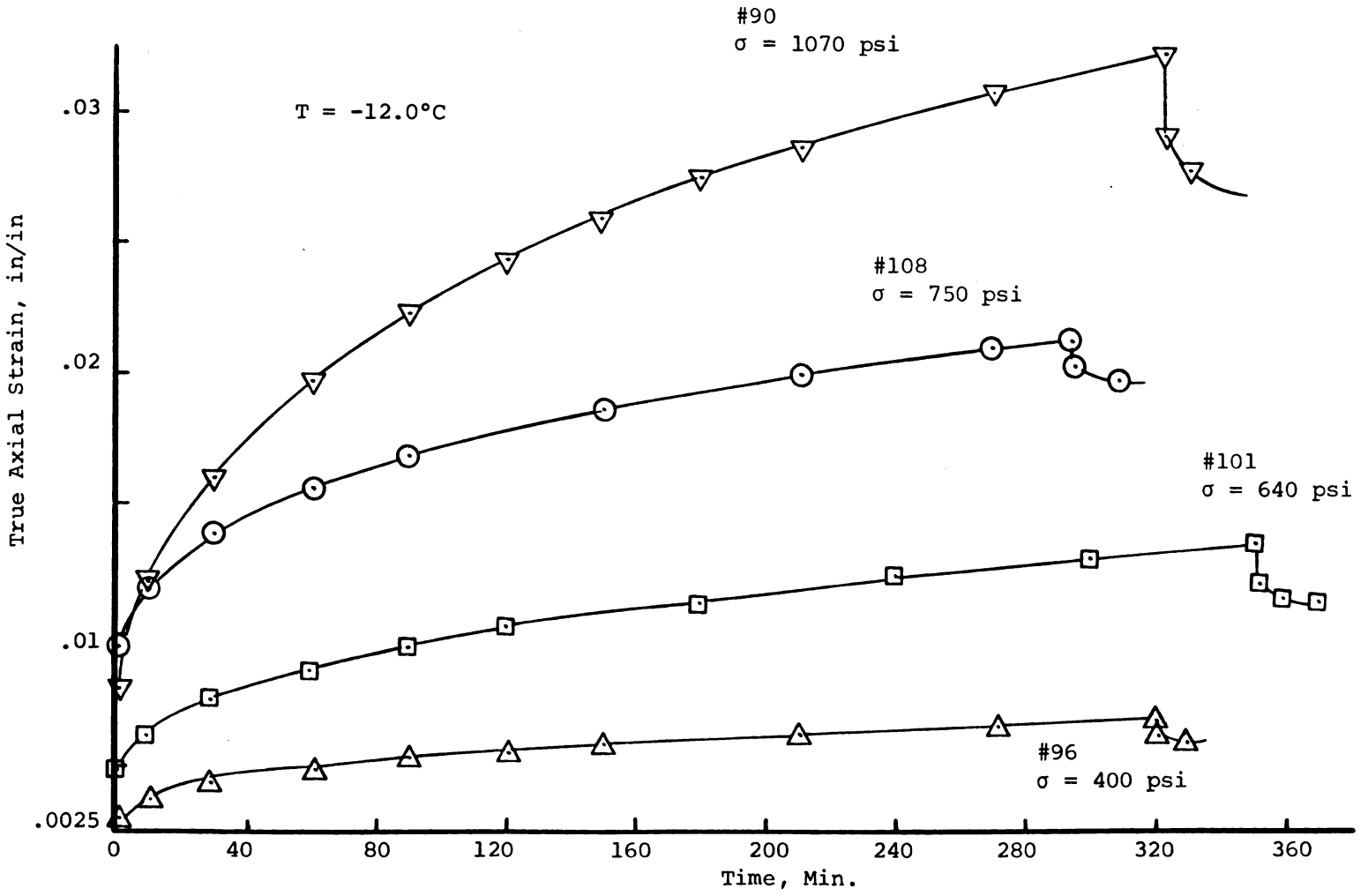

Figure 5-12.--Uniaxial stress creep curves for high ice contents.

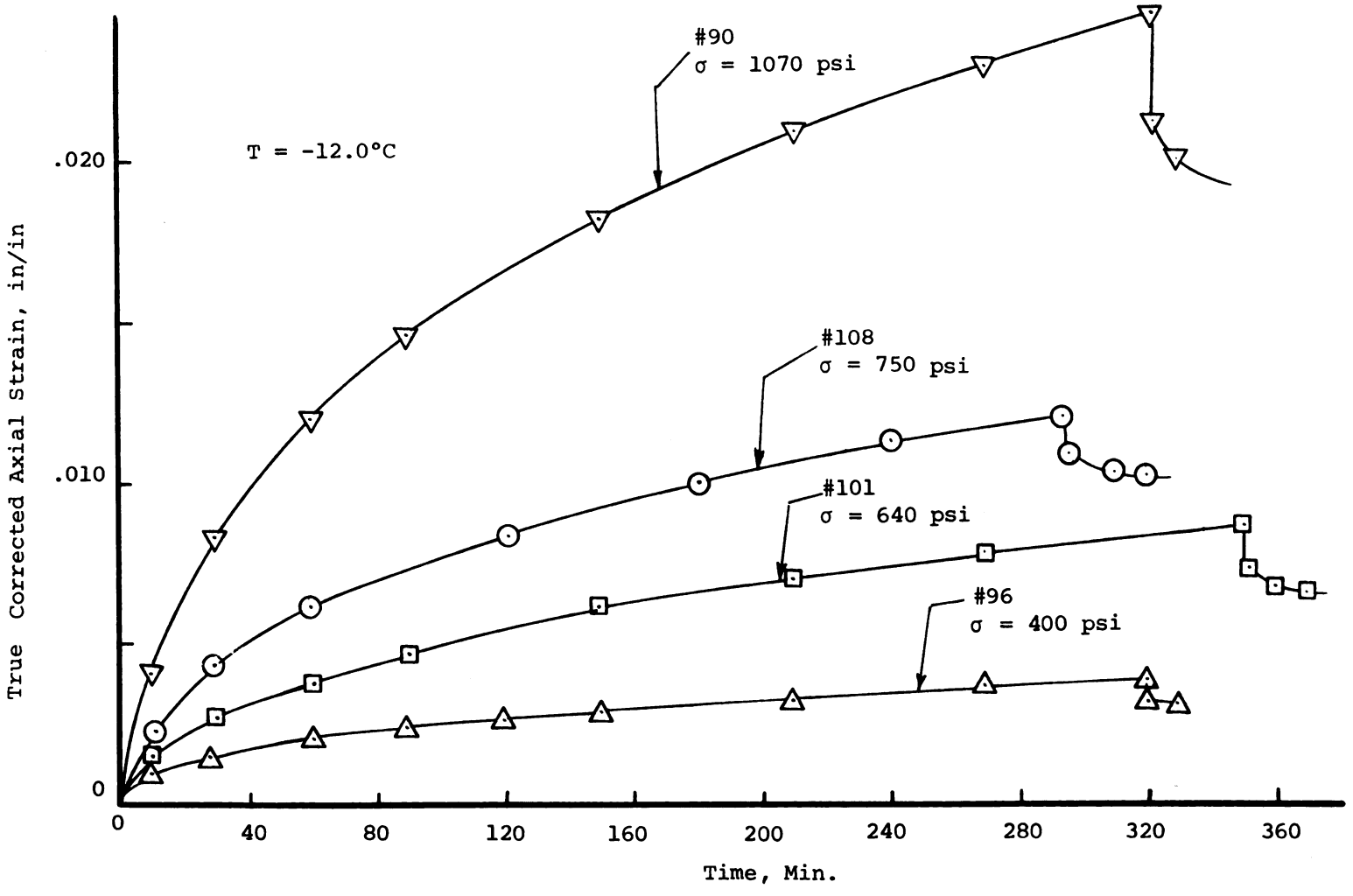

Figure 5-13.--Corrected uniaxial stress creep curves for high ice contents.

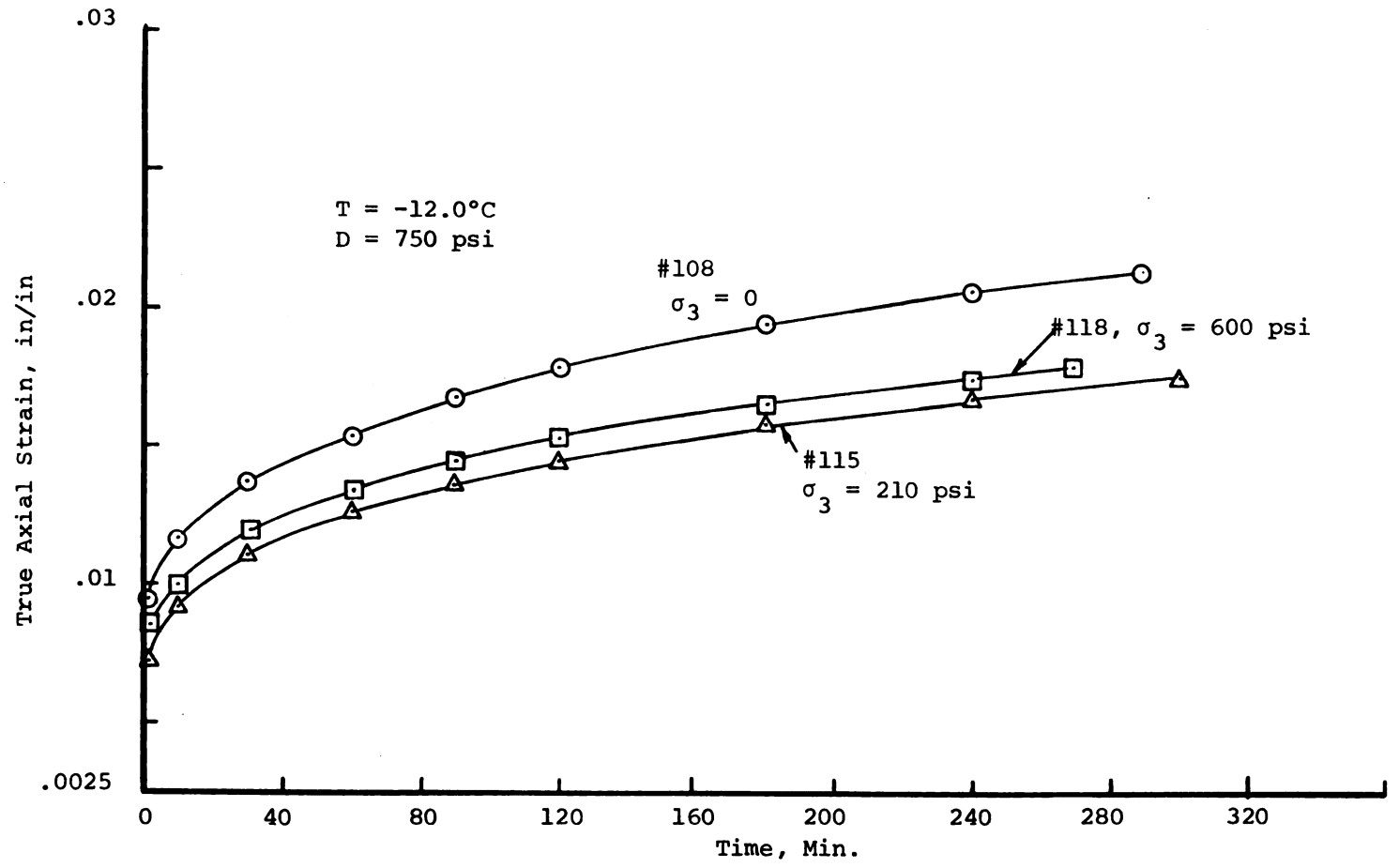

Figure 5-14.--Constant axial load creep with constant confining pressure.

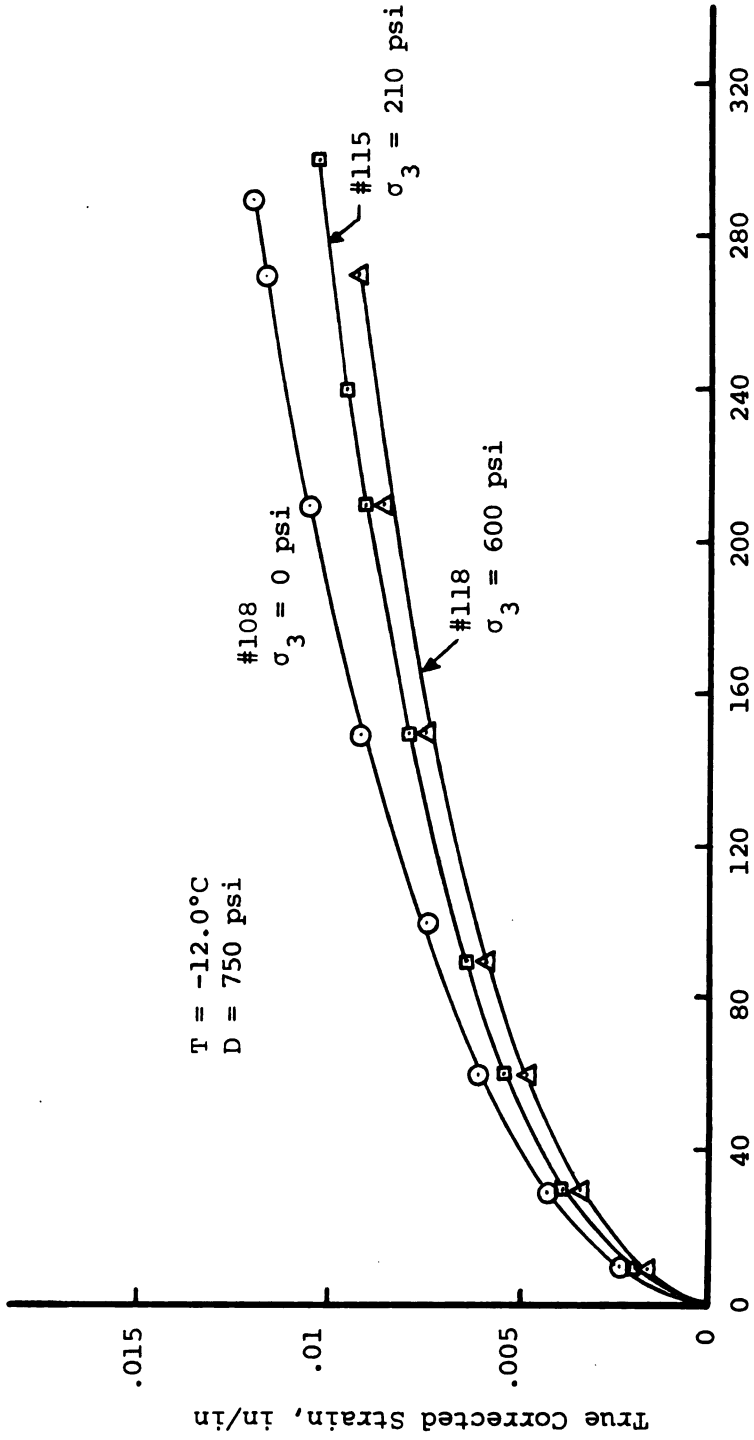

Figure 5-15.--Corrected constant axial load creep with constant confining pressure.

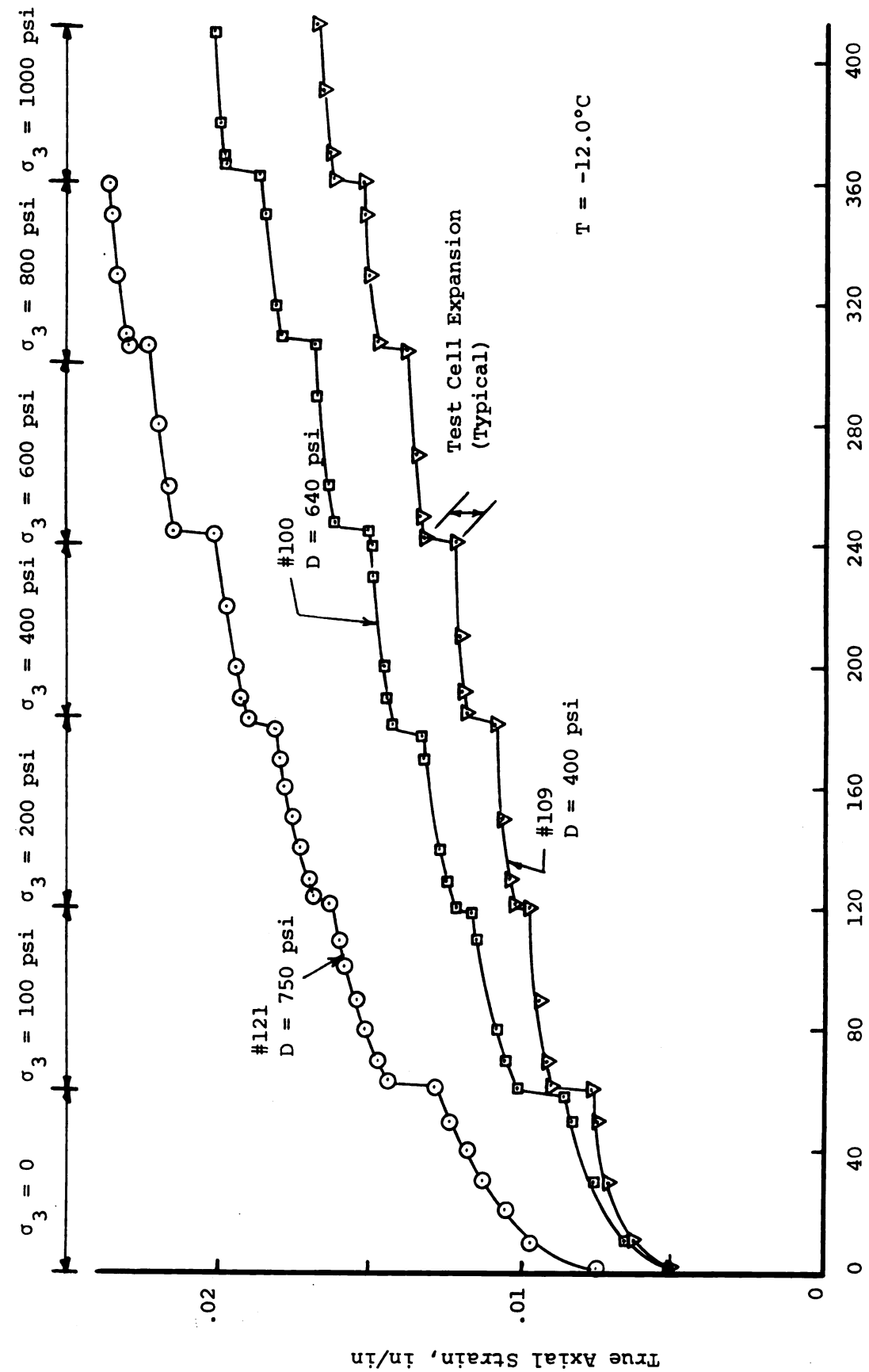

Figure 5-16.--Step-stress creep for high ice content.

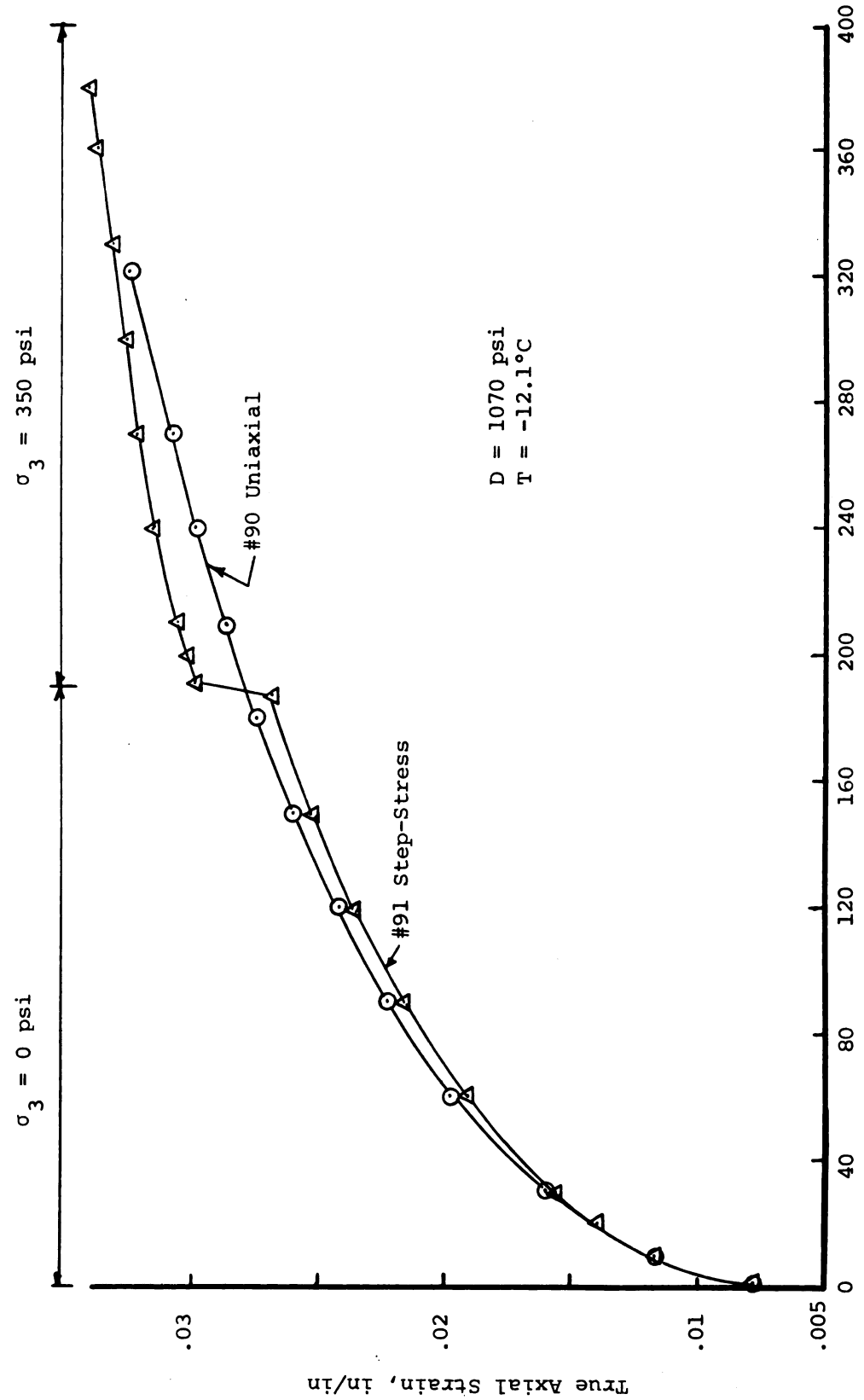

Figure 5-17.--Uniaxial and step stress creep for high ice content.

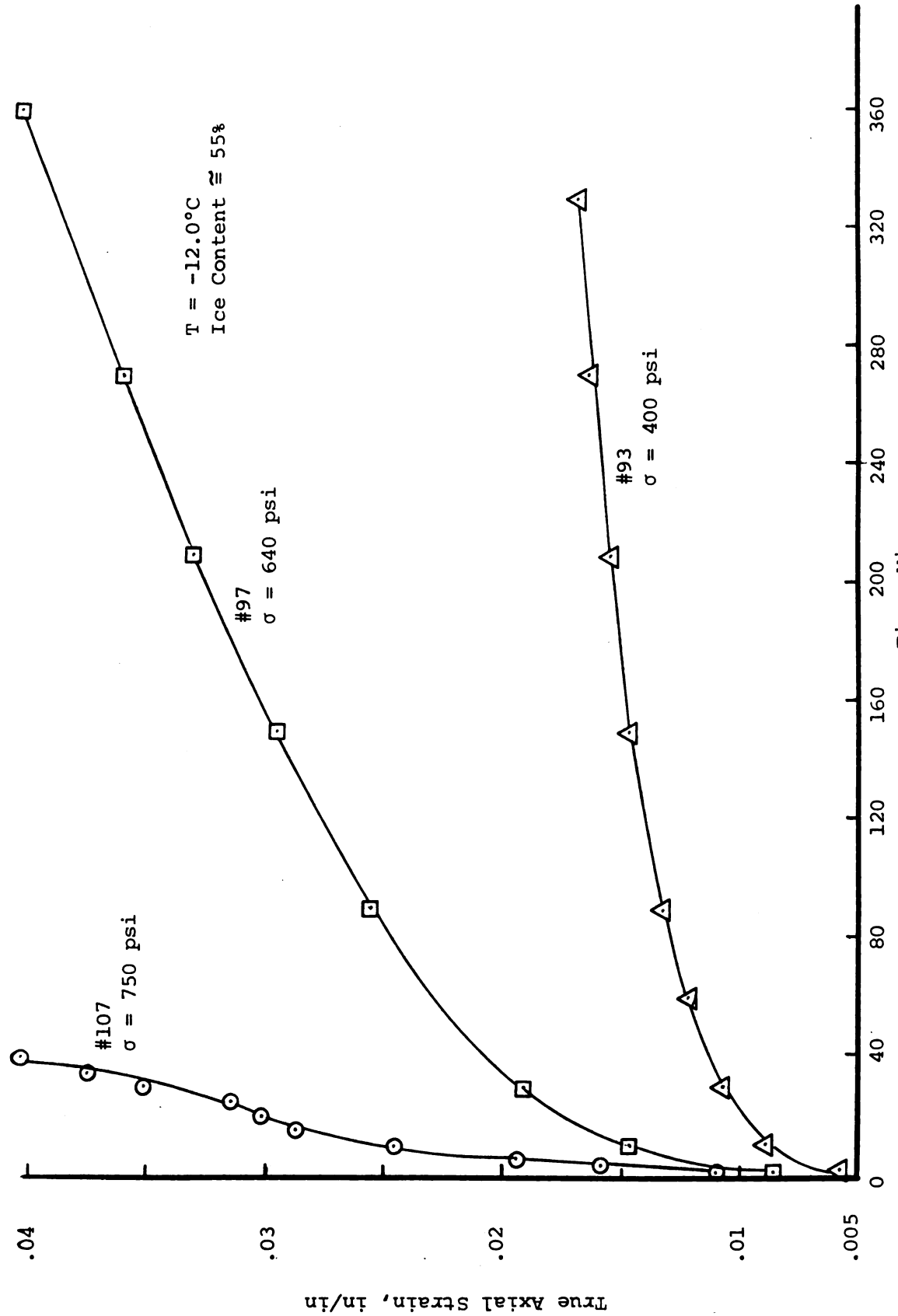

Figure 5-18.--Uniaxial stress creep for reduced ice content.

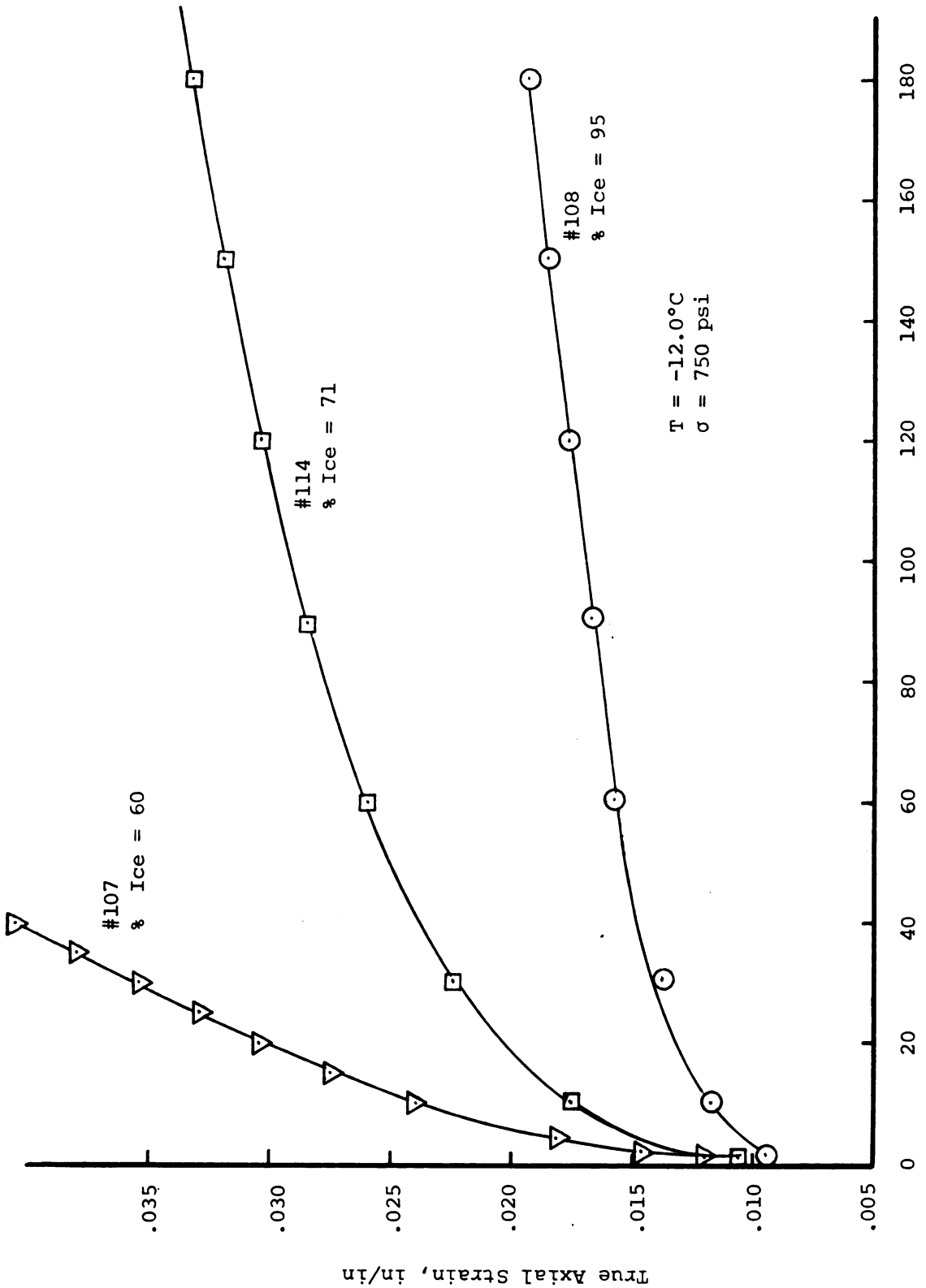

Figure 5-19.--Effect of ice content on uniaxial stress creep.

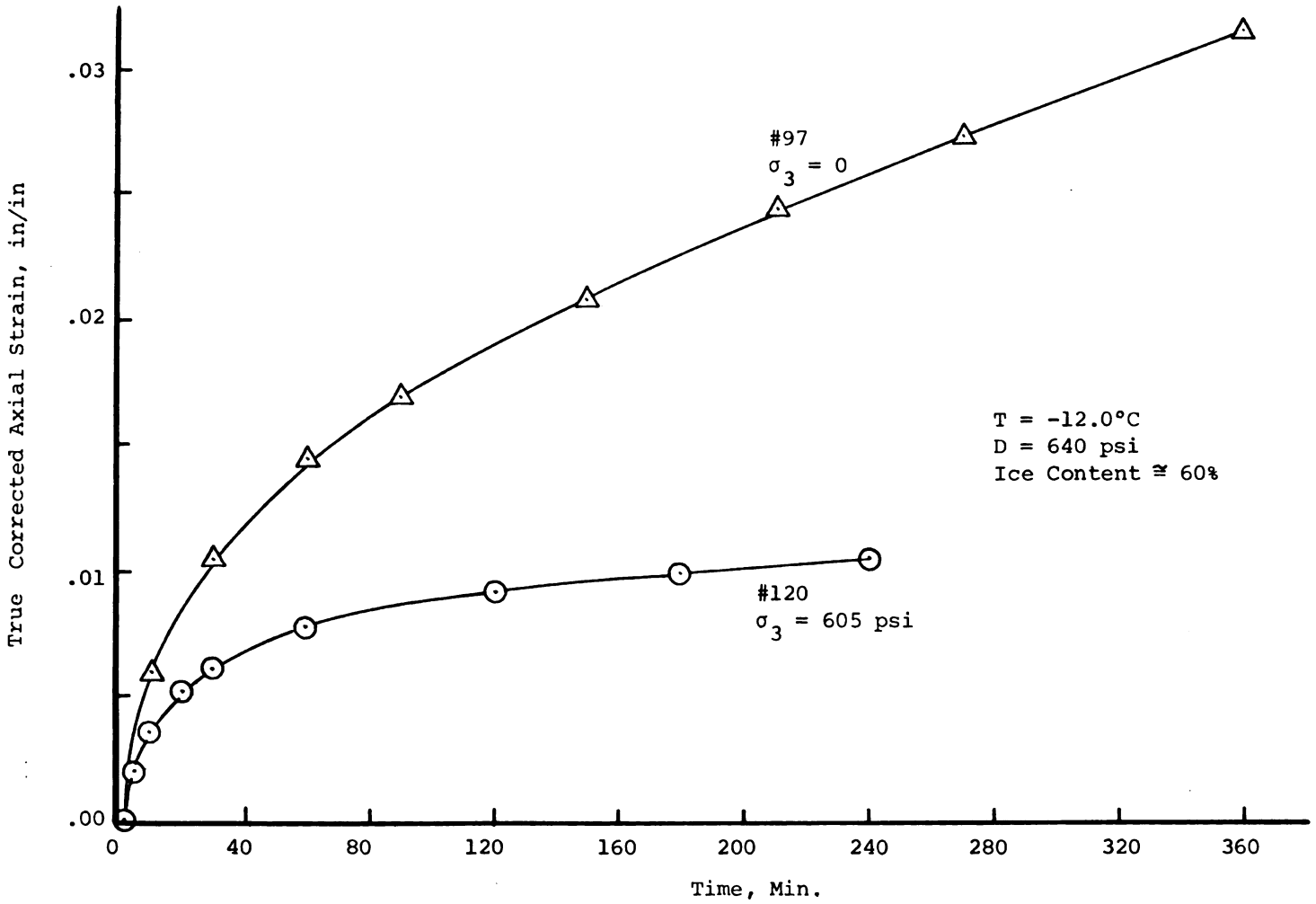

Figure 5-20.--Corrected constant axial load creep with constant confining pressure and reduced ice content.

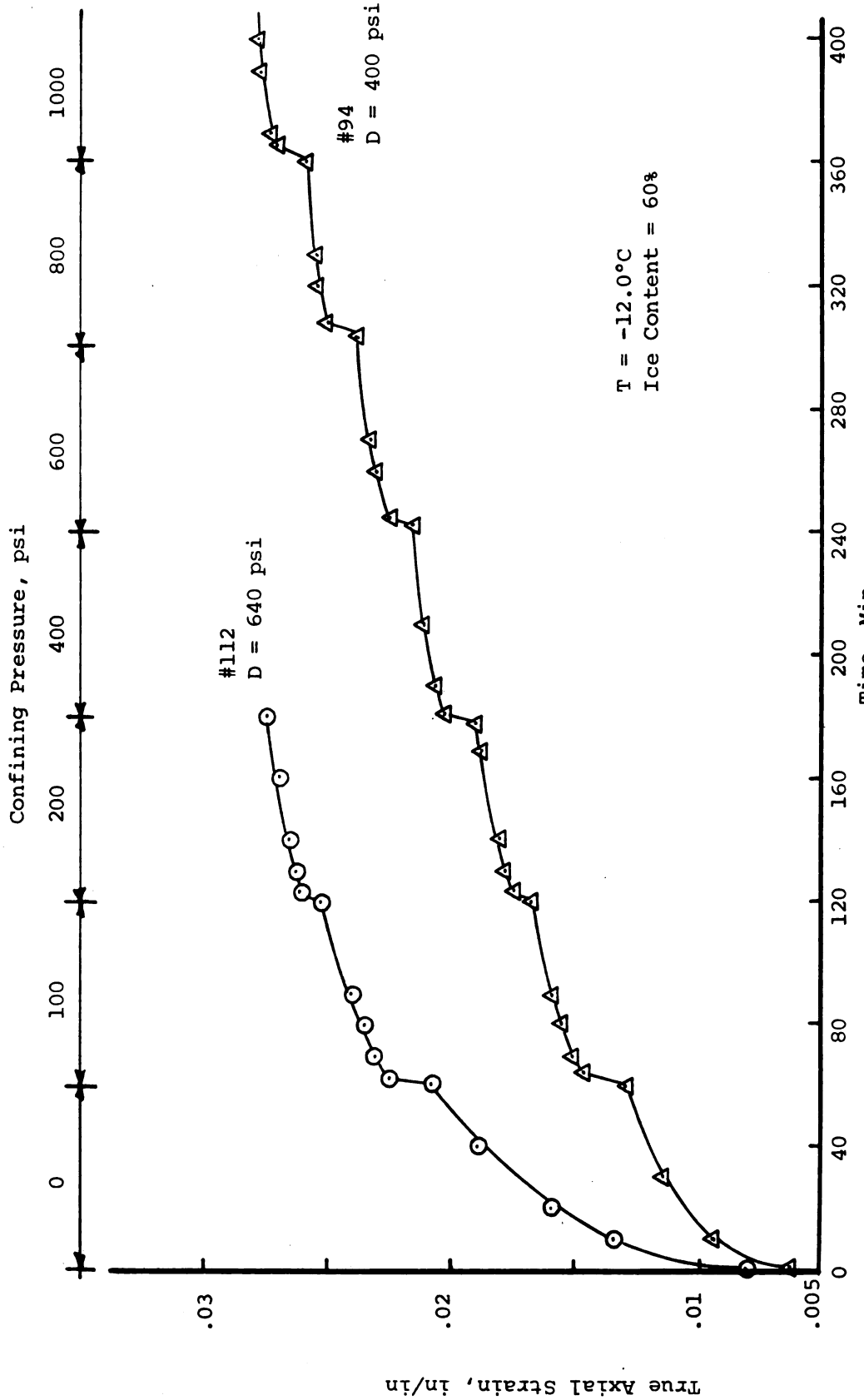

Figure 5-21.--Step-stress creep for reduced ice content, D = 400 and 640 psi.

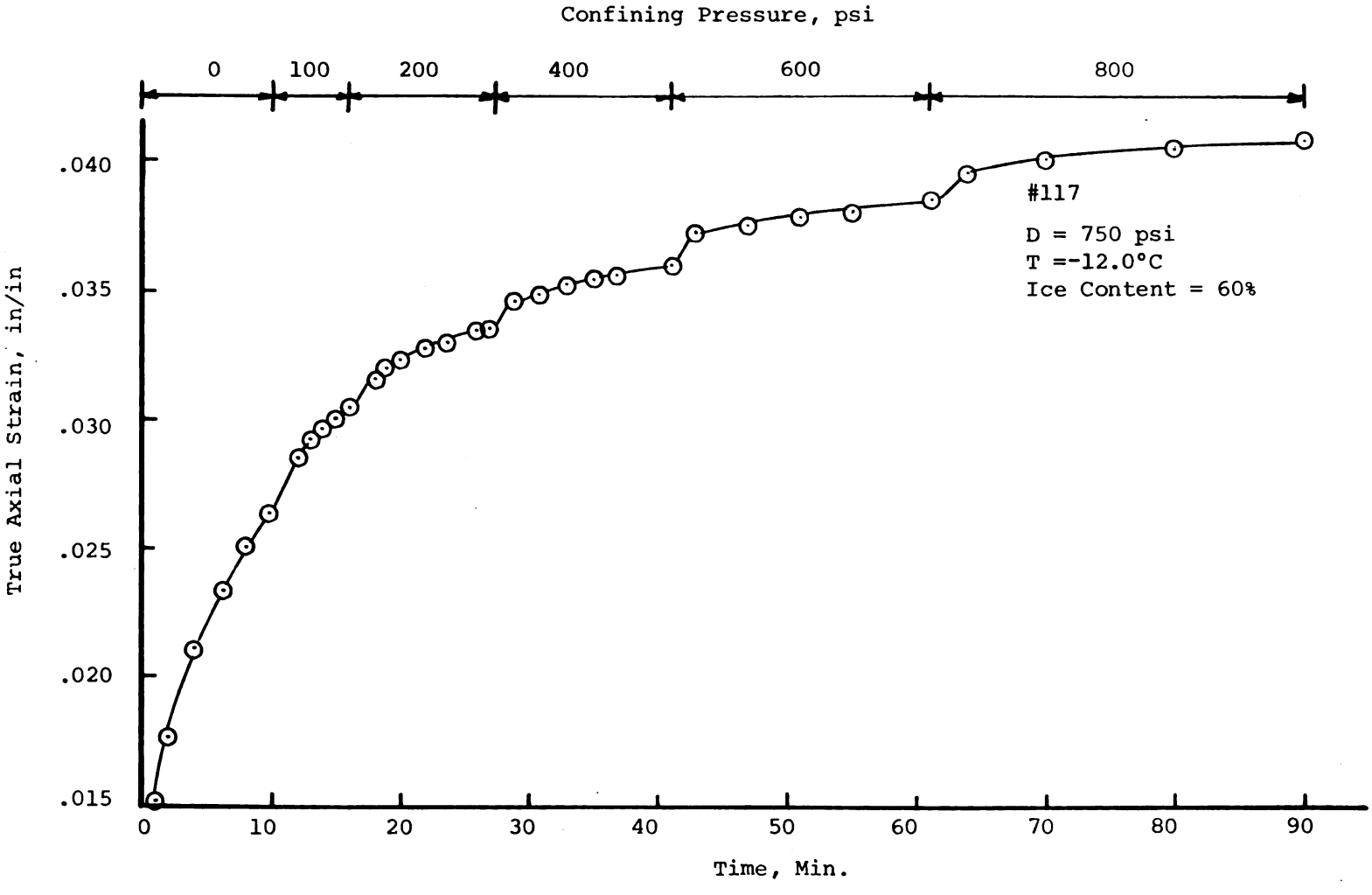

Figure 5-22.--Step-stress creep for reduced ice content, D = 750 psi.

CHAPTER VI

DISCUSSION OF RESULTS

6.1 Factors Controlling Shear Strength

Assuming that shear strength of a sand-ice material is composed of cohesive and frictional components which may be identified and isolated, the effect of various factors on these components can be shown. Vialov (1965b) has shown that the cohesive component of sand-ice is due primarily to confinement by the ice matrix and factors that alter the ice matrix will change the shear strength proportionately. The major cause for variations in the cohesion of the ice matrix is temperature (Vialov, 1965b), with strain rate and ice content having effects that are less well understood. By holding temperature constant, while changing the strain rate or ice content, the effect of these factors was observed.

The frictional component of strength for dense sand-ice materials tested to failure is independent of time, strain rate and ice content, and dependent on the void ratio and confining pressure. The effects of these factors were obtained by testing samples at constant strain rates and various void ratios over a large range of confining pressure.

In the following sections each of the factors which affect the frictional and cohesive component of strength will be discussed. The effect of confining pressure on the various factors will be discussed as it occurs.

6.1.1 Frictional Component

The frictional component of strength for sand-ice materials is dependent on the frictional characteristic of the sand material. Koerner (1970) has identified particle size, shape and gradation as factors which may affect the frictional behavior of single mineral soils. By using only Ottawa sand between the number 20 (0.84mm) and 30 (0.59mm) U. S. Standard sieve size, these factors were minimized. Once these factors have been eliminated, the frictional characteristics of the single mineral sand is dependent on sliding friction, dilatancy, and particle crushing and rearranging. Because of the high volume of sand in the sand-ice samples tested herein, particle to particle contact is likely to occur and sliding friction will develop with deformation. This will be true even if it is assumed that each grain of sand is surrounded by a layer of ice, since the contact pressures that develop will be high enough to cause pressure melting and migration of moisture at contact points. Particle crushing is known (Lee and Seed, 1967) to be small for Ottawa sand tested up to 1000 psi confining pressure and will not contribute

significantly to the frictional component of strength. Thus, the only unaccounted-for component of frictional strength is dilatancy. As the confining pressure increases, the volume changes associated with dilatancy are resisted by the confining pressure resulting in a lower component of strength due to dilatancy, and a lower angle of friction. For sand-ice materials both the applied confining pressure and the confinement due to the ice matrix retard volume changes resulting in a low component of strength due to dilatancy. As a result, the angle of friction for sand-ice materials will be lower than those obtained from unfrozen sands at similar confining pressures.

To verify these observations, volume measurements were taken both before and after testing selected samples. Since the equipment did not allow the measurment of volume changes during the test, total volumetric strain per test was divided by the unit strain at the end of the test to obtain an average change per unit of strain. The results of this procedure, shown in Figure 6-1, permit several observations to be made: (1) volume changes are small and are all negative (increase) for the sand densities tested; (2) volumetric strain per unit strain decrease as confining pressure increases; and (3) volume changes are less for sand-ice materials than for unfrozen sand at equal confining pressures. These observations verify the original assumption that dilatancy must contribute to the strength of sand-ice

materials. However, the fact that the values of volumetric strains are small implies that the contribution to strength will be small. The resulting angle of friction obtained for sand-ice materials should be comparable to those obtained for dense sands at high confining pressures where dilatancy has also been reduced.

6.1.2 Void Ratio (Density)

One of the variables that affects the peak strength is the variation of void ratio between sand-ice samples. This factor has been reported by other investigators (Kapler, 1971; Goughnour, 1967; and Yong, 1963) for sand-ice materials and is an indication that the material retains some of the frictional characteristics of unfrozen sand. A decrease in void ratio for unfrozen sand tends to increase the maximum deviator stress at failure (Koerner, 1970; Lee and Seed, 1967). This is due to dilatancy and particle rearranging and crushing. For sand-ice materials the actual magnitude of the strength increase appears to be dependent upon the confining pressure in addition to the void ratio.

Using uniaxial compression tests, Goughnour and Andersland (1968) showed a bilinear relationship between the volume of sand and peak strength. A similar presentation is shown in Figure 6-2. The majority of the data for this graph was obtained from Goughnour (1967) with additional points added from the tests conducted in this study. The

test procedures and sample preparation were the same for all tests. This figure also shows an increase in peak strength due to changes in temperature and strain rate.

It is interesting to note that above a sand volume of approximately 42 percent the change in slope of the curves at the different temperatures appears related to the ability of the ice matrix to exert various effective stresses in the sample. If the ability of the ice matrix to apply confining pressure is the requirement for increasing the slope of the curves, it would be expected that other factors which increase the cohesive component of strength may also increase the slope of the line. There is an indication in Figure 6-2 that this is the case. The tests conducted at a strain rate of $2.66 \times 10^{-3} min^{-1}$ have a slightly greater slope than the tests conducted at $2.66 \times 10^{-4} min^{-1}$. There is a limitation for which this will occur, since there is a confining pressure at which dilatancy will be prevented and the friction angle will become constant.

The results of increased confining pressure and volume of sand on the peak deviator stress are shown in Figure 6-3. Increased confining pressures serve to increase the maximum deviator stress per unit increase in sand volume. Above 350 psi the increase in maximum deviator stress per unit increase in sand volume appears to be constant, nearly parallel curves. These results reinforce

the previous discussion concerning a limiting value of confining pressure that can cause an increase in the slope of the strength versus percent of sand curves. Lee and Seed (1967) showed that as the confining pressure on unfrozen sand samples increased, the difference in failure stresses between a loose and a dense sample increases up to a maximum value and then remains essentially constant. The same behavior is shown in Figure 6-3 for the sand-ice material. Thus, for sand-ice at low confining pressures, dilatancy contributes to the variations in strength between samples with different void ratios. At high confining pressures the dilatancy component of strength is reduced, producing a fairly constant difference in deviator stress between dense and loose sand-ice samples. This explanation implies that the response of the ice matrix can be considered analogous to higher effective stresses, and variations in sand volume do not increase or decrease that response.

Since the effect of void ratio is influenced by the confining pressure applied to the sample, it is necessary to account for all pressures. For a sand-ice system, there is not only the externally applied confining pressure but an internal increase in effective stresses provided by the ice matrix. If the internal and external pressures are added, it is apparent that the frictional component of strength in sand-ice systems can be compared to unfrozen

sands only if the unfrozen materials are tested at higher confining pressures.

Another indication of the interrelationship of confining pressure and percent of sand by volume can be obtained by plotting the peak stresses in terms of the principal stress ratio. In Figure 6-4 the principal stress ratio versus the percent of sand by volume is shown for various confining pressures. This graph shows that the lower the confining pressure, the more sensitive the principal stress ratio is to changes in sand volume. In fact, at high confining pressure the principal stress ratio is quite insensitive to changes in the sand volume and approaches a constant level. This type of behavior is also typical of unfrozen sands at high confining pressure (Lee and Seed, 1967).

6.1.3 Relative Ice Content

In order to magnify the frictional characteristics of a sand-ice material, tests on samples with reduced ice content were conducted. To relate strength to a function of ice content, the term "percent of ice" is used. The percent of ice is defined as the volume of ice divided by the volume of voids multiplied by 100. The calculation of the volume of ice is determined by dividing the weight of water in a sample by the density of ice at -12.0° C ($0.91848\ gm/cm^3$).

Kaplar (1971), Vialov (1965b), and Yong (1963) have shown that strength of sand-ice materials decrease approximately linearly with a decrease in the percent of ice in the sample. These results were obtained for unconfined tests with no indication of the effects of confining pressure. The results of confined compression tests on samples with different ice contents are shown in Figure 6-5. Values for the high percent of ice were obtained from Figure 6-3 using the same volumes of sand as contained in the reduced ice samples. This figure indicates a linear and constant decrease in deviator stress with reduced ice content for all confining pressures. Since each line of equal confining pressure has a different volume of sand, the reduction in strength due to changes in the ice content is independent of both confining pressure and volume of sand. From this result it can be concluded that the reduction in strength is due entirely to a loss of cohesion and samples at reduced ice content will have the same frictional characteristics as samples at high ice contents.

To compare the significance of the percent of ice for various confining pressures a plot of reduction in strength versus confining pressure is shown in Figure 6-6. The reduction in strength is calculated as follows:

$$\frac{D_H - D_L}{D_H} \times 100$$

where

D_H = Maximum deviator stress for high percent ice.

D_L = Maximum deviator stress for low percent ice.

This figure indicates that the reduction of strength decreases as the confining pressure increases. This is another indication that strength at high confining pressure is less dependent on the ice matrix and becomes primarily frictional in nature.

6.1.4 Confining Pressure

Previous investigations into the strength behavior of frozen soils have been primarily conducted on samples that were unconfined or at low confining pressures. Yong (1963), Goughnour (1967), and AlNouri (1969) have conducted tests on sand-ice materials at confining pressures up to 150 psi. In order to extend the data of these investigators confining pressures up to 1000 psi were used to determine the effect on the strength of sand-ice materials. This range of pressures has been used on unfrozen sand by Lee and Seed (1967). The data from this study was used to interpret the results for frozen sand.

Typical stress-strain behavior for unconfined and confined tests is shown in Figure 6-7. These tests indicate that for low confining pressures the curves progress through an initial period of high stress increase per unit strain

followed by partial yielding leading ultimately to failure. The sample with the higher confining pressure behaves in a similar fashion up through the initial yield point. However, after this point additional strengthening due to dilatancy and sliding friction takes place and there is a long, fairly linear increase in stress, progressing eventually to failure. Similar results have been observed in unfrozen materials with a cohesive matrix (Schmertmann and Osterberg, 1960) where the initial yield point is identified as matrix yield.

An indication of the relative magnitudes of the proportions of shear strength due to cohesion and friction is given, by a graph of principal stress ratio versus confining pressure in Figure 6-8. When compared to unfrozen Ottawa sand values obtained from Lee and Seed (1967) it is apparent that for low values of confining pressure, the shear strength of frozen sand is primarily nonfrictional and dependent on the strength of the ice matrix. As the confining pressure increases, the principal stress ratio for sand-ice decreases and approaches the value for unfrozen sand. However, even at high confining pressure, there is a small component of strength due to the ice matrix. This plot also gives an indication of the shape of the failure envelope since decreasing values of the principal stress ratio with increasing confining pressure correspond to a progressive flatting of Mohr's envelope.

If the same results are plotted on logarithmic scales as shown in Figure 6-9, a bilinear relationship occurs with the area of transition in the region between 100-200 psi confining pressure. Later sections show that creep test results give a similar change in behavior for these pressure ranges.

Another effect of confining pressure on the stress-strain characteristics of a sand-ice sample is an increase in axial strain at failure. Axial strain at failure is plotted against the confining pressure in Figure 6-10. The data shows that as confining pressure increases the strain at failure also increases. This behavior is similar to sands as reported by Vesic and Clough (1968), and Lee and Seed (1967). However, when compared to unfrozen sands, the strains at failure are substantially less for sand-ice materials. For reduced ice content samples, there is also an increase in strain at failure with increasing confining pressure, but the strain at failure has decreased compared to the results for high ice content samples.

6.1.5 Failure Criteria

Using the Mohr-Coulomb theory to describe the time dependent strength of sand-ice materials, the results of the constant strain rate tests are summarized by the p-q diagram shown in Figure 6-11. Data for unfrozen sand (Lee

and Seed, 1967) are also plotted as an aid in comparing the results and identifying the components of strength. If the ordinate to the unfrozen K_f failure line is considered to be caused by sliding friction, dilatancy, and particle crushing; the remaining distance to the sand-ice failure line must be attributed to the ice matrix. What is of interest is the consistency of this value regardless of the value of the normal stress. Over the entire range of confining pressure this component varies from only 330-260 psi. This implies that confining pressure has no significant effect on the component of strength due to the ice matrix. If the results of the constant axial strain rate tests on polycrystalline ice are used, the values of calculated q are nearly the same as the value of the cohesive component shown in the p-q diagram for the sand-ice material. Since the value of the cohesive component is nearly constant, it may be concluded that the ice matrix applies a pseudo-confining pressure analogous to a higher effective stress that is also nearly constant. The magnitude of this pressure may be obtained by evaluating the horizontal stress increment obtained by projecting a line from a point on the sand-ice K_f failure line to a point on the unfrozen sand K_f failure line. For high ice content samples this value is approximately 600 psi.

When the angle of inclination of the K_f failure line in the p-q diagram is measured, it decreases slightly with increasing values of normal stress but is approximately 26 degrees. This gives an angle of 29.2 degrees on the failure plane. This value is low when compared to the friction angle for unfrozen sands, which are typically 37-45 degrees depending on the initial void ratio. However, the friction angle for unfrozen sands at high confining pressures is less than the value at low confining pressures. Lee and Seed (1967) obtained a value of approximately 30 degrees for high confining pressure tests on Ottawa sand with an initial void ratio of 0.49. For unfrozen sands the reduction in the angle of friction is due to a decrease in the dilatancy component of strength as confining pressure increases. The same effect is produced in sand-ice materials by the combination of the applied confining pressure and the pseudo-confining pressure caused by the ice matrix. If sand-ice samples with a different initial void ratio were plotted, the result would be a downward displacement of the failure envelope as the void ratio increased. This does not mean that the cohesive component will decrease, since the failure plane for unfrozen sand will also be displaced. The result shown previously on the effect of void ratio indicated that at high confining pressures, the change in strength per increase in void ratio is constant and not dependent on the ice matrix.

Also shown on the p-q diagram (Figure 6-11) are the results of the constant strain rate tests on reduced ice content samples. The observations for these samples are similar to those for the high ice content discussed above. Again it is apparent that at failure a full frictional component is mobilized and the reduction in strength is due entirely to a reduction in the cohesive component.

The net result is that sand-ice materials tested to failure has strength characteristics that can be divided into a cohesive component due to the ice matrix and a component due to friction. It has been shown that the frictional component can be related to the behavior of unfrozen sands at high confining pressure. The cohesive component is the part of strength which will be most responsive to variable test conditions and controls the time dependent characteristics of the shear strength. In addition, the cohesive component of strength is dependent on the percent of ice in the sample and for given conditions of temperature and strain rate is nearly constant at failure.

6.2 Creep Behavior

In order to describe the creep behavior of sand-ice materials for various stress levels, it is necessary to determine the effect of confining pressure on creep.

This section presents the results of uniaxial, confined and step-stress creep tests on high and reduced ice content samples for confining pressures up to 1000 psi.

Throughout this section constant deviator stress will be shown as a function of the peak deviator stress obtained from the constant axial strain rate tests. The term M will be used to describe this relationship, where M is equal to the ratio of constant deviator stress for the creep test divided by the peak deviator stress from the constant strain rate test conducted at a similar confining pressure. For example if the creep test conditions are:

constant deviator stress, $(\sigma_1-\sigma_3)$ = 1070 psi

confining pressure, σ_3 = 350 psi

volume of sand, = 63.6%

ice content, = 100%

Then from Figure 6-3 the maximum deviator stress would be equal to 2360 psi and

$$M = \frac{1070 \text{ psi}}{2360 \text{ psi}} \times 100 = 45.5\%$$

Values of M for all creep tests have been calculated and are shown in Table 5-3 and 5-4.

6.2.1 High Ice Content

To show the effect of applied stress on the creep behavior of sand-ice materials at high ice contents, the results of uniaxial creep tests conducted at 400, 640, 750 and 1070 psi are plotted as a logarithm of strain rate versus strain in Figure 6-12. The near linear relationship for each stress level indicates that for the time of load application for these tests, the creep strains are small and the strain rates are decreasing at a constant logarithmic rate. These tests have not reached the steady state region of a typical creep curve since this would require a horizontal segment of the strain rate versus time curves. The low values of strain also imply that this should be a region of little volume change. The actual values of volume change that were measured at the end of each test are noted on the figures. Through 750 psi the volume decreased as would be expected for low values of strain. Goughnour (1968) made volumetric measurements during uniaxial creep tests and constant strain rates tests, and demonstrated that an increase in volume will be associated with the matrix yield which is required prior to the mobilization of the dilatancy component of friction. Thus, for the stress levels applied in this series the creep behavior is primarily dependent on the ice matrix and the component of friction associated with solid to solid contacts. Any attempt to

determine an effective angle of friction within this region as proposed by AlNouri (1969) should result in low values since the loads applied are not great enough to mobilize the full frictional value of the sand particles, and the component due to interlocking of the particles.

The effect of confining pressure on a constant deviator stress creep test is to increase the slope of the line of strain rate versus strain as indicated in Figure 6-13. This supports the observation by Andersland and AlNouri (1970) that strain rate decreases with increased mean stress. This may be explained by noting that an increase in confining pressure increases the level of normal stress applied to the sample. Part of this increase is carried directly by particle to particle contact and part is carried by particle to ice contact. When the p-q values for typical sand-ice tests are calculated, the results may be plotted as shown in Figure 6-14. It can be seen that for the unconfined samples, a large portion of the total applied stress must be carried by the ice matrix (F). As confining pressure is applied to the system the stress circle moves to the right and the shear strength required of the ice will be less (G), and the strain rate will decrease, since creep is primarily a function of the shear stress applied to the ice matrix. This mechanistic

picture of creep assumes that the frictional component of strength due to sliding friction is mobilized during the application of the axial stress. For a dense material prepared in themanner described herein, it appears reasonable that this be the case, since the packing is such that grain to grain contact is assured. In order for a sample to proceed to failure, it would be necessary for the Mohr's circle for the test condition to become tangent to the failure plane for the frozen soil. This may occur, since the cohesive component of strength decreases with time causing a downward displacement of the failure envelope. A comparable reduction in strength occurs in overconsolidated clays at large strains. For sand-ice materials time serves the same purpose as the large strains required for the clays.

Step-stress tests have been used (AlNouri, 1969) as a method of determining the steady state creep rate at different levels of confining pressure. When using this method of testing, the axial load is held constant and the major and minor principal stresses are changed by an amount equal to the change in confining pressure. Since the principal stresses are changed by equal amounts, the deviator stress is held constant. With step-stress testing it is assumed that the sample structure remains

the same prior to and immediately after changing the confining pressure and any changes in the creep rate are due only to the change in confining pressure.

The results for step-stress creep tests plotted as logarithm of strain rate versus strain for three levels of constant deviator stress are shown in Figures 6-15 to 6-17. In these tests each new increment of confining pressure causes an increase in the slope of the curves. As noted in Figure 6-12, a decrease in axial stress produced a similar increase in slope. For the step-stress tests the deviator stress was constant and the confining pressures were altered. Therefore, increasing the confining pressure has the same effect as decreasing the applied stress for a uniaxial test.

As each increment of confining pressure was applied, the strain rate increased. Then follows a period of decreasing strain rate until the next increment of pressure was applied. The initial increase in strain rate was dependent upon the deviator stress and the strain of the sample. At low stresses the samples show the greatest change in strain rates due to confining pressure. This is an indication of the greater structural dependency of the system at lower stresses. At low deviator stress levels the strain that took place during an increment of confining pressure was small and the structure remains nearly constant. When

the next increment of confining pressure was applied, the deviator stress and structure were nearly the same as for the previous increment and the initial response of the material was the same.

The step-stress creep tests involved increments of confining pressures applied at one hour intervals. To give an idea of the time effect on the strain rate, a sample with a constant deviator stress of 1070 psi was tested with zero confining pressure for three hours and then a confining pressure of 350 psi was applied for three hours. The logarithm of strain rate versus strain in Figure 6-18 demonstrates that time does not alter the basic characteristics of the curve and a decrease in strain rate takes place in a manner similar to the tests with confining pressures applied at one hour intervals.

The results of the step-stress creep tests are summarized in Figure 6-19. Andersland and AlNouri (1970) demonstrated that when the logarithm of secondary creep rate was plotted against a stress factor, Σ, a straight line relationship appeared for confining pressures up to 150 psi and time increments of one-half hour. The data summarized in Figure 6-19 indicate that the relationship predicted by Andersland and AlNouri (1970) are correct for low confining pressures. However, for confining pressure in excess of 200 psi the strain rates predicted

by their equation are substantially less than those indicated by the experimental results.

In addition to the increase in strain rate at higher confining pressure, it appears that the equation used by Andersland and AlNouri (1970) is dependent upon the time interval at which the strain rates are obtained. The equation can be changed to reflect this by making the intercept term a function of time as shown below:

$$\dot{\varepsilon} = b(t) \exp(m\Sigma) \qquad (6\text{-}1)$$

where Σ = stress factor = $D-\sigma_m$

m = absolute value of the slope of the line

b = time dependent intercept on the Σ axis

Figure 6-19 also indicates that strain rate is most responsive to changes in confining pressure for the range of 0-200 psi. Above 200 psi confining pressure, the strain rate continues to decrease with increased confining pressure; however, the change per increment is much smaller and approaches a constant at the higher levels of confining pressure. This implies that confining pressure changes the creep characteristics by a mechanism that is mobilized at low confining pressure. From these results it appears that in order to adequately predict strain rates using a stress factor as described by Andersland and AlNouri (1970), a bilinear relationship that is a function of time and confining pressure will be required.

When the results of the step-stress creep tests are summarized as shown in Figure 6-20, the interrelationship between stress difference and confining pressure is more clearly shown. To eliminate time dependency in this presentation, time intervals equal to one hour were selected. Changes in slope for lines of equal confining pressures indicate a definite dependency of strain rate upon the confining pressure. For a given deviator stress the strain rates decrease as the confining pressure increases. The exact functional relationship can be derived empirically since a linear relationship on a semi-log plot has the basic form:

$$\dot{\varepsilon} = b(t) \exp (mD) \qquad (6\text{-}2)$$

Taking logarithms of both sides results in the expression

$$\log \dot{\varepsilon} = \log b(t) + (m \log e) D \qquad (6\text{-}3)$$

where (m log e) is the absolute value of the slope of the lines of equal confining pressure and b is the intercept on the ordinate. To determine the relationship between the slope, m, and the value of confining pressure, m is plotted against confining pressures as shown in Figure 6-21. The results of this graph exhibit a bilinear relationship of slope versus confining pressure. From this figure the equation for the slope m as a function of confining pressure is:

$$m_i = C_i + G_i \sigma_3 \qquad (6\text{-}4)$$

where m_i = value of slope for the line of equal confining pressure.

$i = 1$, for confining pressure equal to or less than 200 psi.

$i = 2$, for confining pressure greater than 200 psi.

C_i = intercept of the i^{th} segment of the m versus confining pressure graph.

G_i = slope of the i^{th} segment of the m versus confining pressure graph.

Combining this expression with the equation 6-3 results in the following expressions:

$$\log \dot{\varepsilon} = \log b(t) + [(C_i + G_i \sigma_3) \log e\, D] \qquad (6\text{-}5)$$

$$\dot{\varepsilon} = b(t) \exp [(C_i + G_i \sigma_3) D] \qquad (6\text{-}6)$$

$$\dot{\varepsilon} = b(t) \exp (C_i D) \exp (G_i \sigma_3 D) \qquad (6\text{-}7)$$

Equation 6-7 is of the same form as that describing the rate process theory. For the range of confining pressures studied (up to 1000 psi) an equation can be derived to describe the strain rate of a sand-ice sample. Using equation 6-7, the coefficient C_i and G_i must be determined for the appropriate ranges of confining pressure. From Figure 6-21, when confining pressure is equal to or less than 200 psi

$$m_1 = C_1 + G_1\sigma_3 \tag{6-8}$$

where $C_1 = 2.97 \times 10^{-3}$ min^{-1}/psi

$G_1 = -6.04 \times 10^{-6}$ min^{-1}/psi

likewise for confining pressures greater than 200 psi

$$m_2 = C_2 + G_2\sigma_3 \tag{6-9}$$

where $C_2 = 1.98 \times 10^{-3}$ min^{-1}/psi

$G_2 = -1.03 \times 10^{-6}$ min^{-1}/psi

The resulting equation for the entire range of confining pressures is:

$$\dot{\varepsilon} = b(+)\ \exp(C_i D)\ \exp(G_i \sigma_3 D) \tag{6-10}$$

when

$\sigma_3 \leq 200$ psi $\quad b(60) = 4.7 \times 10^{-6}$ min^{-1}

$C_1 = 2.97 \times 10^{-3}$ min^{-1}/psi

$G_1 = -6.04 \times 10^{-6}$ min^{-1}/psi

$\sigma_3 > 200$ $\quad b(60) = 4.7 \times 10^{-6}$ min^{-1}

$C_2 = 1.98 \times 10^{-3}$ min^{-1}/psi

$G_2 = -1.03 \times 10^{-6}$ min^{-1}/psi

The bilinear relationship noted for this equation may be explained for a sample at low confining pressures. When the sample is loaded instantaneously, numerous micro-cracks form at the sand-ice interface because some of the sand grains apply stresses to the ice in excess of the instantaneous ice crystal strength. Increased confining pressure prevents the cracks from forming, resulting in a more homogeneous material with greater strength and lower creep rates. Equation 6-10 shows that strain rates are most responsive to confining pressures below 200 psi. The term b(t) in the equation has no physical significance but is an indication of the minimum strain rate that will be encountered in the range for which the equation is applicable.

The previous discussion has indicated that given the results of step-stress creep tests, a family of curves may be constructed that will allow the calculation of strain rates for various combinations of confining pressures and deviator stress. This method has the disadvantage of being time dependent. It would be much more helpful if the creep characteristics of the sand-ice material could be obtained independent of time.

It was observed that the strain rate decreases in an exponential fashion either after the initial application of the deviator stress (uniaxial tests, Figure 6-12) or

after the application of increments of confining pressure (Figures 6-15, 6-16, and 6-17). If the slopes of these lines are calculated and are plotted versus the percent of maximum deviator stress M as shown in Figure 6-22, a band of points is obtained. Using the results of this graph it is possible to approximate the decrease in strain rate for any test condition as long as the initial elastic strains and the percent of maximum deviator stress are known. The curvature of the graph as M approaches zero is an indication that the response of the sand-ice materials to low levels of applied stress is different and the approximation would not be valid in this region. On the other end of the scale it is expected that the curve would be nonlinear as M approached 100 percent. From the data shown here, a range of 20-75 percent of the maximum deviator stress can be used for the approximation. For samples that progress to failure, the strain rate versus strain graph exhibits an initial linear portion followed by an upward curvature as the sample approaches the beginning of the tertiary region of creep. The results shown in Figure 6-22 can be used only to describe the linear portion of the curve.

6.2.2 Reduced Ice Content

Since creep is related to the strength of a material, it would be expected that for a given constant axial stress

and void ratio, reduced ice content samples would have greater creep response than high ice content samples.

In Figure 6-23, the results of uniaxial creep tests at 400, 640 and 750 psi are shown. It is apparent that these samples, as with the high ice content samples, exhibit typical strain rate versus strain characteristics. For the low level of axial stress (400 psi), the sample exhibits linear characteristic for the entire duration of the test. At higher levels of axial stress (750 psi) the sample has not only an initial linear portion, but also a segment of increasing strain rate. This is the type of behavior that would be expected of a sample that progresses to failure. The intermediate level of axial stress (640 psi) exhibits the initial linear portion and a small region of decreasing strain rate. These curves indicate that reducing the ice content does not alter the basic characteristics of the creep and any differences between high and low ice content samples are in magnitude only.

If the applied deviator stress is related to the maximum shear strength of sand-ice samples for reduced ice content (as was done for the high ice content samples in the previous section) it is possible to define the term M, percent of maximum deviator stress, for the reduced ice content samples. In order to generalize the use of this term, it is necessary to show the relationship between the percent of maximum deviator stress for high and

reduced ice contents. It can be shown intuitively, that for any given percent of maximum deviator stress, the shear stress carried by the ice is constant and the response of the system will be essentially constant.

Considering any failure plane with a shear force resulting from the applied force, then:

$$\tau_H = \frac{P_H}{A_{HI}+A_{HS}} \quad \text{and} \quad \tau_L = \frac{P_L}{A_{LI}+A_{LS}} \tag{6-11}$$

where τ_H = shear stress resulting from applied load on high ice content samples

τ_L = shear stress resulting from applied load on low ice content samples

P_H = force causing shear for high ice content samples

P_L = force causing shear for low ice content samples

A_{HI} = area of ice, high ice content

A_{LI} = area of ice, low ice content

A_{HS} = area of sand, high ice content sample

A_{LS} = area of sand, low ice content sample

For a constant percent of maximum deviator stress

$$M_H = M_L$$

where M_H = percent of maximum deviator stress high ice content sample

M_L = percent of maximum deviator stress low ice content sample.

Assuming that the shear forces are proportional to the applied loads:

$$P_H = P_{H\ max} \times M_H \text{ and } P_L = P_{L\ max} \times M_L$$

with $P_{H\ max}$ = maximum shear force resulting from the maximum deviator stress high ice content

$P_{L\ max}$ = maximum shear force resulting from the maximum deviator stress low ice content

For any given sample, let j equal the ice content expressed as a decimal fraction. Then the area of ice is proportional to the ice content in the sample, and

$$A_{HI} = \frac{A_{LI}}{j} \qquad (6\text{-}12)$$

Since P max is proportional to the maximum applied loads, and the maximum applied loads are proportional to the ice content of the sample, as shown in Figure 6-5

$$P_{H\ max} = \frac{P_{L\ max}}{j}$$

Using the Adhesion Theory of Friction (Lambe and Whitman, 1969), which states that an increase in normal loads must mean a proportional increase in area of contact between two bodies, the area of sand contact is:

$$A_{HS} = \frac{A_{LS}}{j}$$

Substituting these relationships into equation 6-11 and solving:

$$\tau_H = \frac{P_{L\ max} M_H}{(A_{LI}+A_{LS})} \tag{6-13}$$

and

$$\tau_L = \frac{P_{L\ max} M_L}{(A_{LI}+A_{LS})} \tag{6-14}$$

but,

$$M_H = M_L$$

and, therefore

$$\tau_H = \tau_L$$

The above proof obviously is not rigorous because of the assumptions regarding the distribution of forces and the increase in area due to the applied loads. However, the proof is useful for supporting the initial assumption that given a percent of maximum deviator stress, the resulting creep characteristics should be the same. Using this fact, the results from the tests on the reduced ice content samples are presented in a fashion similar to the high ice content samples.

A plot of strain rate versus strain for the various ice contents is shown in Figure 6-24. This figure demonstrates the invariance of creep behavior with respect to ice content. As an additional indication of the effect of various percents of ice, an intermediate percentage of ice of 70 percent has been included. At the applied axial stress of 750 psi the three different ice contents produce curves similar to those obtained by increasing the axial stress and holding the percent ice constant as was shown in Figure 6-23.

As with the high ice content, there was a test in which the sample was subjected to high confining pressure for the entire test period. The results of test plotted as strain rate versus strain in Figure 6-25 shows that the effect of confining pressure is immediately apparent. The confined sample has a steadily decreasing strain rate through the entire test and has undergone much less strain than the unconfined sample. The substantial increase in slope of the curves as the percent of maximum deviator stress was reduced from 71 percent to 34 percent is apparent.

The results of the step-stress creep tests on reduced ice content samples shown in Figures 6-26 to 6-28 include three levels of deviator stress used for the high ice content samples. The increase in slope of the curves with decrease in percent of maximum deviator stress is common to all the step-stress creep tests conducted, and

indicates a definite response to increased confining pressures. Figure 6-28 is particularly interesting in this respect. For the uniaxial test, the sample proceeded into the tertiary range within 45 minutes after application of the axial stress of 750 psi. As the increments of confining pressure were applied, the creep rate decreased and at the end of the test there was no sign of failure, even though the time of the test was 90 minutes. Since the increments of confining pressure were applied at various time intervals, it may be misleading if strain rates obtained from Figure 6-28 are compared to strain rates from the other tests with lower percents of maximum shear stress.

Figure 6-29 is a plot of the stress factor Σ versus strain rate for the reduced ice samples. As with high ice content samples, there is a definite bilinear behavior. Reduced ice content samples are also more responsive to confining pressure in the 0-200 psi range.

In order to describe the creep behavior of reduced ice samples, it is possible to modify equation 6-7 such that the peak deviator stress is a function of the ice content. Therefore, an expression relating the deviator stress for the high and low ice contents can be written:

$$D_L = D_H \, f(j) \qquad (6\text{-}15)$$

D_H = Deviator stress high ice content

D_L = Deviator stress low ice content

assuming that the function is linear, as shown in Figure 6-5, then:

$$D_H = \frac{D_L}{J} \qquad \sigma_3 = \text{constant} \qquad (6\text{-}16)$$

Substituting this expression into equation 6-7, results in an equation for creep in terms of the applied deviator stress for reduced ice content and the percent of ice.

$$\dot{\varepsilon} = b(t)\ \exp(C_i \frac{D_L}{J}) \exp\ (G_i \sigma_3 \frac{D_L}{J}) \qquad (6\text{-}17)$$

If the parameters $b(t)$, C_i, and G_i are obtained from equation 6-10, it is possible to obtain strain rates for a time interval of one hour. The calculated and experimental results are tabulated in Table 6-1. The data show a good correlation between measured and calculated values and support equation 6-17 for calculating strain rates for reduced ice samples.

Presentation of the creep test results as a function of percent of maximum deviator stress and the slope factor K in Figure 6-30 confirms the trend of increasing K with increasing values of M as was shown for high ice content samples.

From the discussion of results for the reduced ice content samples it can be stated that the creep characteristics of these samples are essentially the same as for the high ice content samples. If the two test series are related by the factor M, percent of maximum deviator stress, the formulations obtained for high ice content may be used. It is noted that considerable scatter occurs for some of the tests on the reduced ice samples. This scatter was due to difficulty in making duplicate low ice content samples. Even though the same amounts of sand and water were added to each sample, it is probable that the distribution of water in the pore spaces for the unsaturated condition may be different between any two samples, resulting in slightly different ice contents on the plane of maximum shear.

It was originally assumed that a reduction in the percent of ice in a sample would accelerate the creep response so that it would be possible to study a wider range of loading conditions in a shorter amount of time. This has not proven to be the case. Rather, it has been demonstrated that for a given percent of maximum deviator stress the creep characteristics are essentially the same for both the high and low ice content samples. This fact may be useful in conducting experiments on frozen sand-ice materials where limited loading capabilities are available or for the analysis of partially saturated sand-ice systems.

TABLE 6-1.--Calculated versus measured strain rates using Equation 6-17, reduced ice content.

Sample No.	% Ice	D_L	Confining Pressure	Calc. Strain Rate Eq 6-17	Measured Strain Rate
	%	psi	psi	min^{-1}	min^{-1}
93	60.8	400	0	$3.3x10^{-5}$	$4.2x10^{-5}$
97	58.8	640	0	$1.10x10^{-5}$	$1.1x10^{-5}$
120	64.6	640	600	$1.7x10^{-5}$	$3.6x10^{-5}$
94	59.4	400	0	$3.5x10^{-5}$	$4.5x10^{-5}$
			100	$2.2x10^{-5}$	$2.5x10^{-5}$
			200	$1.5x10^{-5}$	$1.8x10^{-5}$
			400	$1.3x10^{-5}$	$1.5x10^{-5}$
			600	$1.2x10^{-5}$	$1.3x10^{-5}$
			800	$1.06x10^{-5}$	$1.2x10^{-5}$
			1000	$.89x10^{-5}$	$.9x10^{-5}$
98	60.0	640	0	$11.0x10^{-5}$	$9x10^{-5}$
			100	$5.7x10^{-5}$	$5.4x10^{-5}$
			200	$3.1x10^{-5}$	$2.7x10^{-5}$

Time of Measured Strain Rate = 60 min

Temp. = 12.0° C

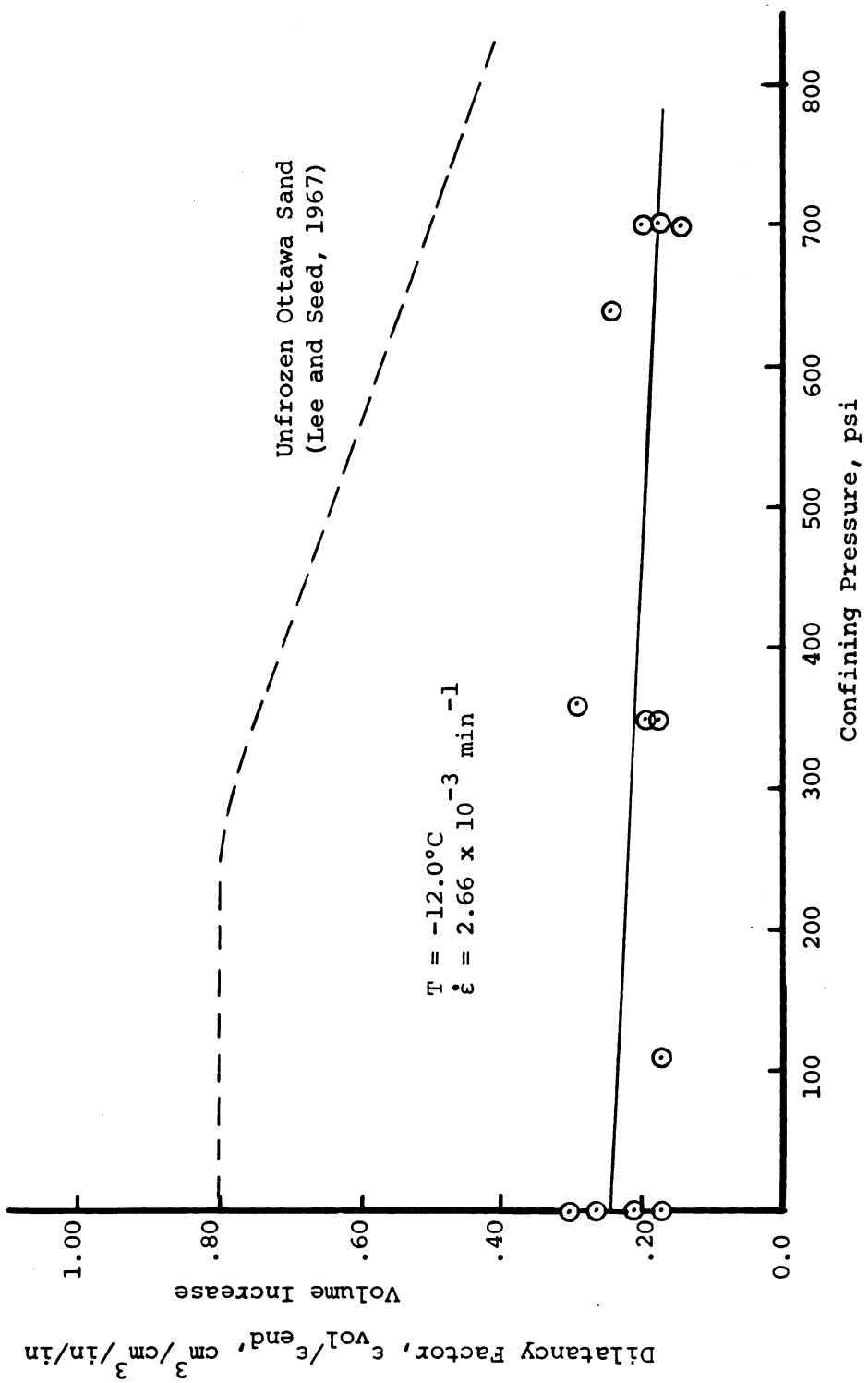

Figure 6-1.--Effect of confining pressure on volume change.

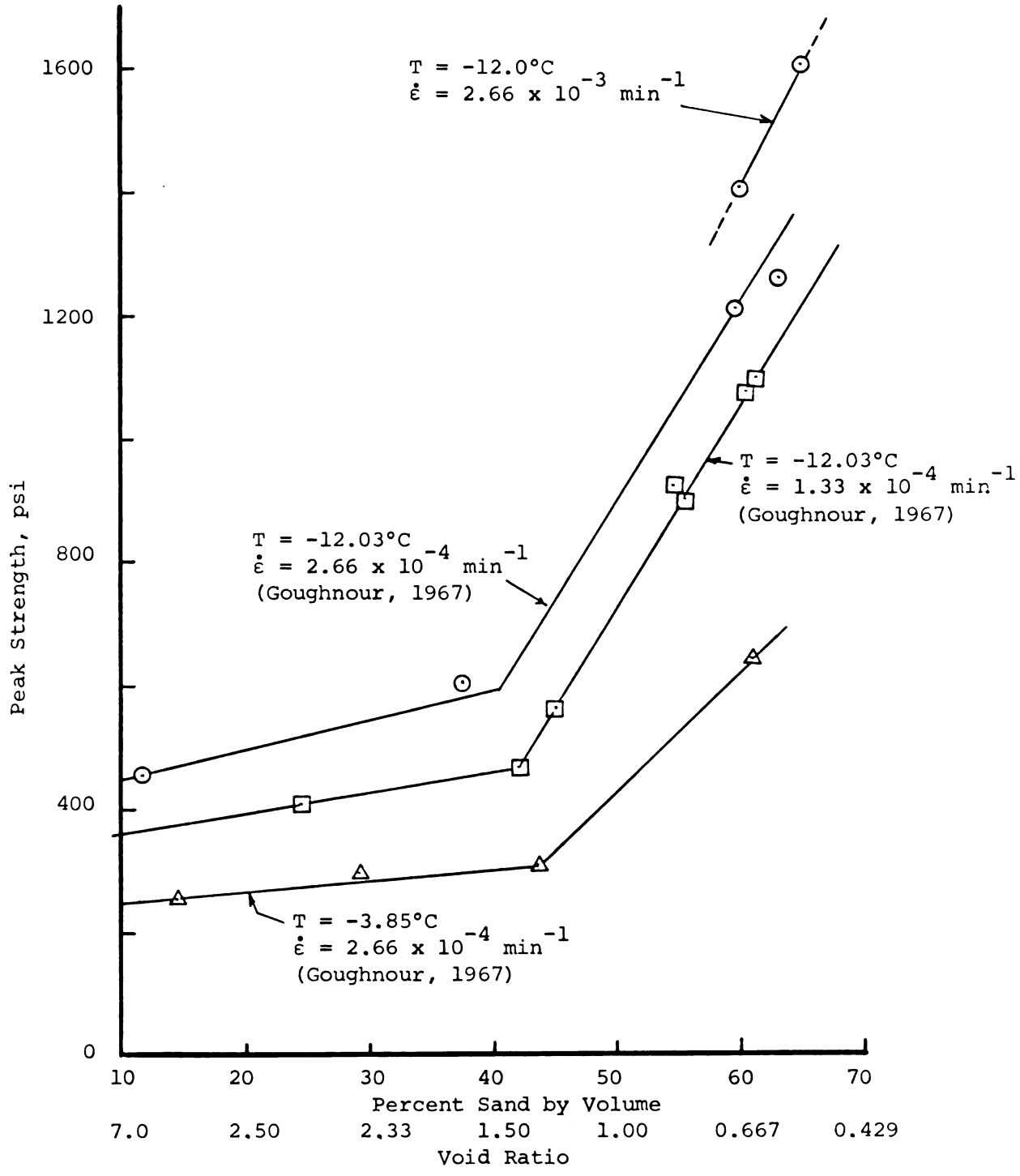

Figure 6-2.--The effect of percent sand, temperature, and strain rate on peak strength.

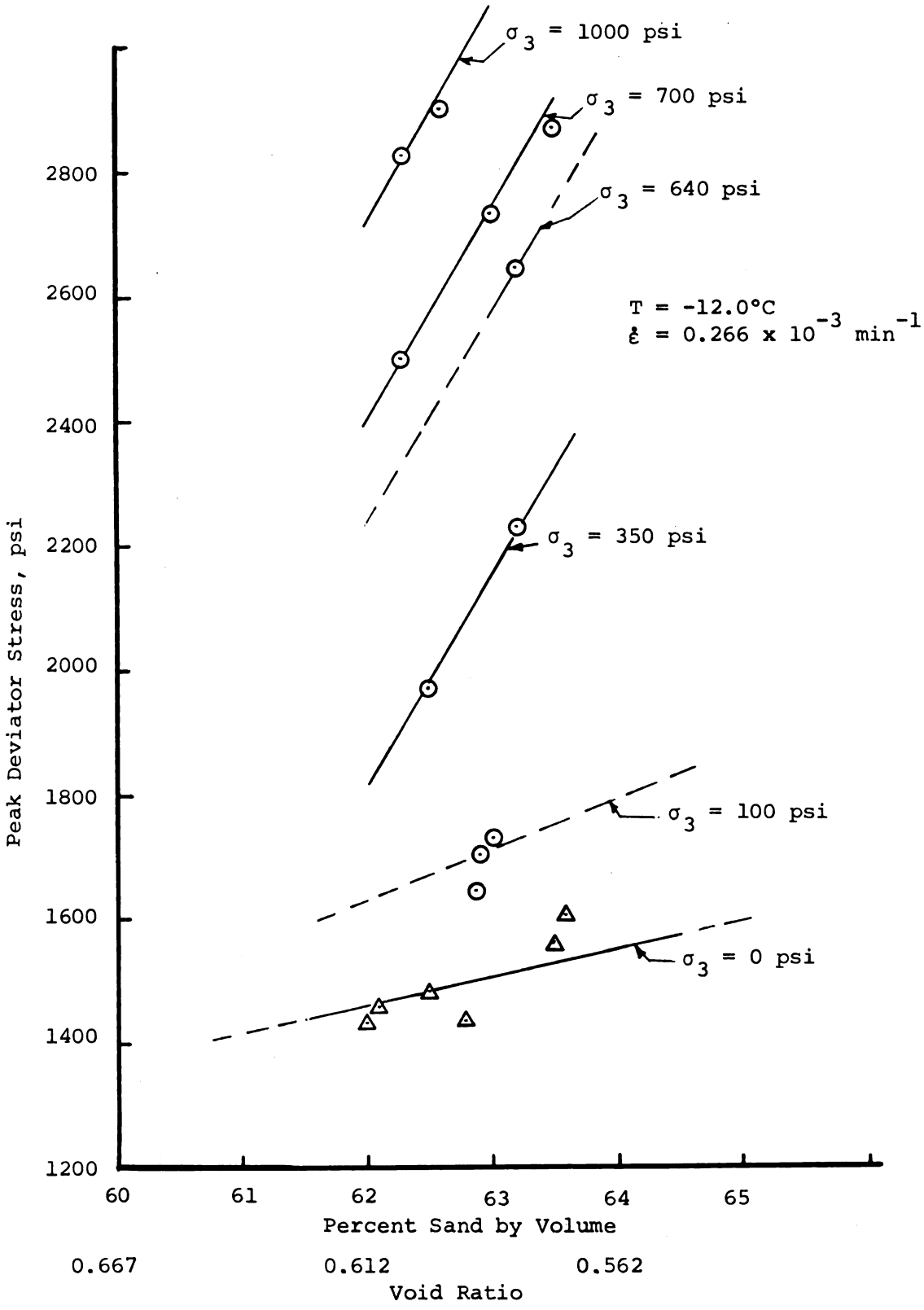

Figure 6-3.--Effect of confining pressure and void ratio on strength

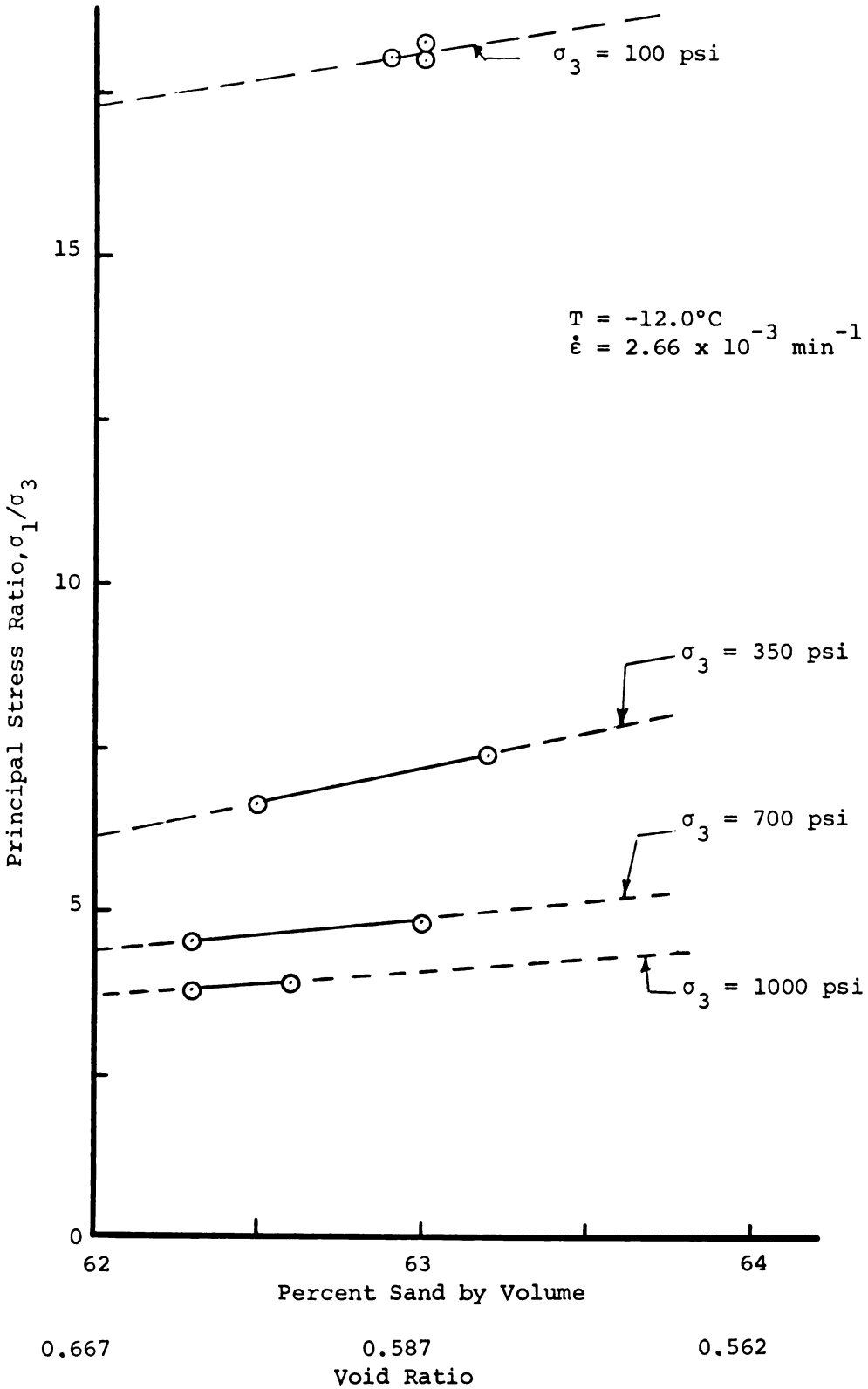

Figure 6-4.--Effect of confining pressure and void ratio on the principal stress ratio

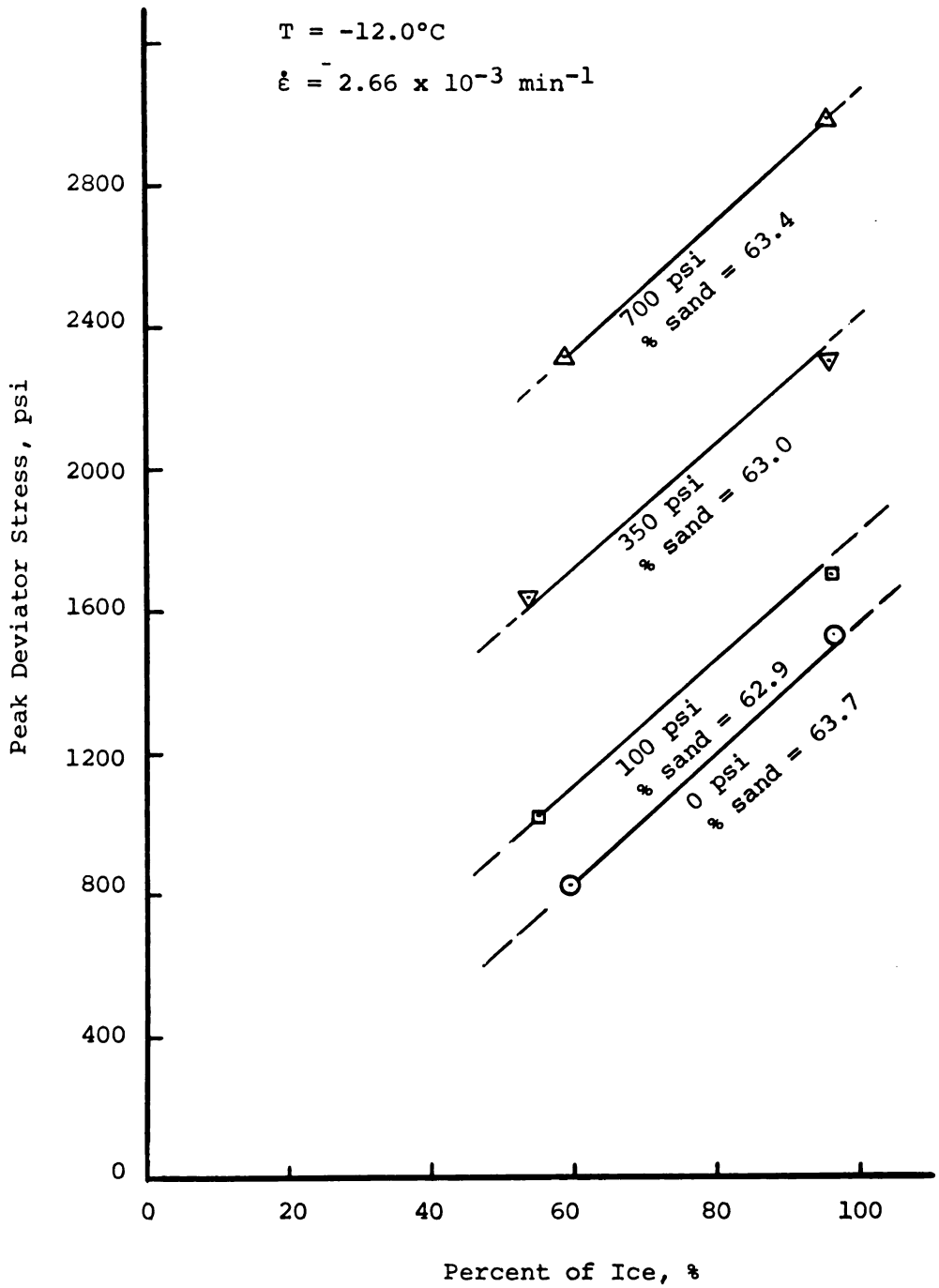

Figure 6-5.--Effect of ice content on strength.

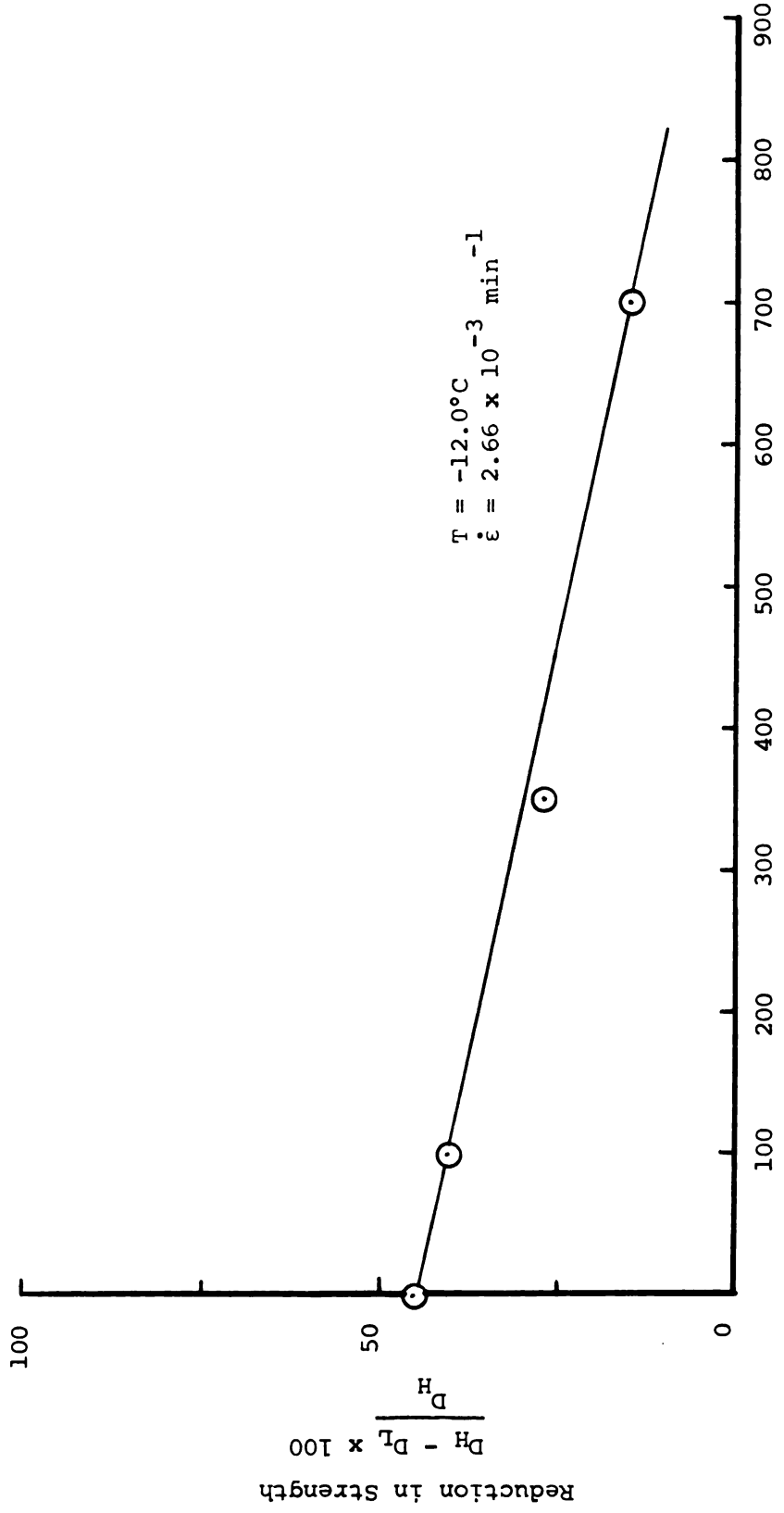

Figure 6-6.--Reduction in strength versus confining pressure.

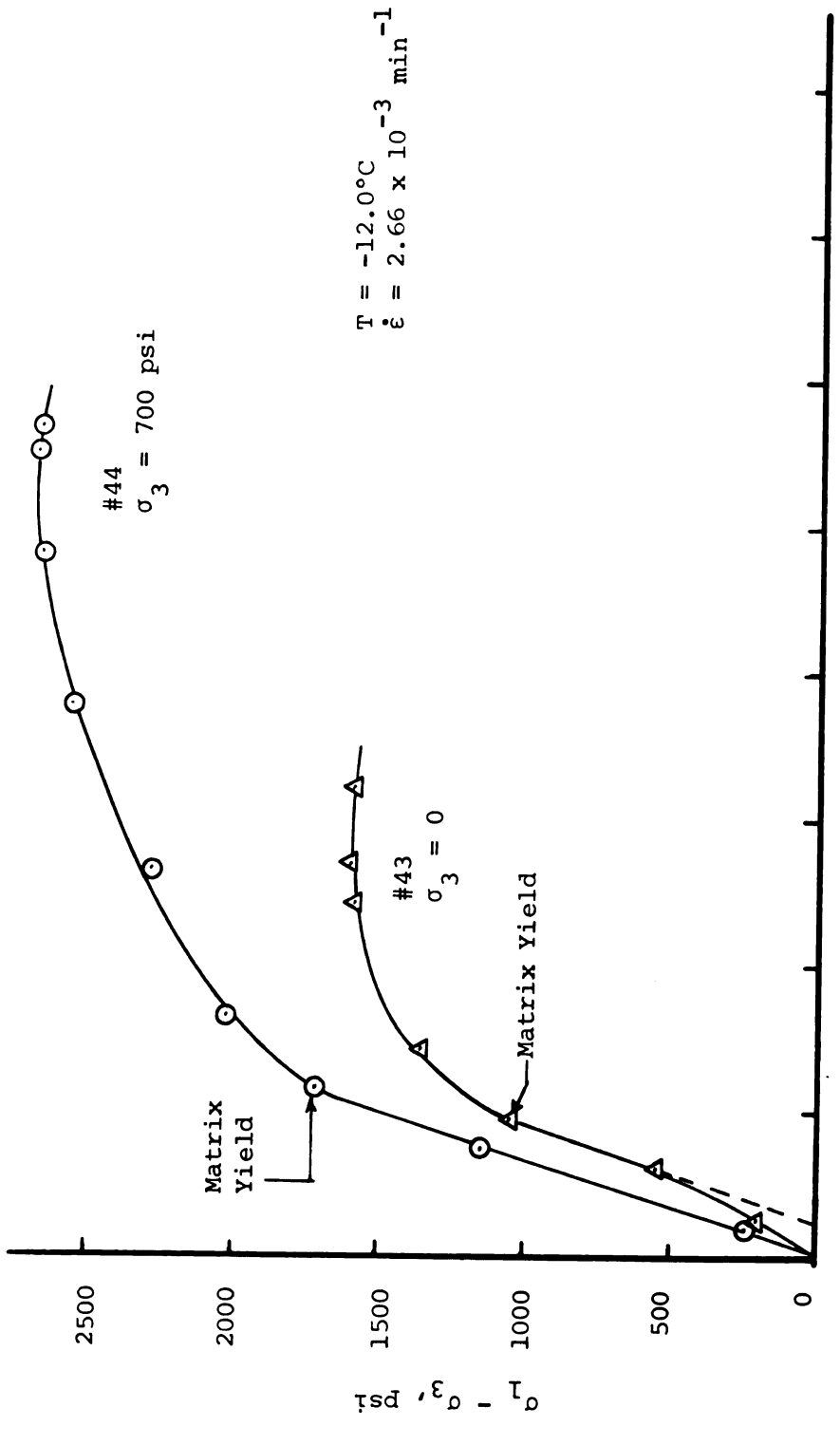

Figure 6-7.--Typical effect of confining pressure on sand-ice.

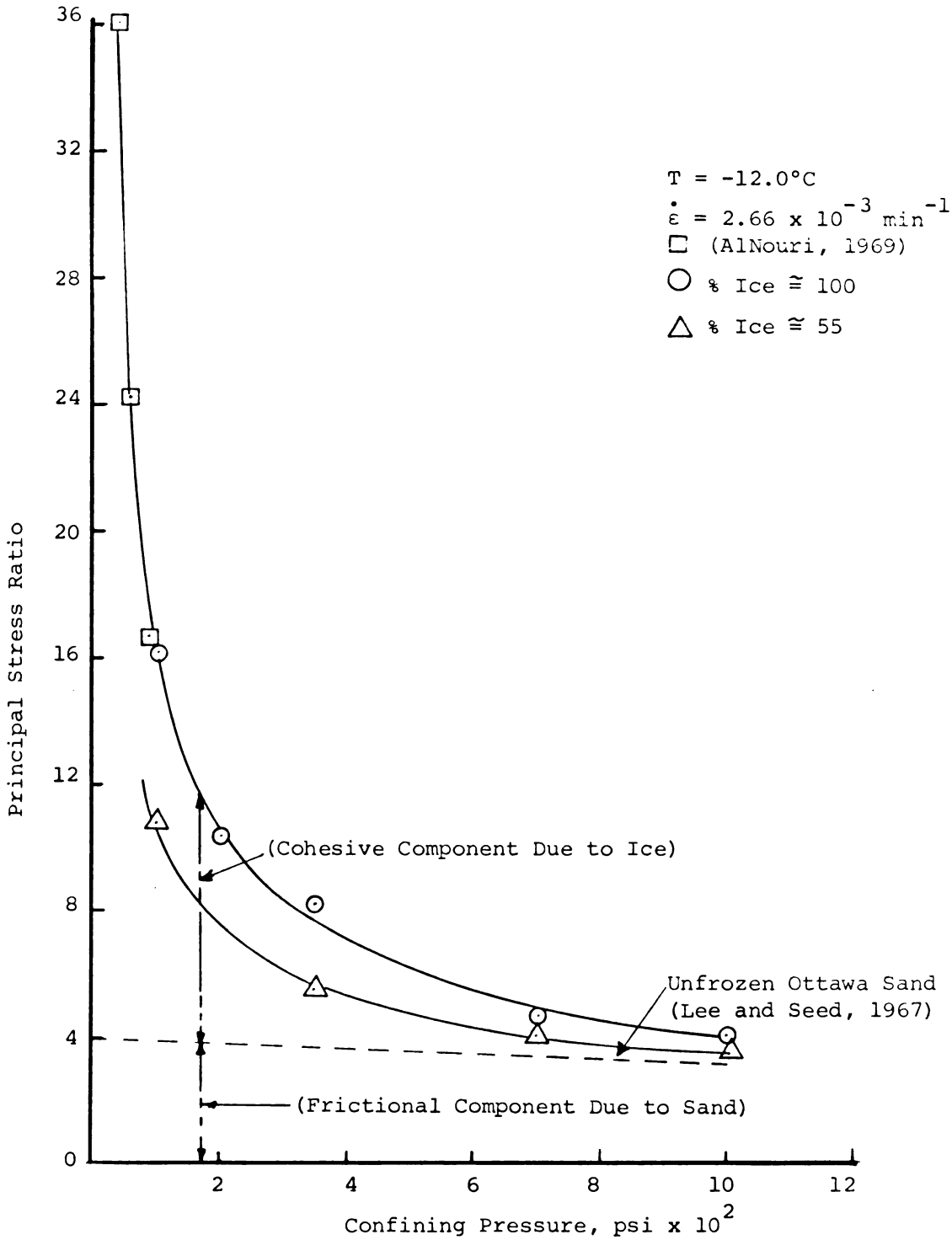

Figure 6-8.--Principal stress ratio versus confining pressure.

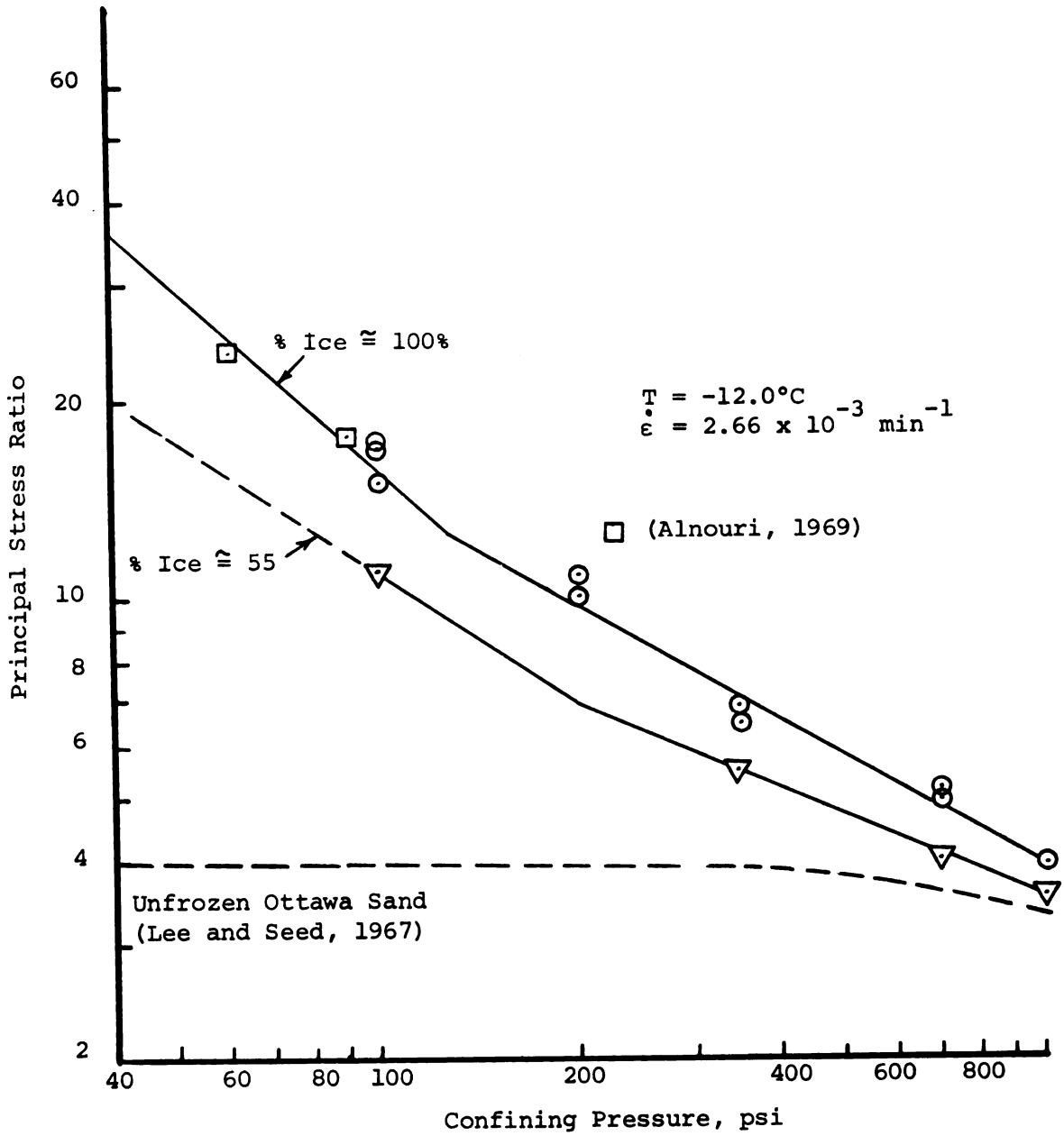

Figure 6-9.--Influence of confining pressure on the principal stress ratio.

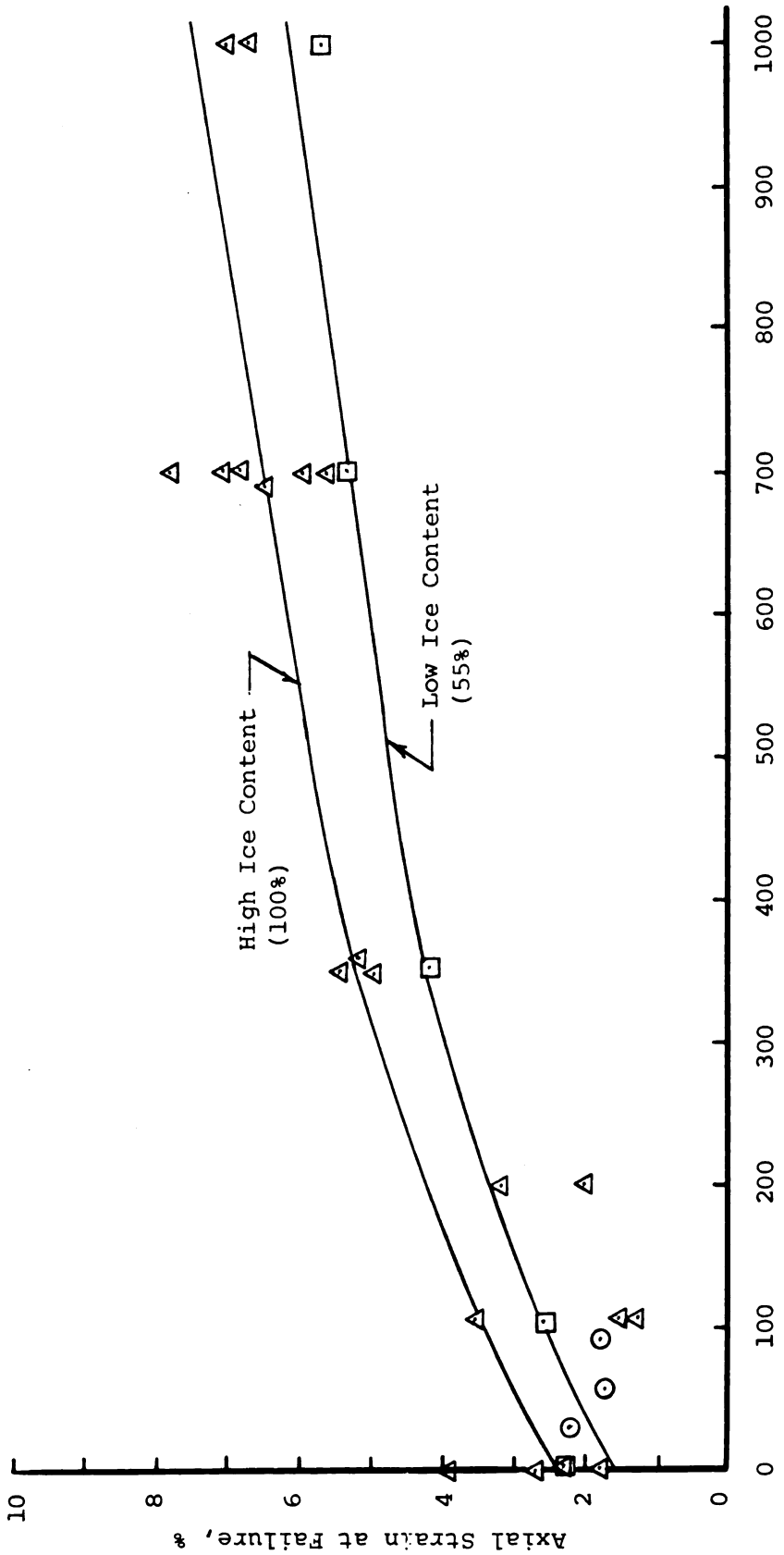

Figure 6-10.--Axial strain at failure for sand-ice samples.

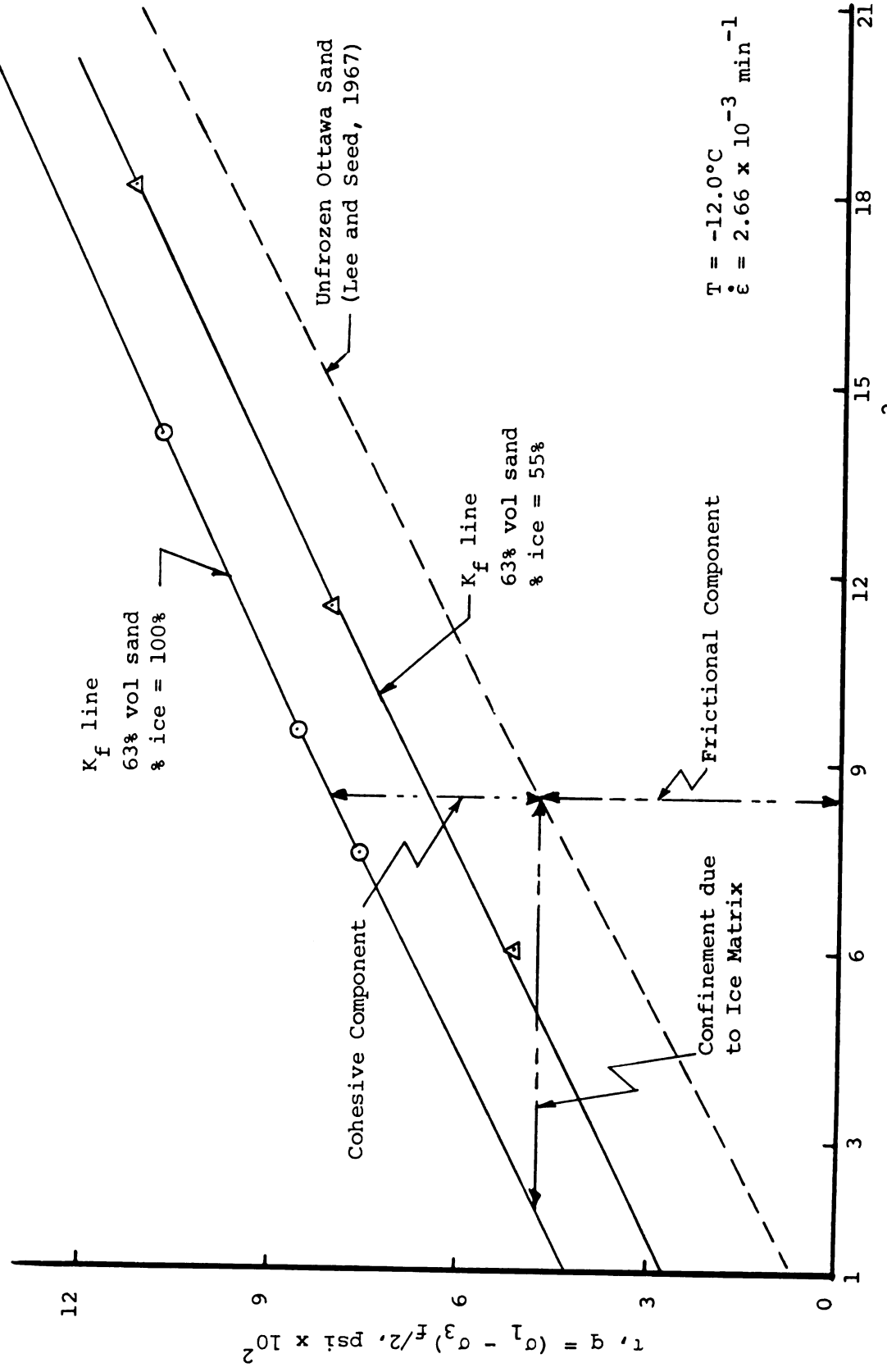

Figure 6-11.--K_f failure line for sand-ice (typical values).

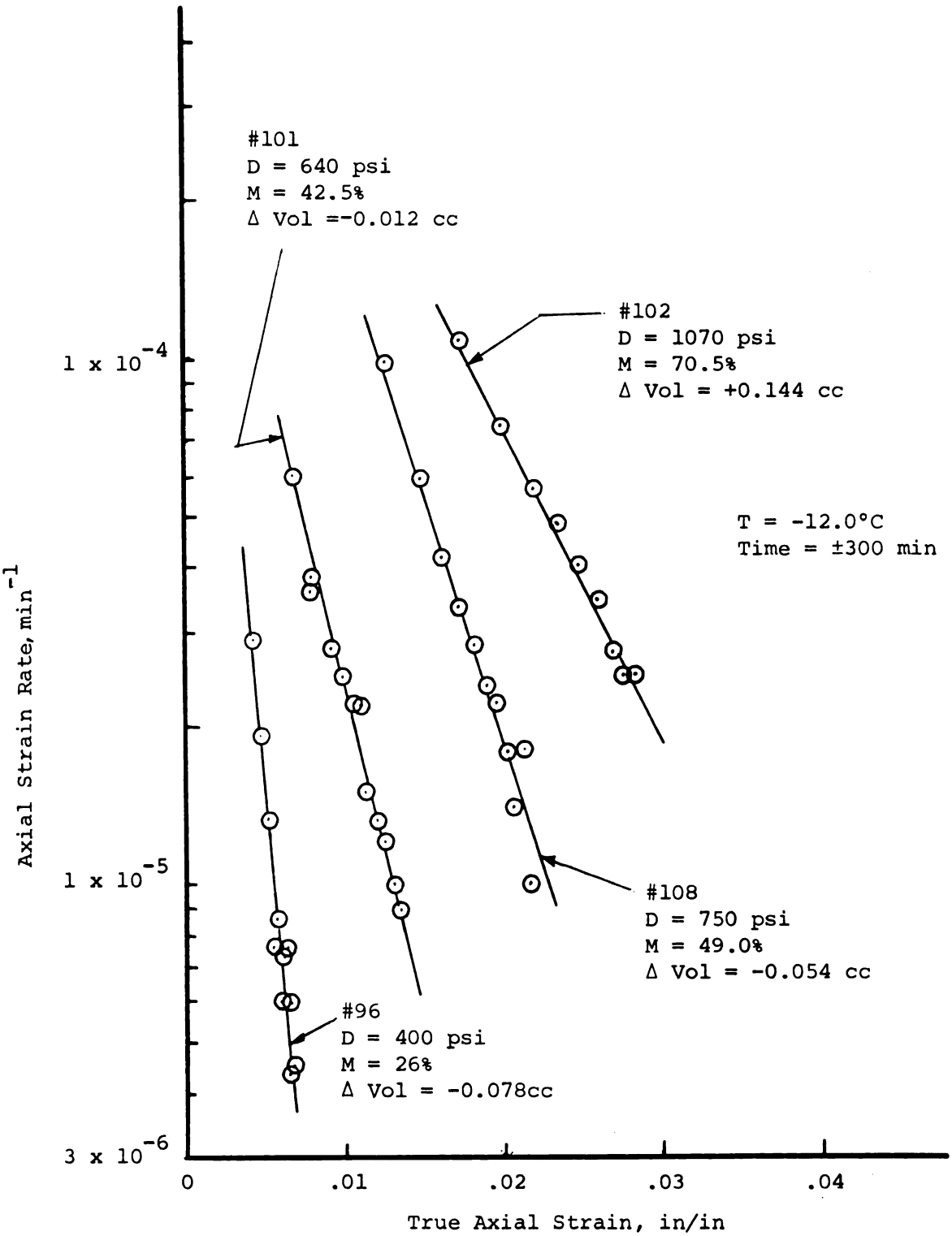

Figure 6-12.--Strain rate versus strain for uniaxial stress creep tests, high ice content.

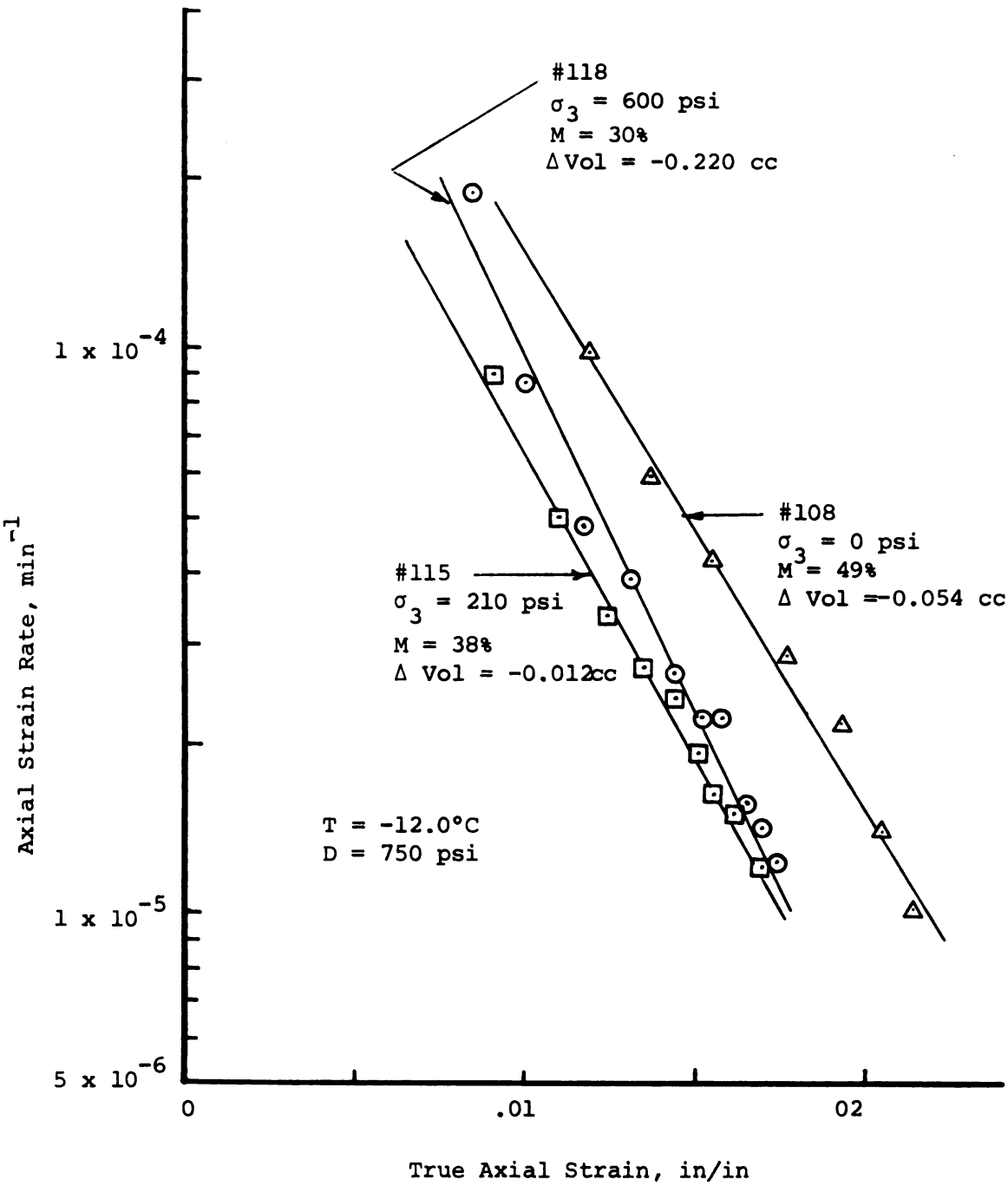

Figure 6-13.--Strain rate versus strain for constant confining pressure test, high ice content.

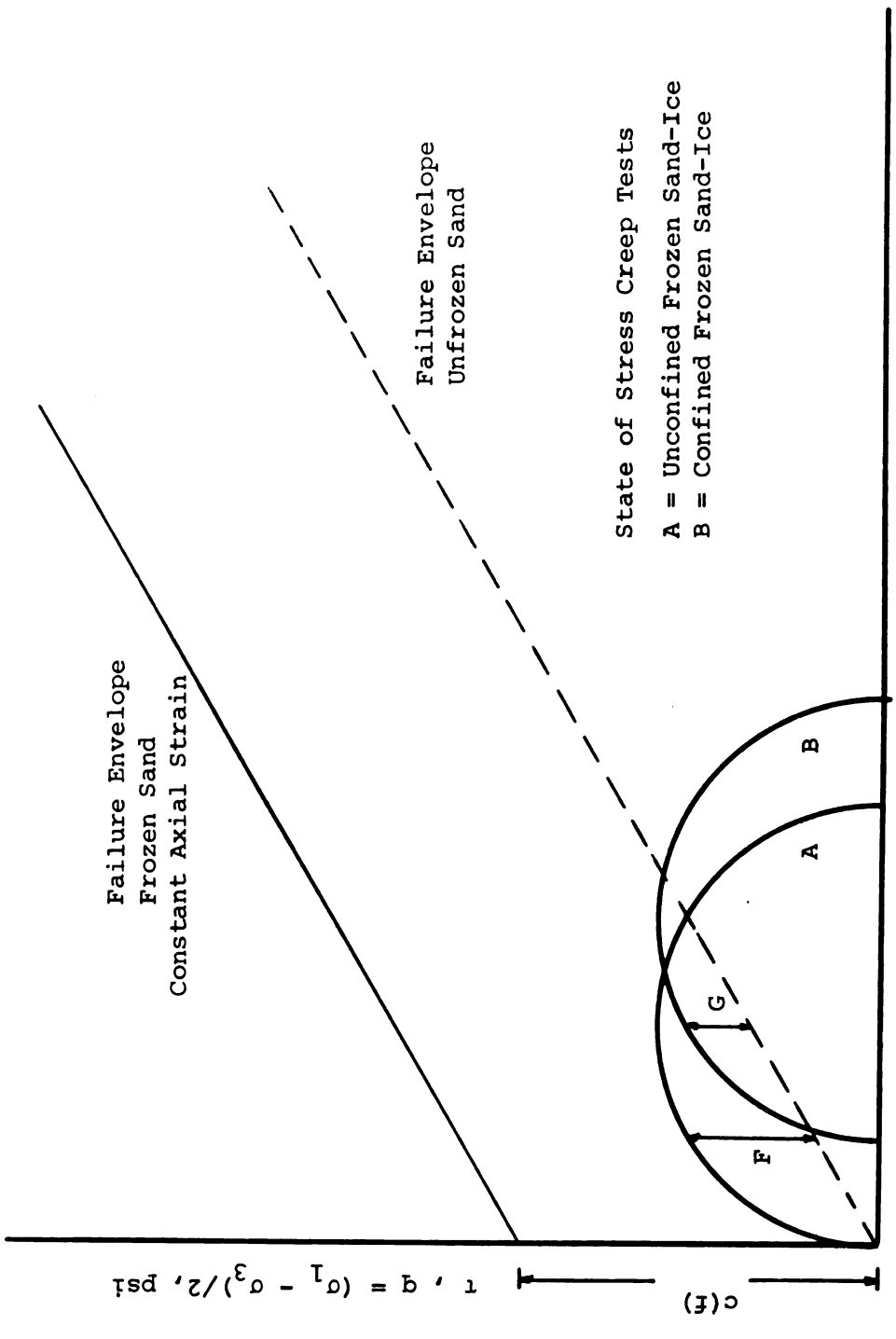

Figure 6-14.--State of stress for uniaxial and confined creep tests.

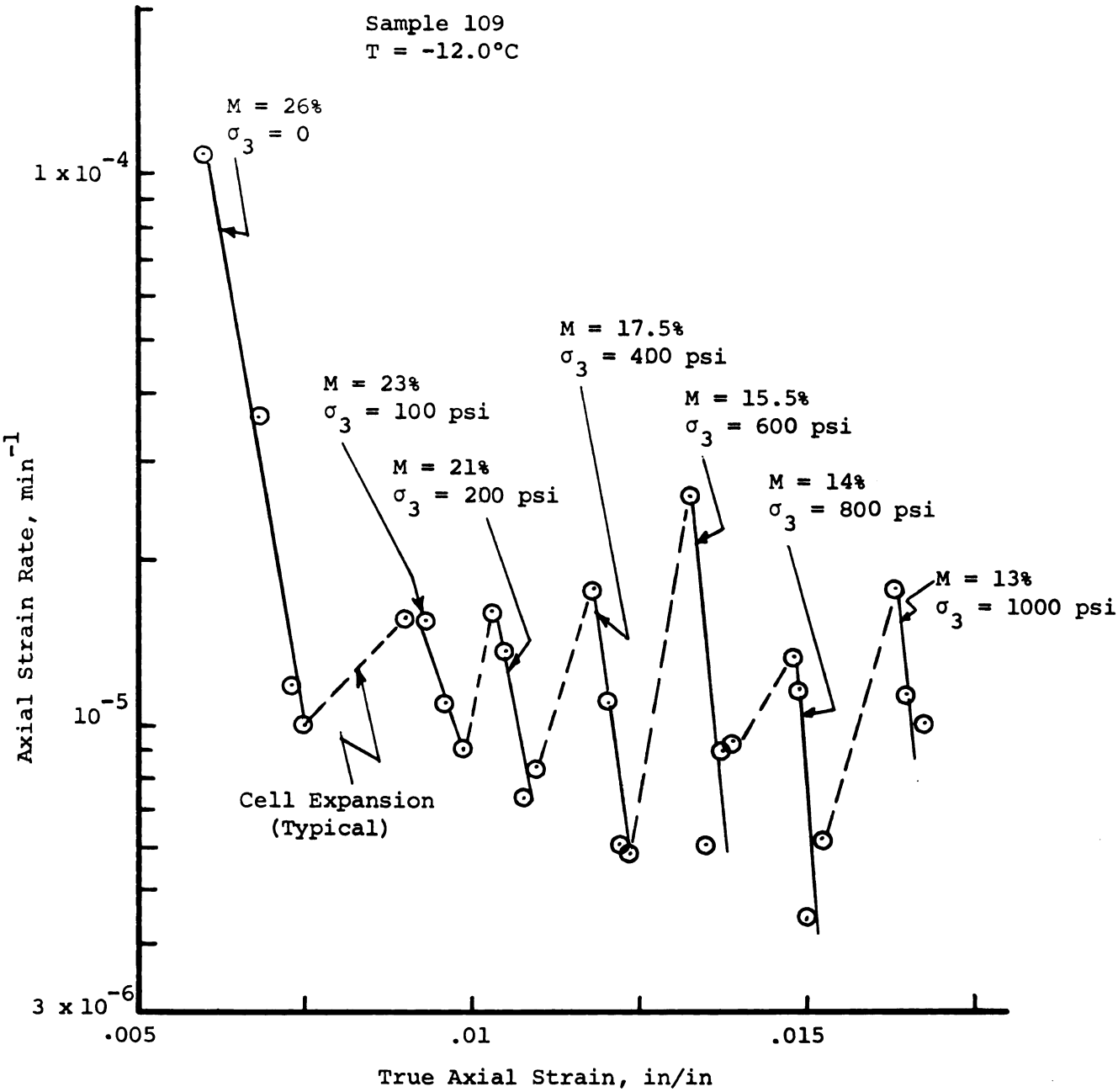

Figure 6-15.--Step-stress creep behavior for a deviator stress of 400 psi, high ice content.

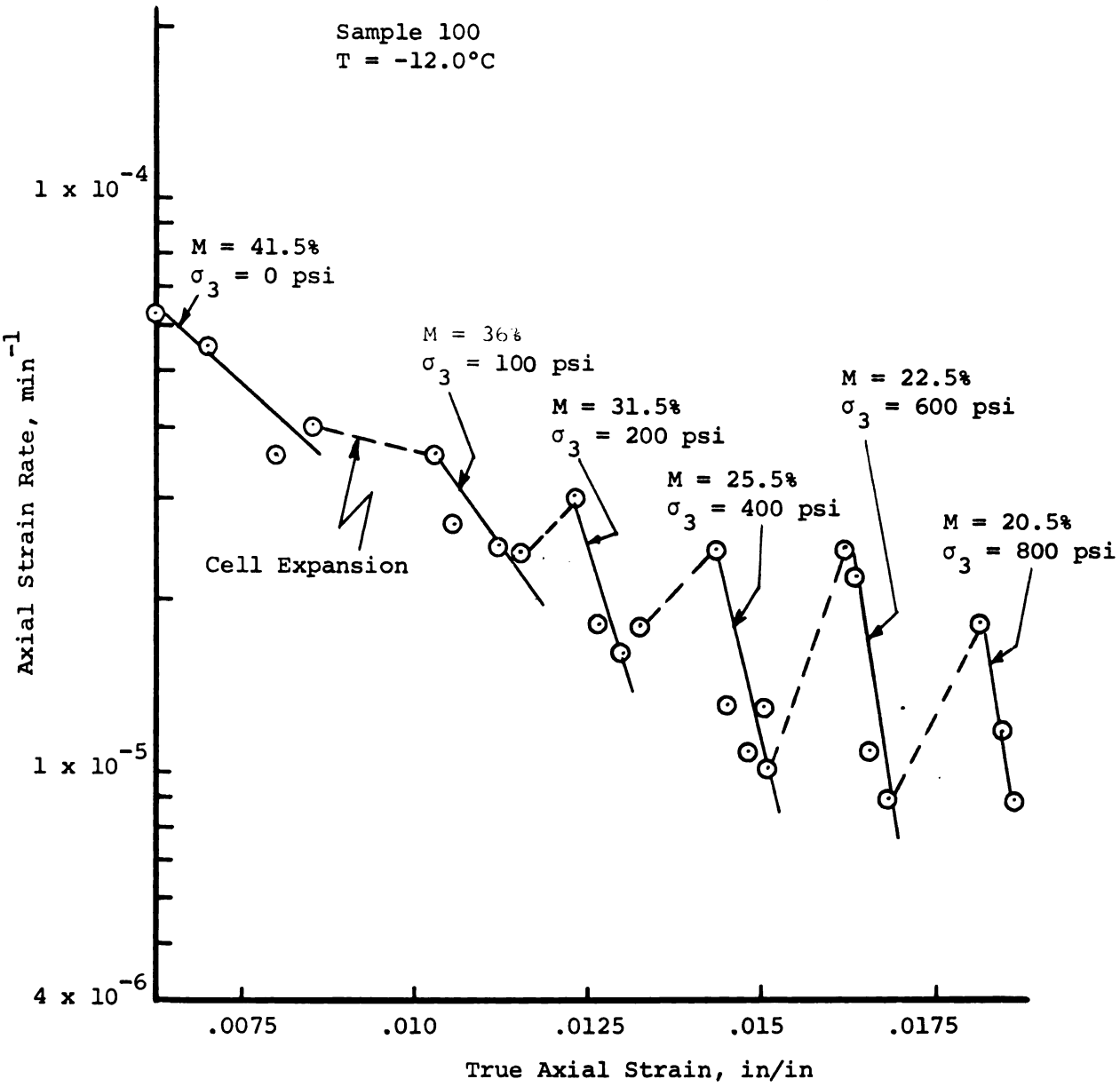

Figure 6-16.--Step-stress creep behavior for a deviator stress of 640 psi, high ice content.

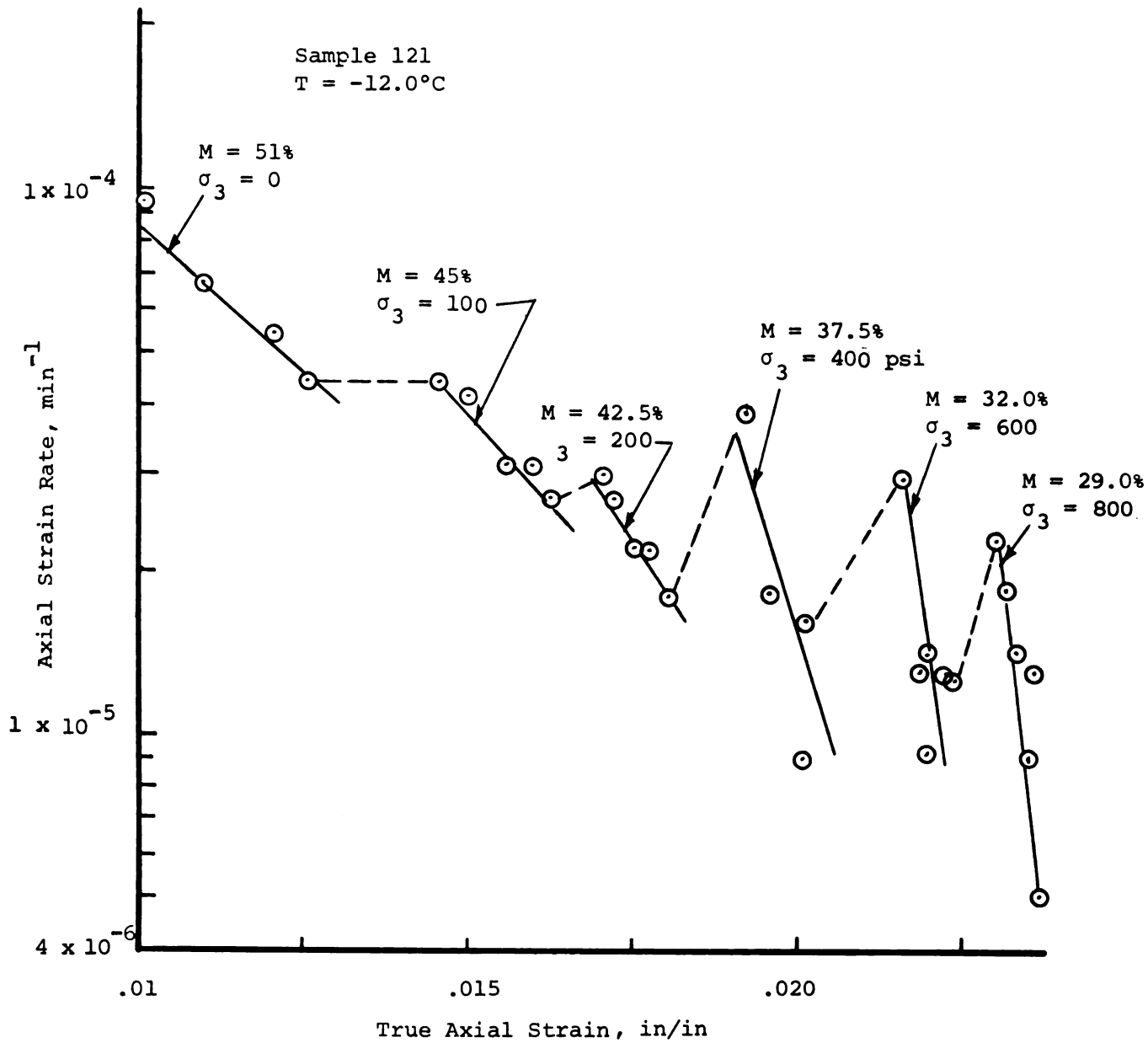

Figure 6-17.--Step-stress creep behavior for a deviator stress of 750 psi, high ice content.

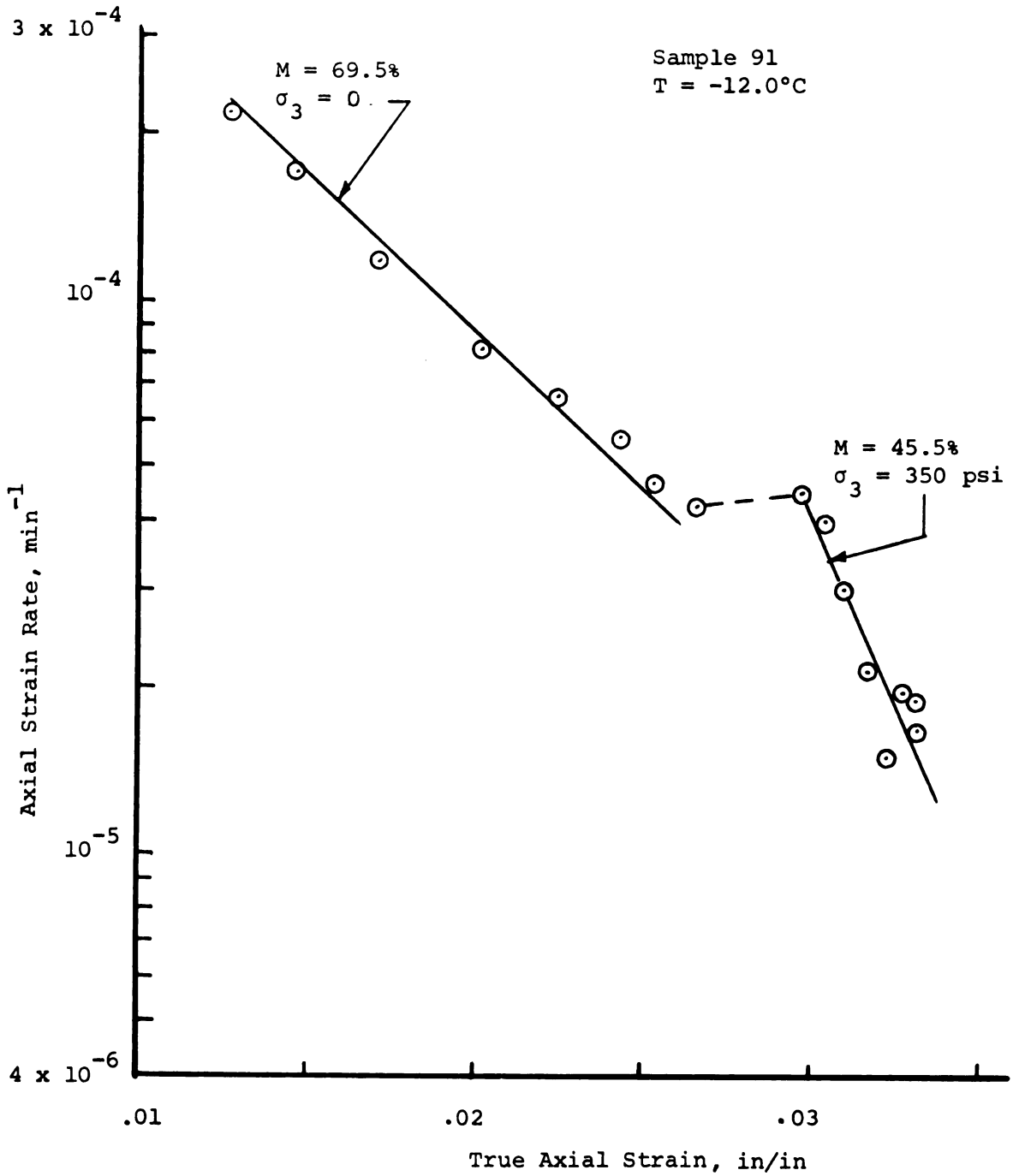

Figure 6-18.--Step-stress creep behavior for a deviator stress of 1070 psi, high ice content.

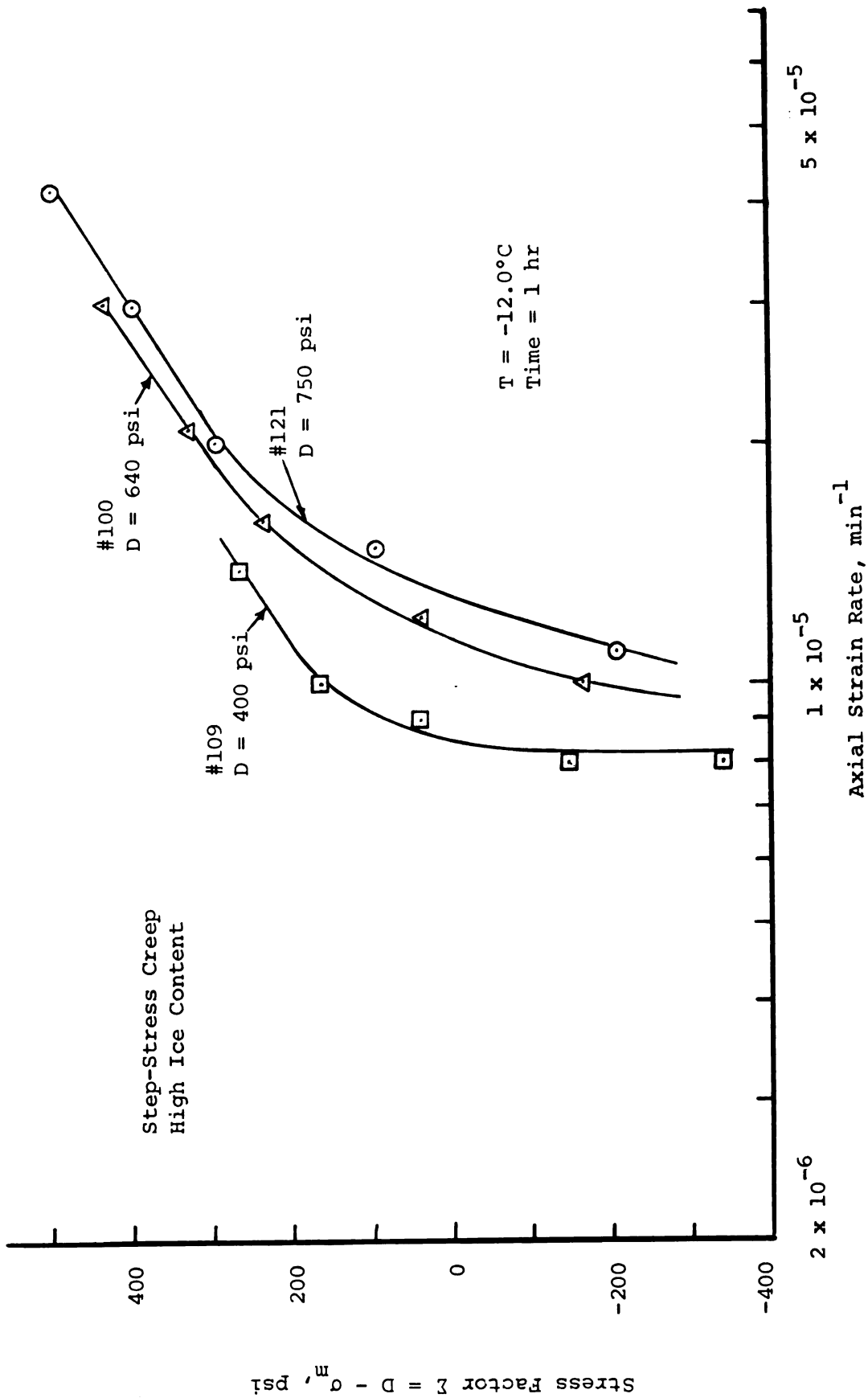

Figure 6-19.--Strain rate versus stress factor Σ.

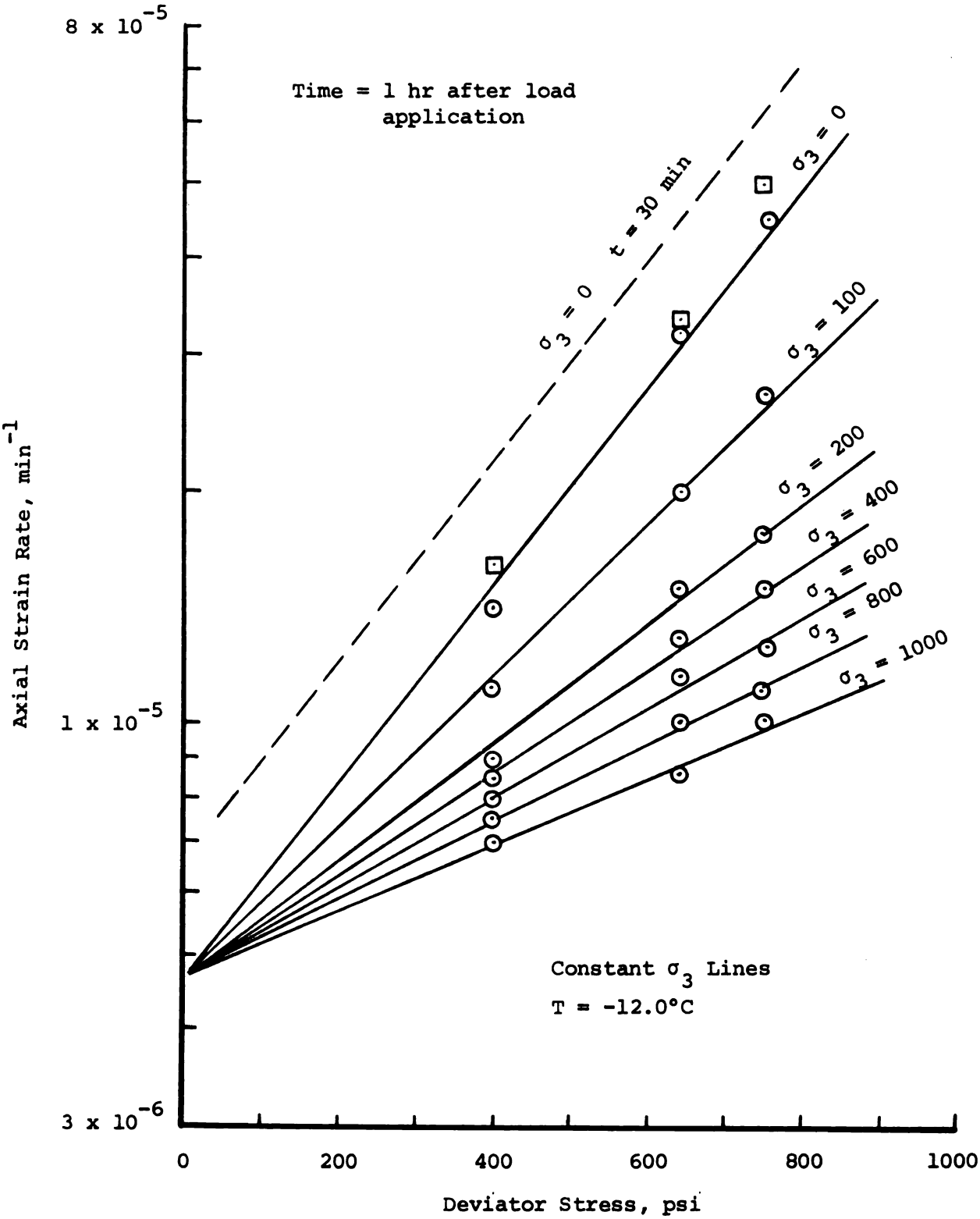

Figure 6-20.--Effect of confining pressure on strain rate.

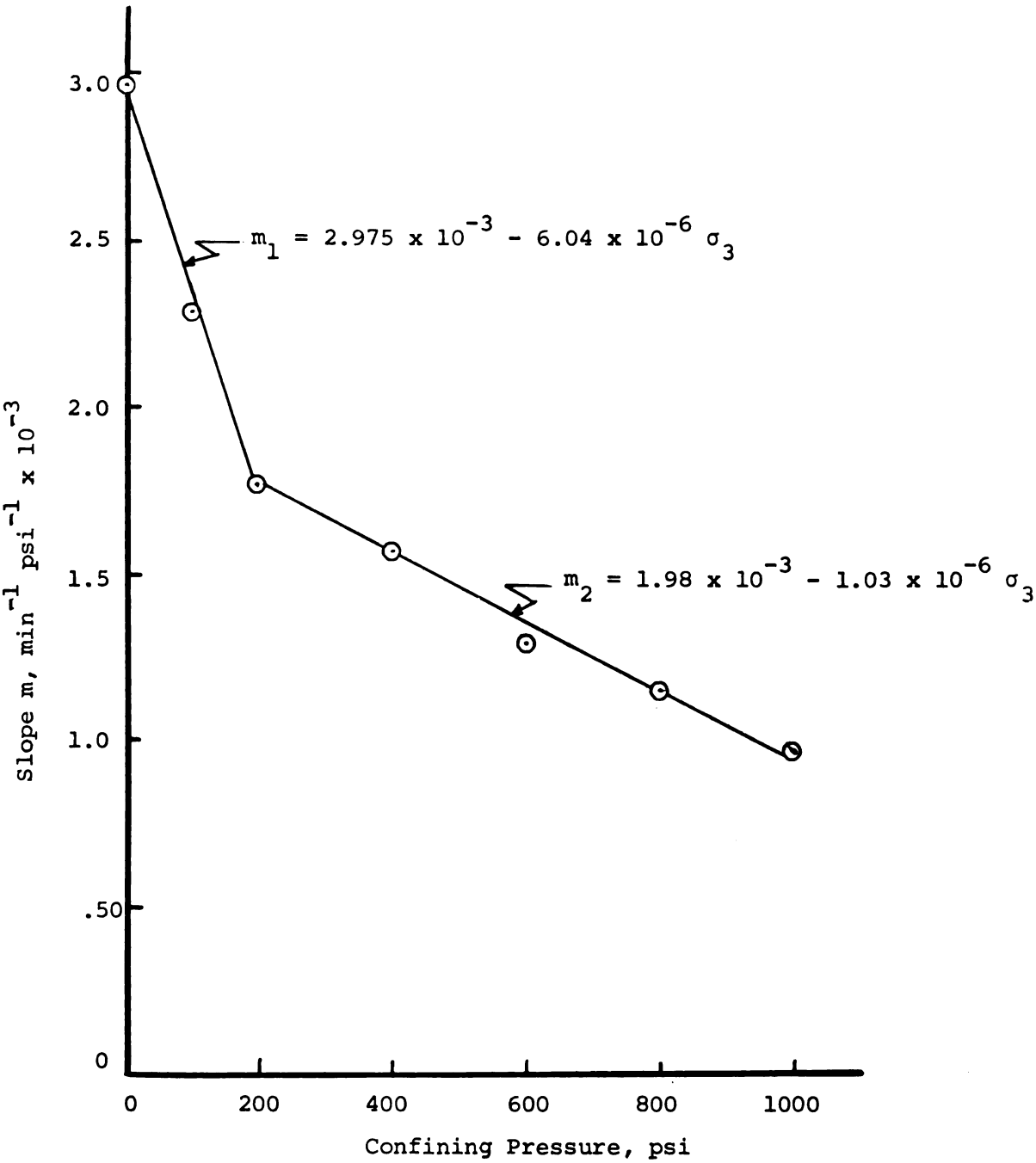

Figure 6-21.--Slope value m versus confining pressure.

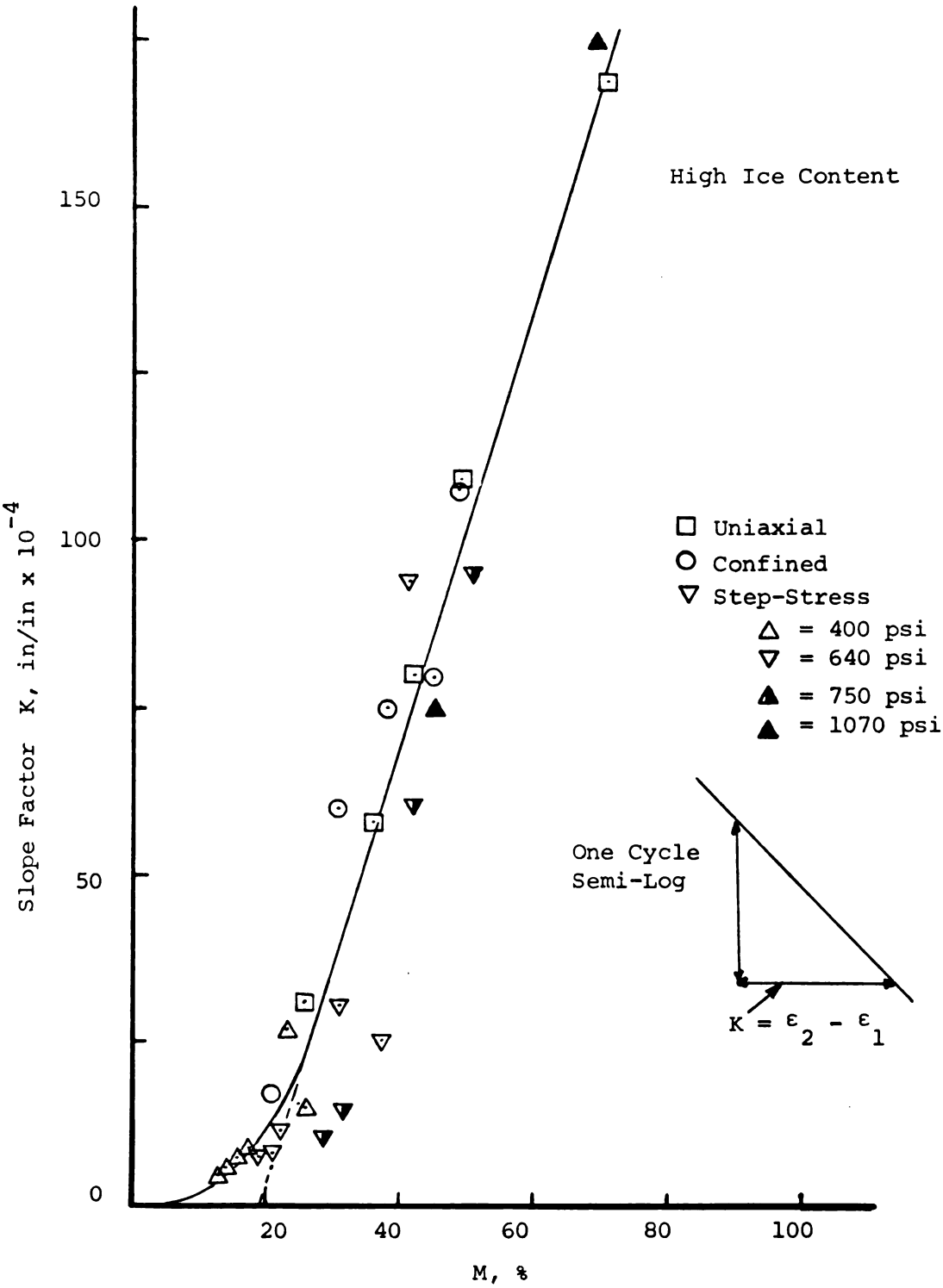

Figure 6-22.--Slope factor K versus percent of maximum deviator stress.

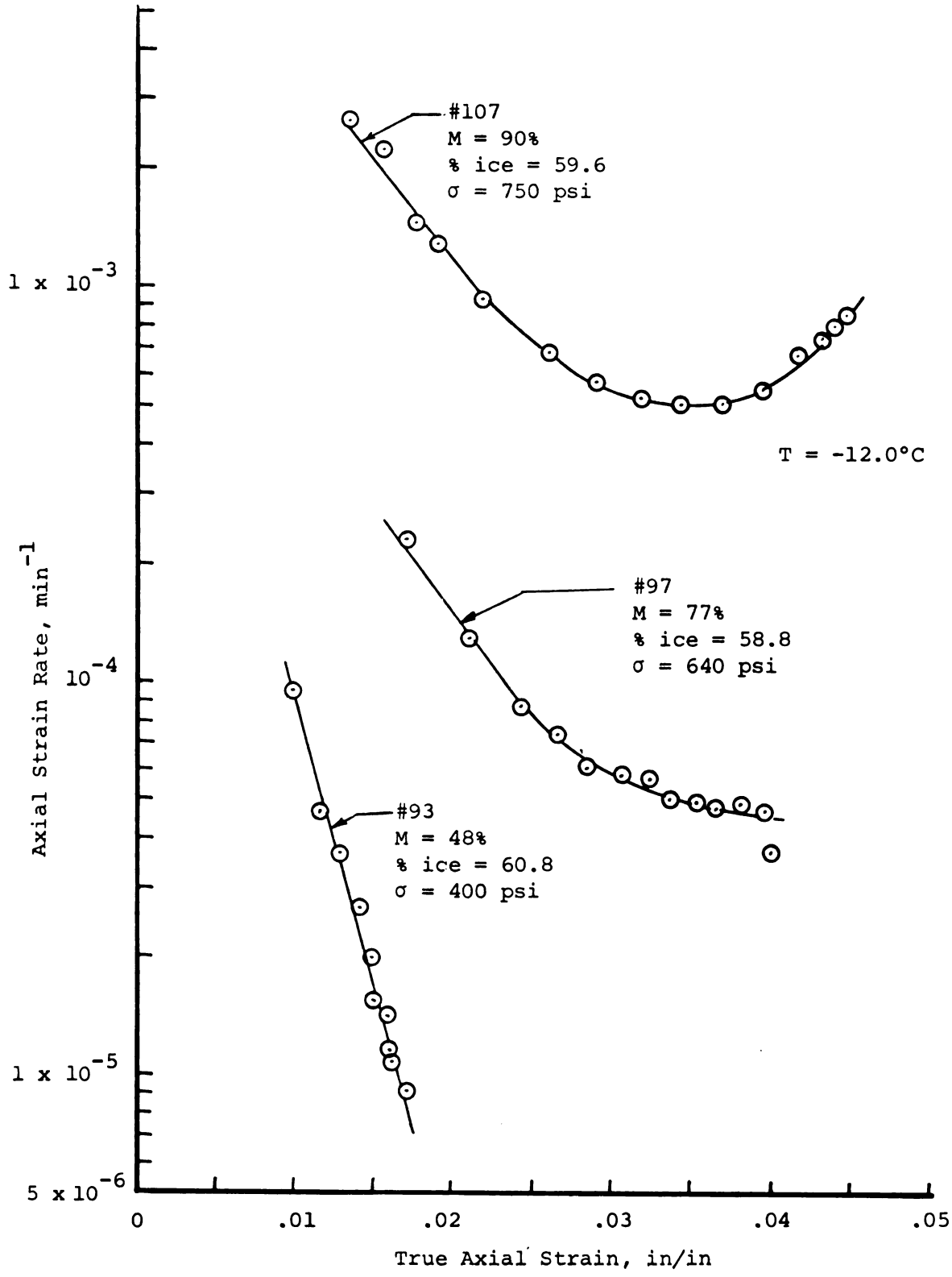

Figure 6-23.--Uniaxial creep test for reduced ice contents.

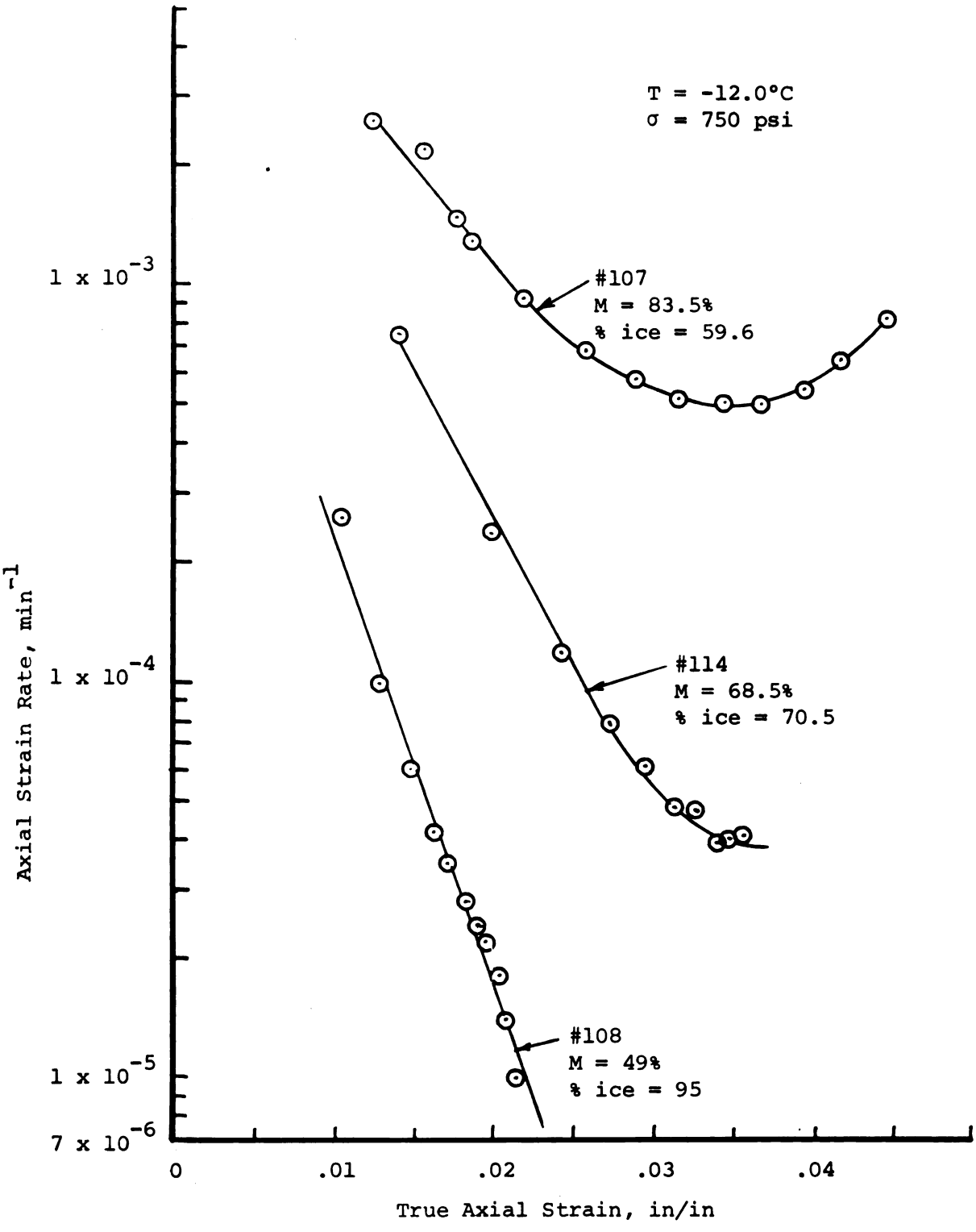

Figure 6-24.--Effect of various levels of ice content on uniaxial creep test behavior.

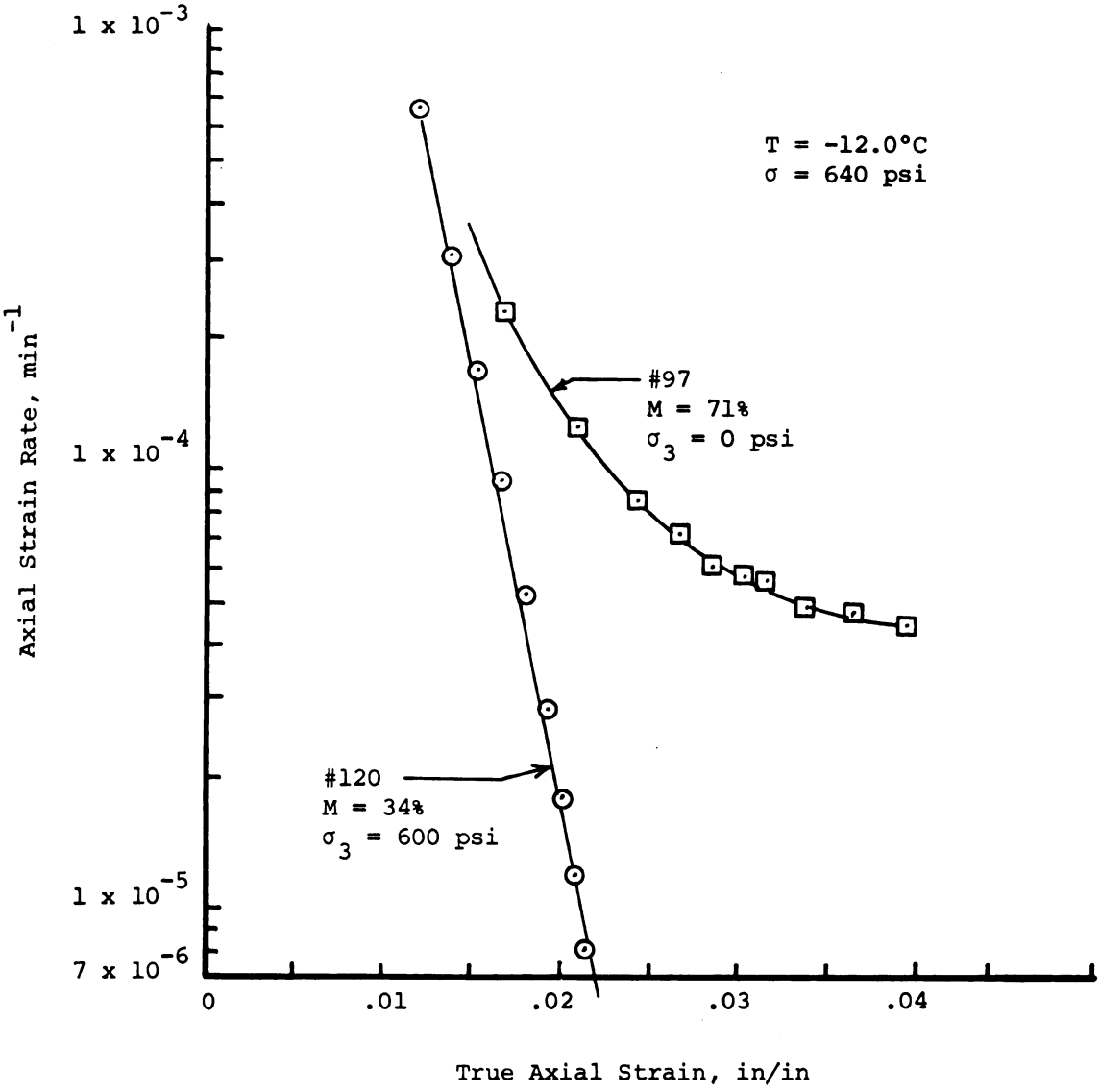

Figure 6-25.--Effect of confining pressure on creep of low ice content samples.

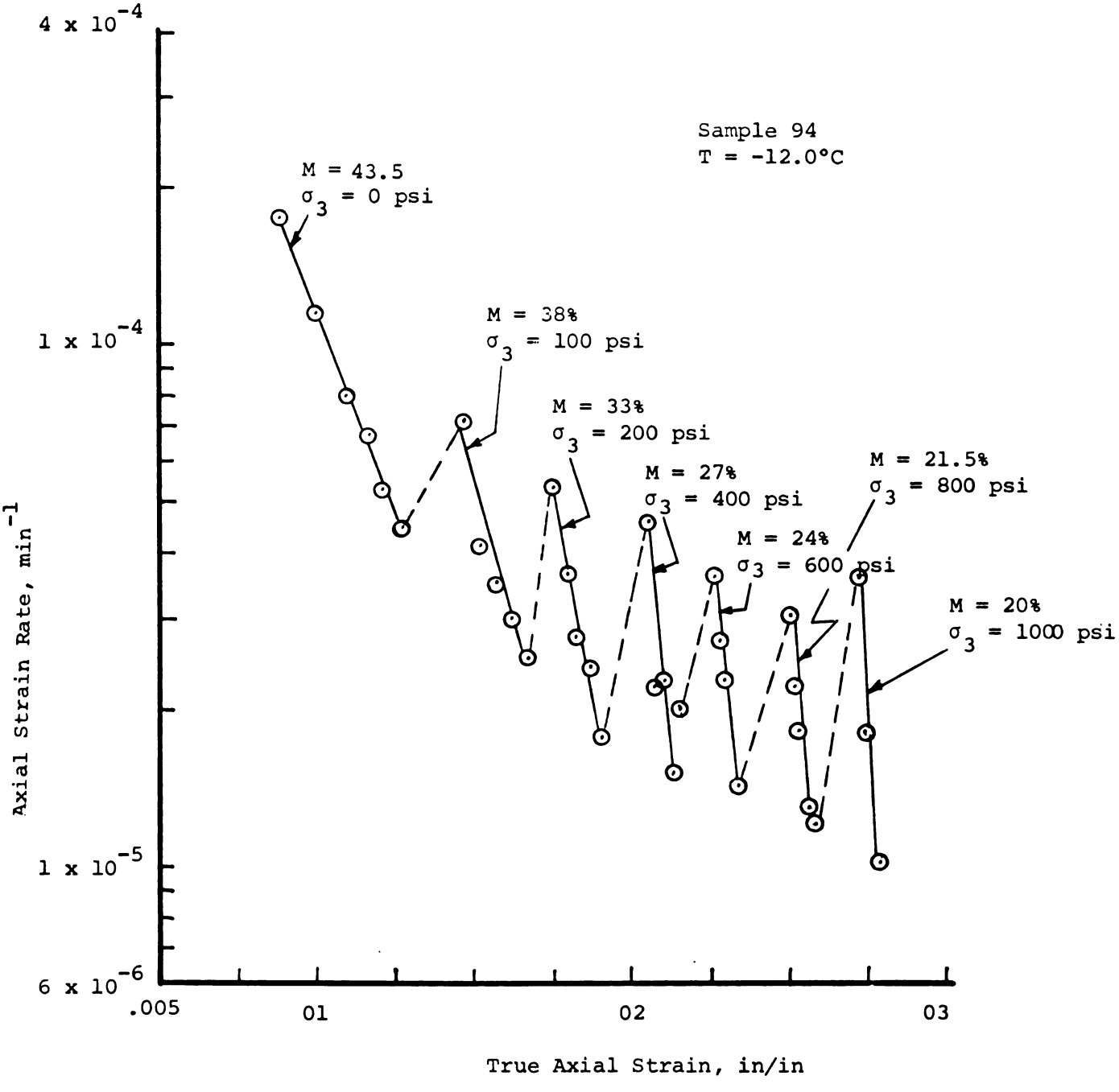

Figure 6-26.--Step-stress creep behavior for deviator stress of 400 psi, low ice content.

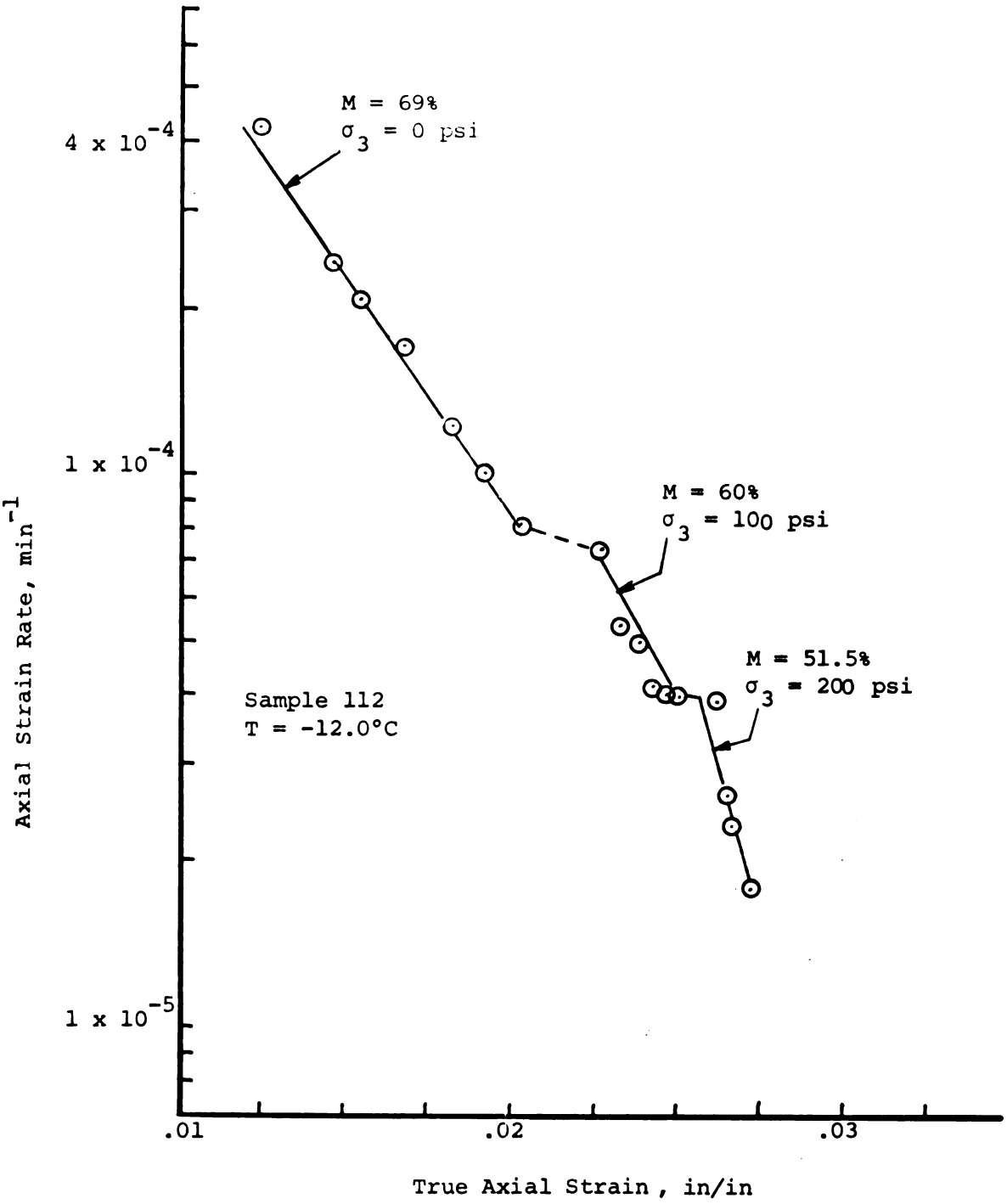

Figure 6-27.--Step-stress creep behavior for a deviator stress of 640 psi, low ice content.

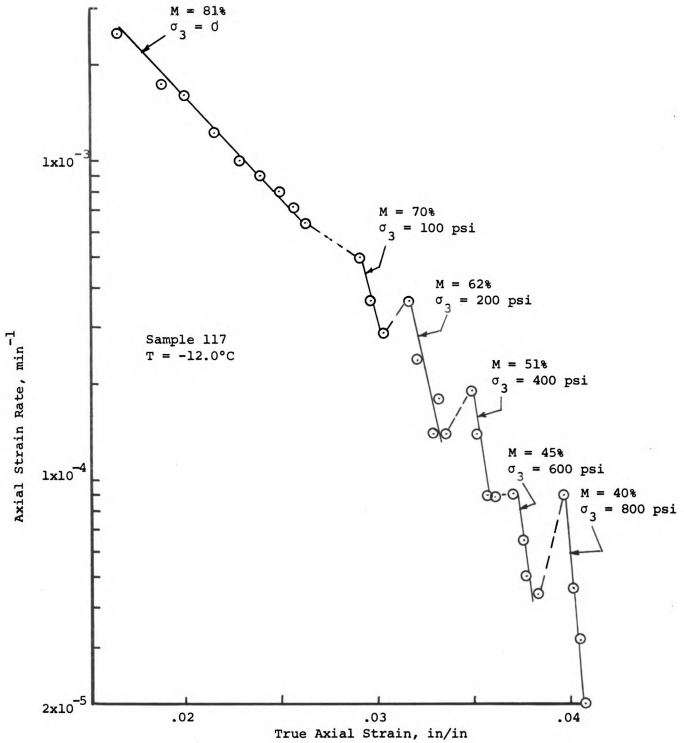

Figure 6-28.--Step-stress creep behavior for a deviator stress of 750 psi, low ice content.

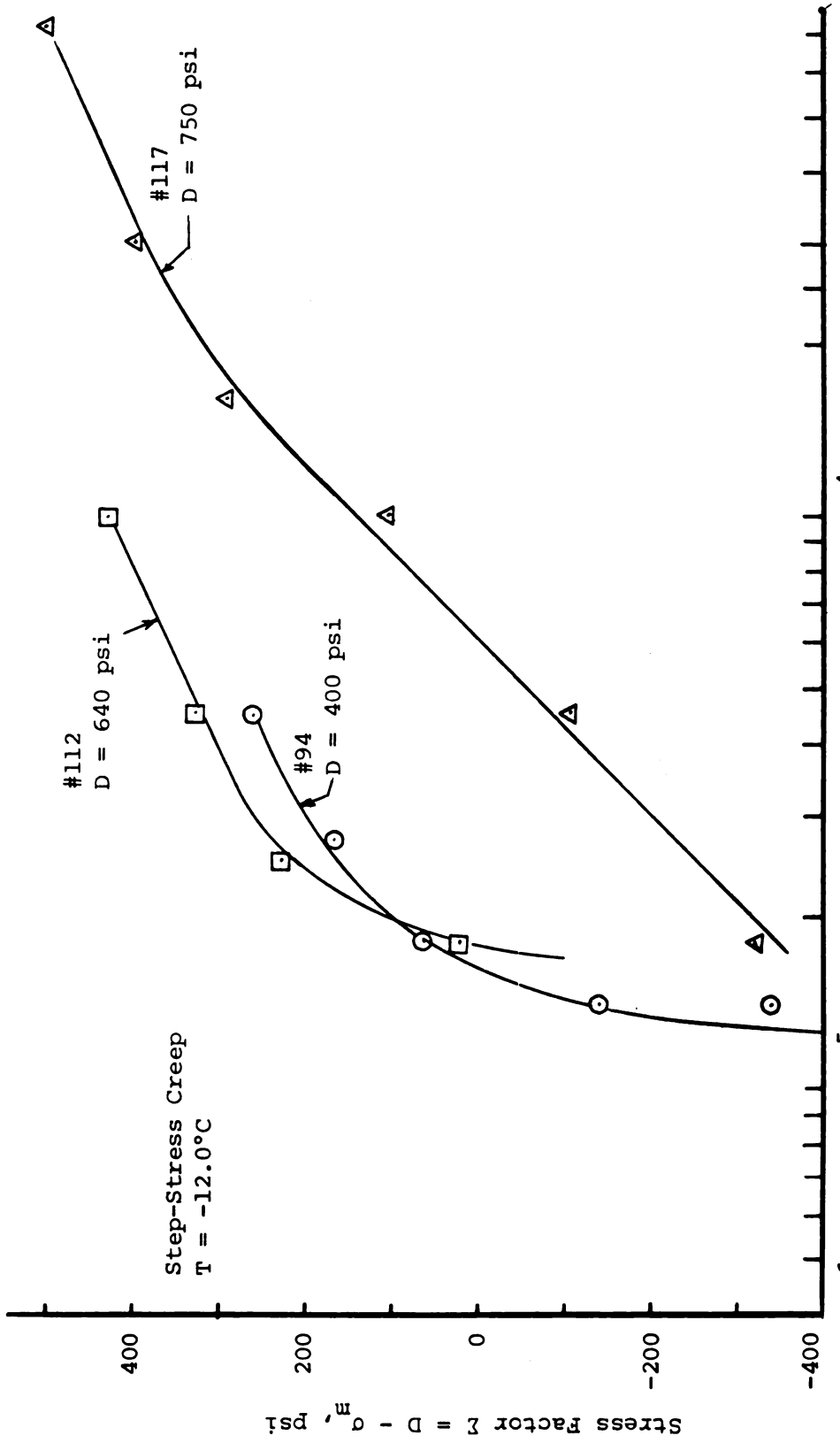

Figure 6-29.--Strain rate versus stress factor Σ for low ice content samples.

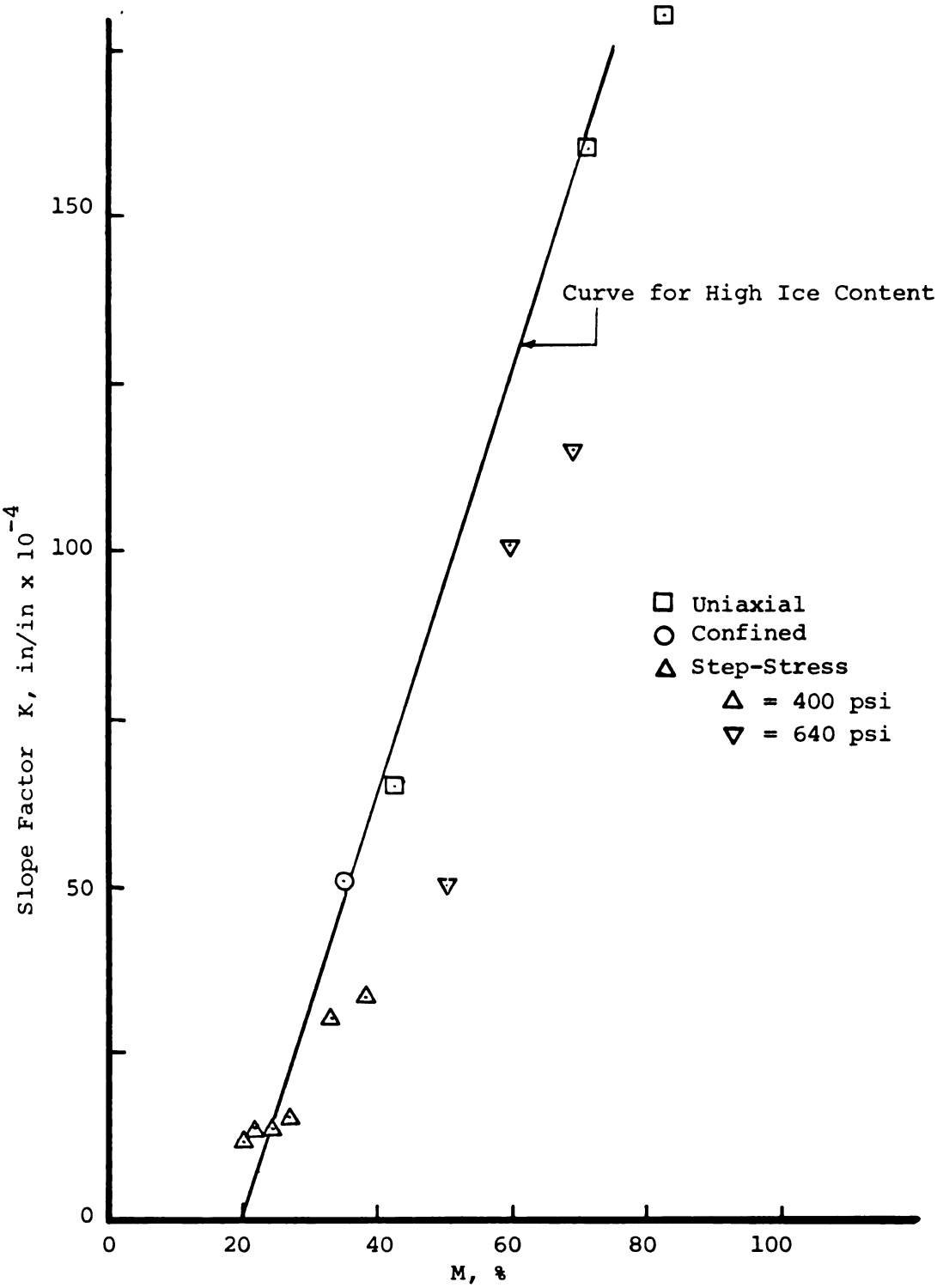

Figure 6-30.--Slope factor K versus percent of maximum deviator stress, low ice content.

CHAPTER VII

SUMMARY AND CONCLUSIONS

7.1 Shearing Resistance

The shearing resistance of sand-ice materials has been studied in terms of the Mohr-Coulomb failure theory in which the shear strength is a summation of a cohesive term and a frictional term. For a constant temperature, it was shown that the cohesive term is dependent on the ice content and strain rate and is independent of the granular component for the percent sand by volume tested. The frictional component was shown to be dependent upon void ratio and independent of the strain rate and ice content. It was observed that the behavior of a sand-ice material is dependent on the magnitude of confining pressure applied to the system. For the unconfined test the ice matrix was the primary contributor to the strength of the material and when the ice matrix yielded, the sample progressed to failure. For confining pressures greater than 200 psi the sand-ice samples showed bilinear stress-strain characteristics. The initial portion of the stress-strain curve was attributed to the ice matrix ending at a matrix yield point. The second portion was due to the development of the frictional component of

strength, which was dependent on the void ratio and the amount of confining pressure. It was shown that dilatancy contributes to the frictional strength of the sand-ice samples. When maximum deviator stresses are used to plot Mohr's circles, the failure envelope exhibits a slight curvature as the normal stress increases. Comparisons with unfrozen sand show that the cohesive and frictional components exist over the entire range of applied stresses. The results indicate a system in which the cohesive component depends on the ice matrix and the frictional component has characteristics similar to those for unfrozen sands tested at high confining pressures. The major conclusions regarding the shear resistance of sand-ice materials are as follows:

1. Dilatancy occurs in sand-ice samples tested to failure and decreases slightly with increasing confining pressure. The dilatancy of sand-ice is less than for unfrozen sands tested at equal condition.

2. A decrease in void ratio (higher density) increases the peak strength for the range of void ratios tested. At higher confining pressures the effect is reduced and the ratio of principal stresses increases only slightly with smaller void ratios.

3. Smaller ice contents reduce the peak strength with a linear dependence on the ice content. This relationship is independent of confining pressure.

4. High confining pressures produce strength characteristics which are predominantly frictional in nature.

5. Failure strains increase as confining pressure increases and decrease slightly with reduced ice content.

6. The failure envelope for sand-ice materials exhibits a slight curvature as normal stress increases, but for engineering design it can be approximated by a straight line. The effective angle of internal friction approximates that for unfrozen sand at high confining pressure. This relationship is independent of the ice content.

7. The cohesive component of strength at failure decreased only slightly with increased confining pressure and remains essentially constant for a constant temperature and strain rate.

7.2 Creep Behavior

The creep behavior of sand-ice materials was shown to follow "classical" behavior exhibited by other materials such as clays, metals and plastics. By conducting uniaxial creep tests at various levels of constant axial stress, the general creep characteristics of the sand-ice materials were obtained. Using these tests as a basis for comparison, the effects of confining pressure

were obtained using step-stress and confined testing techniques. The experimental results show that increases in confining pressure reduce strain rates. Confining pressures below 200 psi have the greater effect whereas above 200 psi creep rates decreases less rapidly with increased confining pressure. Step-stress testing proved useful in predicting the effects of confining pressure so that creep rate could be calculated as a function of the confining pressure and deviator stress. The expression obtained was defined for regions both above and below 200 psi.

Reduced ice contents have no basic effect on the shape of the creep curves. It was shown that the same equations used for high ice content samples can also be used for the reduced ice content samples when the deviator stress was modified. Finally, it was observed that all creep tests could be related by a term called the percent of maximum deviator stress, M. Tests conducted at equal percents of maximum deviator stress produced similar results and the decrease in strain rate for a particular value of M were the same for both high and reduced ice contents. Conclusions concerning the creep of sand-ice materials include:

1. For a constant deviator stress, strain rate is decreased exponentially by increasing confining

pressure. The high and low stress regions appear to be bounded by the common 200 psi stress level.

2. The effect of confining pressure on creep rate is greatest for pressures less than 200 psi.

3. Reduced ice content has no basic effect on the creep characteristics of sand-ice material but at equal deviator stresses, higher strain rates occur for the reduced ice samples.

4. The applied deviator stress for high and reduced ice content samples can be related to the maximum deviator stress obtained from constant strain rate tests by a term M, percent of maximum deviator stress. Samples tested with the same percent of maximum deviator stress exhibit the same creep behavior and the resulting strain rates are equal.

5. The strain rate versus strain curve for sand-ice materials can be approximated using a constant slope factor K, which describes the decrease in strain rate per increment of strain for any given percent of maximum deviator stress.

BIBLIOGRAPHY

BIBLIOGRAPHY

Abdel-Hady, M. A. "Rheological Properties of Bituminous Stabilized Soils." Unpublished Ph.D. dissertation, University of Illinois, 1964.

AlNouri, I. "Time Dependent Strength Behavior of Two Soil Types at Lowered Temperatures." Unpublished Ph.D. dissertation, Michigan State University, 1969.

Andersland, O. B., and Akili, W. "Stress Effects on Creep Rates of a Frozen Clay Soil." Geotechnique, XVII, No. 1 (March, 1967), 27-39.

Andersland, O. B., and AlNouri, I. "Time Dependent Strength Behavior of Frozen Soils." Journal of the Soil Mechanics and Foundations Division, ASCE, XCVI, No. SM4 (July, 1970), 1249-1268.

Anderson, Duwayne M. "Ice Nucleation and the Substrate-Ice Interface." Nature, CCXVI (November, 1967).

Dillon, H. B., and Andersland, O. B. "Deformation Rates of Polycrystalline Ice." Proceedings of International Conference on Physics of Snow and Ice. The Institute of Low Temperature Science, Hokkaido University, Sapporo, Japan, August, 1967.

Glasstone, S.; Laidler, H. J.; and Eyring, H. The Theory of Rate Processes. New York: McGraw-Hill Book Co., Inc., 1941.

Glen, J. W. "The Creep of Polycrystalline Ice." Proceedings of Royal Society of London, Series A, 228, 1955, pp. 519-538.

Gold, T. W. "Deformation Mechanisms in Ice." Chapter 2, Ice and Snow Properties, Processes and Applications. Edited by W. D. Kingery. Cambridge, Mass.: MIT Press, 1963.

Goughnour, R. R. "The Soil-Ice System and the Shear Strength of Frozen Soils." Unpublished Ph.D. dissertation, Michigan State University, 1967.

Goughnour, R. R., and Andersland, O. B. "Mechanical Properties of a Sand-Ice System." Journal of the Soil Mechanics and Foundations Division, ASCE, XCIV, No. SM4 (July, 1968), 923-950.

Halbrook, T. R. "Mechanical Properties of Ice." Unpublished M.S. thesis, Michigan State University, 1964.

Hall, E. B., and Gordon, B. B. "Triaxial Testing with Large Scale High Pressure Equipment." Laboratory Shear Testing of Soils, Special Technical Publication, No. 361, American Society for Testing and Materials, 1963, pp. 315-328.

Hirschfeld, R. C., and Poulous, S. J. "High Pressure Triaxial Tests on a Compacted Sand and an Undisturbed Silt." Laboratory Shear Testing of Soils, Special Technical Publication, No. 361, American Society for Testing and Materials, 1963, pp. 329-341.

Jumikis, A. R. "Natural Freezing." Thermal Soil Mechanics. New Brunswick, N.J.: Rutgers University Press, 1966.

Kaplar, C. W. "Some Strength Properties of Frozen Soils and Effect of Loading Rate." Special Report 159, Cold Regions Research and Engineering Laboratory, Hanover, New Hampshire, June, 1971.

Koerner, R. M. "Effects of Particle Characteristics on Soil Strength." Journal of Soil Mechanics and Foundations Division, XCVI, No. SM4 (July, 1970), 1221-1234.

Ladanyi, B. "An Engineering Theory of Creep of Frozen Soil." Canadian Geotechnical Journal, LXIII (September, 1972), 63-80.

Lambe, T. W., and Whitman, R. V. "Shear Resistance Between Soil Particles." Soil Mechanics. New York: Wiley, 1969.

Lee, K. L., and Seed, H. B. "Drained Strength Characteristics of Sands." Journal of the Soil Mechanics and Foundations Division, ASCE, XCIII No. SM6 (November, 1967), 117-141.

Leonards, G. A., and Andersland, O. B. "The Clay-Water System and the Shearing Resistance of Clays." Research Conference on Shear Strength of Cohesive Soils, ASCE, June, 1960, pp. 793-818.

Mitchell, J. K. "Shearing Resistance of Soils as a Rate Process." Journal of Soil Mechanics and Foundations Division, ASCE, XC, No. SM1 (January, 1964), 29-61.

Mitchell, J. K.; Campanella, R. G.; and Singh, A. "Soil Creep as a Rate Process." Journal of Soil Mechanics and Foundations Division, ASCE, XC, No. SM1 (January, 1964), 29-61.

Pounder, E. R. The Physics of Ice. Oxford: Pergamon Press, 1967.

Sayles, F. J. "Creep of Frozen Soils." Technical Report 190, 1968, Cold Regions Research and Engineering Laboratory, Hanover, New Hampshire.

Schmertmann,J. H., and Osterberg, J. O. "An Experimental Study of the Development of Cohesion and Friction with Axial Strain in Saturated Cohesive Soils." Proc. Research Conference on Shear Strength of Cohesive Soils, ASCE (June, 1960), 643-694.

Scott, F. S. "The Freezing Process and Mechanics of Frozen Ground." Cold Regions Science and Engineering Monograph II-D1, October, 1969, Cold Regions Research and Engineering Laboratory, Hanover, New Hampshire.

Trollope, D. J., and Zafar, S. M. "A Study of Saturated Sand, and Sand: Clay Mixtures in Triaxial Compression." Proc. Second Australia-New Zealand Conference of Soil Mechanics and Foundation Engineering, I (1956), 7-13.

Tsytovich, N. A. "Instability of Mechanical Properties of Frozen and Thawing Soil." Proc. of the Permafrost International Conference, National Academy of Sciences-National Council Publication No. 1287, 1963, pp. 325-331.

Tsytovich. N. A. "Mechanical Properties of Frozen Soils." Highway Research Board Special Report 58 (a translation from Russian), Washington, D.C., 1960.

Vesic, A. S., and Clough, G. W. "Behavior of Granular Materials Under High Stresses." Journal of Soil Mechanics and Foundations Division, ASCE, XCIV, No. SM3 (June, 1968), 661-688.

Vialov, S. S., ed. "Rheological Properties and Bearing Capacity of Frozen Soils." Translation 74, 1965a, Cold Regions Research and Engineering Laboratory, Hanover, New Hampshire.

_____. "The Strength and Creep of Frozen Soils and Calculations for Ice-Soil Retaining Structures." Translation 76, Cold Regions Research and Engineering Laboratory, Hanover, New Hampshire, 1965b.

Warder, David J. "Behavior and Analysis of a Model Soil-Ice Barrier." Unpublished Ph.D. dissertation, Michigan State University, 1969.

Whitman, R. V. "The Behavior of Soils Under Transient Loading." Proc. Fourth International Conference of Soil Mechanics and Foundations Engineering, Vol. 1, London, 1957, pp. 207-210.

Yong, R. N. "Soil Freezing Considerations in Frozen Soils Strength." Proc. of the Permafrost International Conference, National Academy of Sciences-National Research Council Publication No. 1287, 1963, pp. 315-319.

APPENDICES

TABLE A-1

CONSTANT AXIAL STRAIN RATE TEST DATA

TABLE A-1.--Constant Axial Strain Rate Test Data.

SAMPLE NUMBER 1

TEMPERATURE = -12.0° C
STRAIN RATE = 2.66 x 10^{-3} min^{-1}
PERCENT SAND = 61.6
PERCENT ICE = 99.8
TOTAL VOLUME CHANGE = NA
CONFINING PRESSURE = 0 psi

TIME (MIN.)	DEFL. (INS.)	LOAD (LBS.)
1.0	0.001	95.0
2.0	0.003	160.0
3.0	0.007	250.0
4.0	0.009	360.0
5.0	0.012	510.0
6.0	0.016	725.0
7.0	0.019	945.0
8.0	0.024	1125.0
9.0	0.030	1285.0
10.0	0.035	1345.0
11.0	0.041	1395.0
12.0	0.047	1395.0
13.0	0.052	1395.0
14.0	0.058	1360.0
15.0	0.064	1150.0

SAMPLE NUMBER 2

TEMPERATURE = -12.0° C
STRAIN RATE = 2.66 x 10^{-3} min^{-1}
PERCENT SAND = 62.1
PERCENT ICE = 92.8
TOTAL VOLUME CHANGE = NA
CONFINING PRESSURE = 0 psi

TIME (MIN.)	DEFL. (INS.)	LOAD (LBS.)
0.0	0.0	0.0
1.0	0.0004	60.0
2.0	0.0018	175.0
3.0	0.0048	330.0
4.0	0.0078	540.0
5.0	0.0110	815.0
6.0	0.0147	1055.0
7.0	0.0190	1245.0
8.0	0.0241	1350.0
9.0	0.0291	1415.0
10.0	0.0346	1455.0
11.0	0.0399	1480.0
12.0	0.0458	1495.0
13.0	0.0508	1495.0
15.0	0.0445	0.0

SAMPLE NUMBER 4

TEMPERATURE = -12.0° C
STRAIN RATE = 2.66 x 10^{-3} min^{-1}
PERCENT SAND = 63.5
PERCENT ICE = 97.4
TOTAL VOLUME CHANGE = NA
CONFINING PRESSURE = 0 psi

TIME (MIN.)	DEFL. (INS.)	LOAD (LBS.)
0.0	0.0000	0.0
0.5	0.0004	20.0
1.0	0.0017	65.0
1.5	0.0039	105.0
2.0	0.0063	135.0
2.5	0.0086	175.0
3.0	0.0116	220.0
4.0	0.0144	330.0
5.0	0.0170	475.0
6.0	0.0210	670.0
7.0	0.0251	875.0
8.0	0.0290	1100.0
9.0	0.0343	1265.0
10.0	0.0394	1360.0
11.0	0.0452	1400.0
12.0	0.0508	1400.0
13.0	0.0564	1400.0
14.0	0.0627	1380.0
15.0	0.0686	1345.0
16.0	0.0752	1290.0
17.0	0.0814	1230.0
18.0	0.0870	1160.0
19.0	0.0888	1088.0
20.0	0.0905	1010.0
21.0	0.0922	925.0
22.0	0.0938	860.0
23.0	0.0956	810.0
24.0	0.0976	770.0
24.5	0.0987	750.0

TABLE A 1.--Continued.

SAMPLE NUMBER 5

TEMPERATURE = -12.0° C
STRAIN RATE = 2.66 x 10^{-3} min^{-1}
PERCENT SAND = 62.5
PERCENT ICE = 94.5
TOTAL VOLUME CHANGE = NA
CONFINING PRESSURE = 0 psi

TIME (MIN.)	DEFL. (INS.)	LOAD (LBS.)
0.0	0.0000	0.0
1.0	0.0010	10.0
2.0	0.0043	125.0
3.0	0.0078	240.0
4.0	0.0108	425.0
5.0	0.0146	640.0
6.0	0.0196	830.0
7.0	0.0238	1030.0
8.0	0.0289	1170.0
9.0	0.0344	1255.0
10.0	0.0408	1325.0
11.0	0.0455	1360.0
12.0	0.0509	1400.0
13.0	0.0569	1435.0
14.0	0.0617	1465.0
15.0	0.0677	1495.0
16.0	0.0740	1515.0
17.0	0.0800	1540.0
18.0	0.0861	1550.0
19.0	0.0905	1545.0
20.0	0.0965	1540.0
21.0	0.1028	1535.0
22.0	0.1084	1530.0
23.0	0.1148	1520.0
24.0	0.1202	1505.0
25.0	0.1267	1480.0
26.0	0.1327	1445.0
27.0	0.1402	1405.0
28.0	0.1459	1355.0
29.0	0.1515	1300.0
30.0	0.1581	1240.0
31.0	0.1642	1180.0
32.0	0.1707	1115.0
33.0	0.1763	1045.0
34.0	0.1830	990.0
35.0	0.1886	930.0

SAMPLE NUMBER 7

TEMPERATURE = -12.0° C
STRAIN RATE = 2.66 x 10^{-3} min^{-1}
PERCENT SAND = 62.9
PERCENT ICE = 94.5
TOTAL VOLUME CHANGE = NA
CONFINING PRESSURE = 0 psi

TIME (MIN.)	DEFL. (INS.)	LOAD (LBS.)
0.0	0.0000	0.0
1.0	0.0026	65.0
2.0	0.0054	170.0
3.0	0.0084	330.0
4.0	0.0117	555.0
5.0	0.0154	800.0
6.0	0.0186	1005.0
7.0	0.0231	1205.0
8.0	0.0283	1310.0
9.0	0.0341	1345.0
10.0	0.0401	1360.0
11.0	0.0461	1360.0
12.0	0.0522	1360.0
13.0	0.0586	1350.0
14.0	0.0647	1340.0
15.0	0.0708	1325.0
16.0	0.0769	1310.0
17.0	0.0829	1280.0
18.0	0.0887	1245.0
19.0	0.0948	1215.0
20.0	0.1010	1190.0
21.0	0.1072	1170.0
22.0	0.1133	1150.0
23.0	0.1193	1130.0
24.0	0.1255	1110.0
25.0	0.1318	1100.0
26.0	0.1384	1085.0
27.0	0.1449	1080.0
28.0	0.1512	1065.0

TABLE A-1.--Continued.

SAMPLE NUMBER 8

TEMPERATURE = -12.0° C
STRAIN RATE = 1.33×10^{-3} min^{-1}
PERCENT SAND = 62.9
PERCENT ICE = 96.0
TOTAL VOLUME CHANGE = NA
CONFINING PRESSURE = 0 psi

TIME (MIN.)	DEFL. (INS.)	LOAD (LBS.)
0.0	0.0	0.0
1.0	0.0006	0.0
2.0	0.0020	45.0
3.0	0.0034	90.0
4.0	0.0050	145.0
5.0	0.0067	210.0
6.0	0.0085	270.0
7.0	0.0104	355.0
8.0	0.0125	460.0
9.0	0.0146	580.0
10.0	0.0168	690.0
11.0	0.0192	780.0
12.0	0.0217	870.0
14.0	0.0270	1020.0
16.0	0.0336	1130.0
18.0	0.0394	1205.0
20.0	0.0454	1265.0
22.0	0.0514	1320.0
24.0	0.0574	1360.0
26.0	0.0633	1390.0
28.0	0.0694	1420.0
30.0	0.0755	1445.0
32.0	0.0816	1470.0
34.0	0.0878	1495.0
36.0	0.0937	1515.0
38.0	0.0998	1535.0
40.0	0.1061	1550.0
42.0	0.1126	1555.0
44.0	0.1188	1555.0
46.0	0.1250	1555.0
48.0	0.1312	1545.0
50.0	0.1375	1535.0
52.0	0.1436	1515.0
54.0	0.1498	1500.0
56.0	0.1560	1475.0
58.0	0.1623	1455.0
60.0	0.1688	1435.0

SAMPLE NUMBER 10

TEMPERATURE = -12.0° C
STRAIN RATE = 2.66×10^{-3} min^{-1}
PERCENT SAND = 63.0
PERCENT ICE = 95.0
TOTAL VOLUME CHANGE = NA
CONFINING PRESSURE = 355 psi

TIME (MIN.)	DEFL. (INS.)	LOAD (LBS.)
0.0	0.0000	0.0
1.0	0.0037	165.0
2.0	0.0080	345.0
3.0	0.0126	540.0
4.0	0.0172	765.0
5.0	0.0222	960.0
6.0	0.0276	1115.0
7.0	0.0331	1225.0
8.0	0.0388	1310.0
9.0	0.0447	1385.0
10.0	0.0505	1455.0
11.0	0.0564	1515.0
12.0	0.0621	1575.0
13.0	0.0680	1635.0
14.0	0.0738	1695.0
15.0	0.0796	1760.0
16.0	0.0856	1830.0
17.0	0.0914	1890.0
18.0	0.0974	1945.0
19.0	0.1032	1985.0
20.0	0.1091	2005.0
21.0	0.1152	2015.0
22.0	0.1214	2010.0
23.0	0.1277	1985.0
24.0	0.1338	1950.0
25.0	0.1399	1905.0
26.0	0.1462	1885.0
27.0	0.1523	1885.0
28.0	0.1585	1885.0
29.0	0.1645	1885.0
30.0	0.1706	1880.0

TABLE A-1.--Continued.

SAMPLE NUMBER 11

TEMPERATURE = -12.0° C
STRAIN RATE = 2.66 x 10^{-3} min^{-1}
PERCENT SAND = 62.9
PERCENT ICE = 95.0
TOTAL VOLUME CHANGE = NA
CONFINING PRESSURE = 105 psi

TIME (MIN.)	DEFL. (INS.)	LOAD (LBS.)
0.0	0.0000	0.0
1.0	0.0040	75.0
2.0	0.0082	155.0
3.0	0.0125	240.0
4.0	0.0169	345.0
5.0	0.0213	480.0
6.0	0.0255	660.0
7.0	0.0305	850.0
8.0	0.0358	1020.0
9.0	0.0411	1170.0
10.0	0.0469	1270.0
11.0	0.0526	1340.0
12.0	0.0584	1405.0
13.0	0.0644	1455.0
14.0	0.0701	1500.0
15.0	0.0761	1540.0
16.0	0.0819	1580.0
17.0	0.0876	1615.0
18.0	0.0936	1640.0
19.0	0.0993	1670.0
20.0	0.1051	1695.0
21.0	0.1112	1720.0
22.0	0.1170	1735.0
23.0	0.1232	1745.0
24.0	0.1292	1755.0
25.0	0.1355	1755.0
26.0	0.1420	1745.0
27.0	0.1481	1735.0
28.0	0.1545	1700.0
29.0	0.1609	1675.0
30.0	0.1672	1635.0

SAMPLE NUMBER 13

TEMPERATURE = -12.0° C
STRAIN RATE = 2.66 x 10^{-3} min^{-1}
PERCENT SAND = 62.8
PERCENT ICE = 97.5
TOTAL VOLUME CHANGE = NA
CONFINING PRESSURE = 350 psi

TIME (MIN.)	DEFL. (INS.)	LOAD (LBS.)
0.0	0.0	0.0
1.0	0.0049	0.0
2.0	0.0106	20.0
3.0	0.0154	110.0
4.0	0.0202	220.0
5.0	0.0248	370.0
6.0	0.0293	560.0
7.0	0.0342	755.0
8.0	0.0393	930.0
9.0	0.0447	1070.0
10.0	0.0503	1180.0
11.0	0.0559	1260.0
12.0	0.0618	1320.0
13.0	0.0676	1365.0
14.0	0.0736	1420.0
15.0	0.0795	1465.0
16.0	0.0855	1510.0
17.0	0.0905	1550.0
18.0	0.0975	1585.0
19.0	0.1036	1615.0
20.0	0.1097	1630.0
21.0	0.1157	1630.0
22.0	0.1219	1615.0
23.0	0.1281	1590.0
24.0	0.1344	1575.0
25.0	0.1404	1570.0
26.0	0.1467	1565.0
27.0	0.1529	1560.0
28.0	0.1591	1550.0
29.0	0.1654	1550.0
30.0	0.1714	1540.0
31.0	0.1777	1530.0
32.0	0.1838	1520.0
40.0	0.1518	0.0

TABLE A-1.--Continued.

SAMPLE NUMBER 14

TEMPERATURE = -12.0° C
STRAIN RATE = 2.66 x 10^{-3} min^{-1}
PERCENT SAND = 62.3
PERCENT ICE = 97.5
TOTAL VOLUME CHANGE = NA
CONFINING PRESSURE = 700 psi

TIME (MIN.)	DEFL. (INS.)	LOAD (LBS.)
0.0	0.0	0.0
1.0	0.0051	100.0
2.0	0.0104	205.0
3.0	0.0154	355.0
4.0	0.0202	545.0
5.0	0.0253	735.0
6.0	0.0302	955.0
7.0	0.0352	1160.0
8.0	0.0406	1325.0
9.0	0.0457	1440.0
10.0	0.0513	1525.0
11.0	0.0571	1605.0
12.0	0.0628	1675.0
13.0	0.0686	1740.0
14.0	0.0743	1800.0
15.0	0.0802	1870.0
16.0	0.0858	1940.0
17.0	0.0920	2010.0
18.0	0.0977	2080.0
19.0	0.1034	2160.0
20.0	0.1098	2230.0
21.0	0.1149	2295.0
22.0	0.1208	2360.0
23.0	0.1265	2425.0
24.0	0.1324	2480.0
25.0	0.1380	2530.0
26.0	0.1438	2575.0
27.0	0.1496	2615.0
28.0	0.1554	2650.0
29.0	0.1614	2685.0
30.0	0.1672	2695.0
31.0	0.1735	2710.0
32.0	0.1793	2725.0
33.0	0.1854	2730.0
34.0	0.1914	2730.0
35.0	0.1974	2730.0
36.0	0.2035	2730.0
36.5	0.2065	2730.0

SAMPLE NUMBER 18

TEMPERATURE = -12.0° C
STRAIN RATE = 2.66 x 10^{-2} min^{-1}
PERCENT SAND = 62.5
PERCENT ICE = 97.0
TOTAL VOLUME CHANGE = +0.193 cc
CONFINING PRESSURE = 700 psi

TIME (MIN.)	DEFL. (INS.)	LOAD (LBS.)
0.0	0.0000	0.0
0.1	0.0048	165.0
0.2	0.0091	400.0
0.3	0.0135	710.0
0.4	0.0180	1090.0
0.5	0.0223	1475.0
0.6	0.0272	1810.0
0.7	0.0324	2055.0
0.78	0.0370	2135.0
0.8	0.0380	2130.0
0.9	0.0453	1815.0

TABLE A-1.--Continued.

SAMPLE NUMBER 19

TEMPERATURE = -12.0° C
STRAIN RATE = 7.07×10^{-5} min^{-1}
= 3.54×10^{-4} min^{-1}
= 1.76×10^{-3} min^{-1}
PERCENT SAND = 62.4
PERCENT ICE = 97.5
TOTAL VOLUME CHANGE = +0.362 cc
CONFINING PRESSURE = 700 psi

TIME (MIN.)	DEFL. (INS.)	LOAD (LBS.)
0.0	0.0000	0.0
25.0	0.0028	75.0
50.0	0.0061	180.0
75.0	0.0092	300.0
100.0	0.0124	425.0
125.0	0.0159	520.0
150.0	0.0196	585.0
175.0	0.0233	645.0
200.0	0.0271	695.0
225.0	0.0308	740.0
234.0	0.0321	745.0
235.0	0.0325	785.0
240.0	0.0357	1000.0
245.0	0.0392	1125.0
250.0	0.0429	1215.0
255.0	0.0466	1275.0
260.0	0.0505	1325.0
265.0	0.0544	1370.0
275.0	0.0621	1445.0
285.0	0.0700	1535.0
295.0	0.0777	1625.0
305.0	0.0856	1730.0
315.0	0.0931	1835.0
325.0	0.1009	1930.0
335.0	0.1085	2000.0
345.0	0.1164	2105.0
355.0	0.1242	2190.0
365.0	0.1319	2265.0
368.5	0.1347	2300.0
369.5	0.1363	2470.0
370.0	0.1392	2675.0
371.0	0.1427	2800.0
272.0	0.1462	2885.0
373.0	0.1500	2940.0
374.0	0.1539	2970.0
375.0	0.1579	2980.0
376.0	0.1618	2975.0
377.0	0.1660	2965.0
377.5	0.1680	2945.0

SAMPLE NUMBER 20 - ICE

TEMPERATURE = -12.0° C
STRAIN RATE = 2.66×10^{-3} min^{-1}
PERCENT SAND = 0
PERCENT ICE = 98.0
TOTAL VOLUME CHANGE = -0.403 cc
CONFINING PRESSURE = 700 psi

TIME (MIN.)	DEFL. (INS.)	LOAD (LBS.)
0.0	0.0000	0.0
0.5	0.0025	60.0
1.0	0.0049	135.0
2.0	0.0098	275.0
3.0	0.0149	415.0
4.0	0.0206	500.0
5.0	0.0264	570.0
6.0	0.0319	635.0
7.0	0.0378	685.0
8.0	0.0436	715.0
9.0	0.0496	740.0
10.0	0.0557	755.0
12.0	0.0679	760.0
14.0	0.0802	750.0
16.0	0.0927	735.0
18.0	0.1047	715.0
20.0	0.1172	700.0
22.0	0.1296	690.0
24.0	0.1418	670.0
26.0	0.1510	665.0
28.0	0.1663	655.0
30.0	0.1784	650.0
32.0	0.1907	640.0
34.0	0.2027	635.0
36.0	0.2151	630.0
37.0	0.2210	630.0

TABLE A-1.--Continued.

SAMPLE NUMBER 21

TEMPERATURE = -12.0° C
STRAIN RATE = 2.66 x 10^{-3} min^{-1}
PERCENT SAND = 63.0
PERCENT ICE = 97.0
TOTAL VOLUME CHANGE = +0.662 cc
CONFINING PRESSURE = 350 psi

TIME (MIN.)	DEFL. (INS.)	LOAD (LBS.)
0.0	0.0	0.0
1.0	0.0047	130.0
2.0	0.0095	320.0
3.0	0.0140	555.0
4.0	0.0187	835.0
5.0	0.0237	1105.0
6.0	0.0292	1305.0
7.0	0.0351	1430.0
8.0	0.0411	1510.0
9.0	0.0477	1560.0
10.0	0.0540	1580.0
11.0	0.0604	1610.0
12.0	0.0688	1635.0
13.0	0.0730	1670.0
14.0	0.0794	1700.0
15.0	0.0856	1730.0
16.0	0.0921	1770.0
17.0	0.0985	1810.0
18.0	0.1048	1840.0
19.0	0.1111	1860.0
20.0	0.1175	1875.0
21.0	0.1238	1895.0
22.0	0.1305	1915.0
23.0	0.1367	1935.0
24.0	0.1431	1955.0
25.0	0.1495	1970.0
26.0	0.1559	1980.0
27.0	0.1622	1985.0
28.0	0.1685	1980.0
29.0	0.1748	1975.0
30.0	0.1814	1945.0
31.0	0.1880	1915.0
32.0	0.1944	1890.0
33.0	0.2011	1890.0
34.0	0.2074	1890.0
34.41	0.2101	1875.0
35.0	0.1633	0.0

SAMPLE NUMBER 22

TEMPERATURE = -12.0° C
STRAIN RATE = 2.66 x 10^{-3} min^{-1}
PERCENT SAND = 62.8
PERCENT ICE = 96.0
TOTAL VOLUME CHANGE = NA
CONFINING PRESSURE = 350 psi

TIME (MIN.)	DEFL. (INS.)	LOAD (LBS.)
0.0	0.0	0.0
1.0	0.0041	130.0
2.0	0.0082	285.0
3.0	0.0125	500.0
4.0	0.0167	755.0
5.0	0.0212	1025.0
6.0	0.0265	1250.0
7.0	0.0318	1395.0
8.0	0.0375	1490.0
9.0	0.0435	1550.0
10.0	0.0493	1575.0
11.0	0.0555	1590.0
12.0	0.0615	1610.0
13.0	0.0676	1630.0
14.0	0.0738	1650.0
15.0	0.0796	1680.0
16.0	0.0857	1720.0
17.0	0.0918	1765.0
18.0	0.0979	1805.0
19.0	0.1040	1830.0
20.0	0.1100	1855.0
21.0	0.1161	1880.0
22.0	0.1222	1890.0
23.0	0.1285	1890.0
24.0	0.1349	1880.0
24.41	0.1374	1870.0
25.0	0.0952	0.0

TABLE A-1.--Continued.

SAMPLE NUMBER 24

TEMPERATURE = -12.0° C
STRAIN RATE = 2.66 x 10^{-3} min^{-1}
PERCENT SAND = 63.0 EST.
PERCENT ICE = 96.0 EST.
TOTAL VOLUME CHANGE = NA
CONFINING PRESSURE = 350 psi

TIME (MIN.)	DEFL. (INS.)	LOAD (LBS.)
1.0	0.0045	205.0
2.0	0.0087	410.0
3.0	0.0129	665.0
5.0	0.0223	1280.0
7.0	0.0334	1470.0
10.0	0.0509	1635.0
13.0	0.0691	1730.0
16.0	0.0869	1885.0
19.0	0.1045	2075.0
22.0	0.1224	2225.0
25.0	0.1404	2285.0
27.0	0.1631	2275.0

SAMPLE NUMBER 26

TEMPERATURE = -12.0° C
STRAIN RATE = 2.66 x 10^{-3} min^{-1}
PERCENT SAND = 62.0
PERCENT ICE = 97.5
TOTAL VOLUME CHANGE =+.656 cc
CONFINING PRESSURE = 0 psi

TIME (MIN.)	DEFL. (INS.)	LOAD (LBS.)
0.0	0.0	0.0
1.0	0.0029	105.0
2.0	0.0059	230.0
3.0	0.0093	355.0
4.0	0.0129	525.0
5.0	0.0168	730.0
6.0	0.0210	945.0
7.0	0.0257	1140.0
8.0	0.0305	1280.0
9.0	0.0360	1370.0
10.0	0.0417	1425.0
11.0	0.0476	1460.0
12.0	0.0536	1470.0
13.0	0.0596	1480.0
15.0	0.0719	1480.0
17.0	0.0843	1470.0
19.0	0.0968	1470.0
21.0	0.1094	1450.0
23.0	0.1221	1410.0
23.62	0.1257	1395.0
24.0	0.1075	0.0

SAMPLE NUMBER 27

TEMPERATURE = -12.0° C
STRAIN RATE = 2.66 x 10^{-3} min^{-1}
PERCENT SAND = 62.5
PERCENT ICE = 96.5
TOTAL VOLUME CHANGE =+0.403 cc
CONFINING PRESSURE = 350 psi

TIME (MIN.)	DEFL. (INS.)	LOAD (LBS.)
0.0	0.0	0.0
1.0	0.0039	175.0
2.0	0.0081	390.0
3.0	0.0124	645.0
4.0	0.0166	930.0
5.0	0.0216	1165.0
6.0	0.0269	1320.0
7.0	0.0325	1430.0
8.0	0.0382	1505.0
9.0	0.0439	1540.0
10.0	0.0499	1600.0
11.0	0.0557	1650.0
12.0	0.0617	1705.0
13.0	0.0675	1760.0
14.0	0.0734	1810.0
15.0	0.0792	1870.0
16.0	0.0850	1930.0
17.0	0.0909	1990.0
18.0	0.0967	2040.0
19.0	0.1028	2070.0
20.0	0.1089	2080.0
21.0	0.1151	2045.0
22.0	0.1214	1985.0
22.41	0.1240	1955.0
23.0	0.1124	0.0

TABLE A-1.--Continued.

SAMPLE NUMBER 28

TEMPERATURE = -12.0° C
STRAIN RATE = 2.66 x 10^{-3} min^{-1}
PERCENT SAND = 62.7
PERCENT ICE = 96.5
TOTAL VOLUME CHANGE = +0.484 cc
CONFINING PRESSURE = 700 psi

TIME (MIN.)	DEFL. (INS.)	LOAD (LBS.)
2.0	0.0095	415.0
3.0	0.0142	760.0
4.0	0.0191	925.0
5.0	0.0241	1120.0
6.0	0.0303	1315.0
8.0	0.0414	1560.0
10.0	0.0529	1740.0
14.0	0.0759	2040.0
18.0	0.0992	2365.0
22.0	0.1224	2680.0
26.0	0.1458	2860.0
29.0	0.1638	2885.0

SAMPLE NUMBER 33

TEMPERATURE = -12.0° C
STRAIN RATE = 2.66 x 10^{-3} min^{-1}
PERCENT SAND = 62.4
PERCENT ICE = NA
TOTAL VOLUME CHANGE = NA
CONFINING PRESSURE = 0 psi

TIME (MIN.)	DEFL. (INS.)	LOAD (LBS.)
1.0	0.0025	95.0
2.0	0.0060	200.0
4.0	0.0139	535.0
6.0	0.0222	1005.0
8.0	0.0330	1225.0
10.0	0.0445	1350.0
12.0	0.0667	1415.0
14.0	0.0689	1465.0
16.0	0.0809	1530.0
18.0	0.0932	1585.0
21.0	0.1118	1630.0
23.0	0.1246	1610.0

SAMPLE NUMBER 34

TEMPERATURE = -12.0° C
STRAIN RATE = 2.66 x 10^{-3} min^{-1}
PERCENT SAND = 62.9
PERCENT ICE = NA
TOTAL VOLUME CHANGE = +0.282 cc
CONFINING PRESSURE = 0 psi

TIME (MIN.)	DEFL. (INS.)	LOAD (LBS.)
1.0	0.0033	190.0
2.0	0.0064	370.0
4.0	0.0144	905.0
6.0	0.0243	1310.0
8.0	0.0355	1490.0
12.0	0.0593	1610.0
16.0	0.0817	1670.0
18.0	0.0958	1720.0

SAMPLE NUMBER 35

TEMPERATURE = -12.0° C
STRAIN RATE = 2.66 x 10^{-3} min^{-1}
PERCENT SAND = 63.0 EST.
PERCENT ICE = NA
TOTAL VOLUME CHANGE = NA
CONFINING PRESSURE = 700 psi

TIME (MIN.)	DEFL. (INS.)	LOAD (LBS.)
1.0	0.0047	295.0
2.0	0.0089	595.0
3.0	0.0134	880.0
4.0	0.0182	1155.0
6.0	0.0286	1530.0
8.0	0.0398	1725.0
10.0	0.0514	1820.0
14.0	0.0748	2020.0
18.0	0.0980	2320.0
22.0	0.1210	2605.0
26.0	0.1444	2775.0
29.0	0.1620	2830.0
30.7	0.1726	2840.0

TABLE A-1.--Continued.

SAMPLE NUMBER 36

TEMPERATURE = -12.0° C
STRAIN RATE = 2.66 x 10^{-3} min^{-1}
PERCENT SAND = 63.5 EST.
PERCENT ICE = 96.0 EST.
TOTAL VOLUME CHANGE = NA
CONFINING PRESSURE = 700 psi

TIME (MIN.)	DEFL. (INS.)	LOAD (LBS.)
1.0	0.0047	320.0
2.0	0.0089	635.0
3.0	0.0134	960.0
4.0	0.0183	1245.0
6.0	0.0286	1640.0
8.0	0.0398	1800.0
10.0	0.0514	1880.0
14.0	0.0751	2085.0
18.0	0.0980	2400.0
22.0	0.1208	2685.0
26.0	0.1438	2870.0
30.0	0.1875	2970.0
32.0	0.1794	2990.0

SAMPLE NUMBER 38

TEMPERATURE = -12.0° C
STRAIN RATE = 2.66 x 10^{-3} min^{-1}
PERCENT SAND = 63.0
PERCENT ICE = 97.0
TOTAL VOLUME CHANGE = +0.559 cc
CONFINING PRESSURE = 700 psi

TIME (MIN.)	DEFL. (INS.)	LOAD (LBS.)
0.0	0.0000	0.0
1.0	0.0044	190.0
2.0	0.0088	470.0
3.0	0.0132	740.0
4.0	0.0179	1010.0
5.0	0.0225	1230.0
6.0	0.0277	1400.0
7.0	0.0330	1530.0
8.0	0.0383	1645.0
9.0	0.0439	1750.0
10.0	0.0492	1840.0
12.0	0.0604	2010.0
14.0	0.0716	2200.0
16.0	0.0827	2375.0
18.0	0.0938	2535.0

SAMPLE NUMBER 38 continued.

TIME (MIN.)	DEFL. (INS.)	LOAD (LBS.)
20.0	0.1052	2675.0
22.0	0.1165	2790.0
24.0	0.1280	2875.0
26.0	0.1397	2920.0
28.0	0.1517	2940.0
29.0	0.1577	2935.0
29.25	0.1591	2935.0
30.0	0.1136	0.0

SAMPLE NUMBER 39

TEMPERATURE = -12.0° C
STRAIN RATE = 2.66 x 10^{-3} min^{-1}
PERCENT SAND = 63.2
PERCENT ICE = 97.0
TOTAL VOLUME CHANGE = +0.696 cc
CONFINING PRESSURE = 360 psi

TIME (MIN.)	DEFL. (INS.)	LOAD (LBS.)
0.0	0.0000	0.0
1.0	0.0042	140.0
2.0	0.0084	320.0
3.0	0.0123	525.0
4.0	0.0166	775.0
5.0	0.0213	995.0
6.0	0.0262	1175.0
7.0	0.0313	1310.0
8.0	0.0366	1420.0
9.0	0.0419	1520.0
10.0	0.0475	1615.0
12.0	0.0582	1775.0
14.0	0.0693	1950.0
16.0	0.0804	2095.0
18.0	0.0917	2215.0
20.0	0.1029	2315.0
22.0	0.1144	2370.0
24.0	0.1259	2375.0
25.0	0.1318	2350.0
26.0	0.1378	2295.0
27.0	0.1017	0.0

TABLE A-1.--Continued.

SAMPLE NUMBER 40

TEMPERATURE = -12.0° C
STRAIN RATE = 2.66 x 10^{-3} min^{-1}
PERCENT SAND = 63.0
PERCENT ICE = NA
TOTAL VOLUME CHANGE = NA
CONFINING PRESSURE = 100 psi

TIME (MIN.)	DEFL. (INS.)	LOAD (LBS.)
1.0	0.0044	100.0
2.0	0.0084	180.0
4.0	0.0165	435.0
6.0	0.0248	910.0
8.0	0.0348	1295.0
10.0	0.0457	1495.0
12.0	0.0573	1630.0
14.0	0.0686	1730.0
16.0	0.0808	1790.0
17.0	0.0868	1790.0
18.0	0.0932	1770.0

SAMPLE NUMBER 41

TEMPERATURE = -12.0° C
STRAIN RATE = 2.66 x 10^{-3}
PERCENT SAND = 62.9
PERCENT ICE = 96.0
TOTAL VOLUME CHANGE = +0.246 cc
CONFINING PRESSURE = 100 psi

TIME (MIN.)	DEFL. (INS.)	LOAD (LBS.)
0.0	0.0000	0.0
1.0	0.0035	80.0
2.0	0.0070	135.0
4.0	0.0162	405.0
6.0	0.0248	865.0
8.0	0.0347	1285.0
10.0	0.0456	1505.0
12.0	0.0572	1645.0
14.0	0.0688	1735.0
16.0	0.0807	1770.0
16.5	0.0838	1755.0
17.0	0.0601	0.0

SAMPLE NUMBER 42

TEMPERATURE = -12.0° C
STRAIN RATE = 2.66 x 10^{-3} min^{-1}
PERCENT SAND = 62.8
PERCENT ICE = 96.0
TOTAL VOLUME CHANGE = +0.240 cc
CONFINING PRESSURE = 0 psi

TIME (MIN.)	DEFL. (INS.)	LOAD (LBS.)
1.0	0.0033	140.0
2.0	0.0062	275.0
3.0	0.0098	440.0
4.0	0.0139	665.0
5.0	0.0185	900.0
6.0	0.0229	1100.0
8.0	0.0338	1345.0
10.0	0.0453	1440.0
12.0	0.0568	1480.0
13.0	0.0627	1485.0
14.0	0.0687	1482.0

SAMPLE NUMBER 43

TEMPERATURE = -12.0° C
STRAIN RATE = 2.66 x 10^{-3} min^{-1}
PERCENT SAND = 63.6
PERCENT ICE = 96.5
TOTAL VOLUME CHANGE = +0.426 cc
CONFINING PRESSURE = 0 psi

TIME (MIN.)	DEFL. (INS.)	LOAD (LBS.)
0.0	0.0000	0.0
1.0	0.0028	100.0
2.0	0.0057	205.0
4.0	0.0141	565.0
6.0	0.0214	1075.0
8.0	0.0319	1385.0
10.0	0.0430	1545.0
12.0	0.0545	1635.0
13.0	0.0604	1660.0
14.0	0.0661	1660.0
15.0	0.0721	1650.0
15.25	0.0737	1640.0
16.0	0.0548	0.0

TABLE A-1.--Continued.

SAMPLE NUMBER 44

TEMPERATURE = -12.0° C
STRAIN RATE = 2.66 x 10^{-3} min^{-1}
PERCENT SAND = 63.5
PERCENT ICE = 96.0
TOTAL VOLUME CHANGE = +0.450 cc
CONFINING PRESSURE = 700 psi

TIME (MIN.)	DEFL. (INS.)	LOAD (LBS.)
0.0	0.0000	0.0
1.0	0.0043	250.0
2.0	0.0084	530.0
4.0	0.0171	1170.0
6.0	0.0265	1740.0
8.0	0.0372	2070.0
10.0	0.0482	2220.0
12.0	0.0595	2355.0
14.0	0.0729	2535.0
16.0	0.0842	2660.0
18.0	0.0954	2800.0
20.0	0.1067	2935.0
22.0	0.1181	3040.0
22.5	0.1210	3050.0
22.75	0.1226	3045.0
24.0	0.0771	200.0

SAMPLE NUMBER 45 - ICE

TEMPERATURE = -12.0° C
STRAIN RATE = 2.66 x 10^{-3} min^{-1}
PERCENT SAND = 0
PERCENT ICE = 98.0
TOTAL VOLUME CHANGE = +0.294 cc
CONFINING PRESSURE = 0 psi

TIME (MIN.)	DEFL. (INS.)	LOAD (LBS.)
0.0	0.0	0.0
1.0	0.0032	120.0
2.0	0.0062	245.0
4.0	0.0148	460.0
6.0	0.0254	590.0
8.0	0.0368	660.0
10.0	0.0485	685.0
12.0	0.0602	685.0
15.0	0.0786	660.0
18.0	0.0967	630.0
21.0	0.1146	615.0
24.0	0.1325	580.0
27.0	0.1503	565.0
30.0	0.1682	560.0
31.75	0.1746	550.0

SAMPLE NUMBER 47

TEMPERATURE = -12.0° C
STRAIN RATE = 5.33 x 10^{-3} min^{-1}
PERCENT SAND = 63.5
PERCENT ICE = 96.5
TOTAL VOLUME CHANGE = +1.00 cc
CONFINING PRESSURE = 700 psi

TIME (MIN.)	DEFL. (INS.)	LOAD (LBS.)
0.0	0.0000	0.0
1.0	0.0084	595.0
2.0	0.0172	1305.0
3.0	0.0270	1865.0
4.0	0.0378	2145.0
5.0	0.0489	2305.0
6.0	0.0601	2455.0
7.0	0.0714	2585.0
8.0	0.0832	2675.0
9.0	0.0952	2770.0
10.0	0.1071	2885.0
11.0	0.1187	2980.0
12.0	0.1305	3035.0
13.0	0.1420	3050.0
14.0	0.1539	3060.0
15.0	0.1658	3050.0
16.0	0.1224	370.0

TABLE A-1.--Continued.

SAMPLE NUMBER 48

TEMPERATURE = -12.0° C
STRAIN RATE = 2.66 x 10^{-3} min^{-1}
PERCENT SAND = 63.7
PERCENT ICE = 96.0
TOTAL VOLUME CHANGE = +0.493 cc
CONFINING PRESSURE = 700 psi

TIME (MIN.)	DEFL. (INS.)	LOAD (LBS.)
0.0	0.0000	0.0
10.0	0.0046	210.0
20.0	0.0092	445.0
30.0	0.0140	675.0
40.0	0.0190	885.0
50.0	0.0236	1065.0
60.0	0.0291	1215.0
70.0	0.0346	1355.0
80.0	0.0400	1475.0
100.0	0.0513	1715.0
120.0	0.0627	1935.0
140.0	0.0739	2145.0
160.0	0.0853	2330.0
180.0	0.0967	2535.0
200.0	0.1082	2695.0
220.0	0.1199	2840.0
240.0	0.1318	2955.0
260.0	0.1435	3025.0
270.0	0.1494	3060.0
275.0	0.1525	3060.0
276.0	0.1072	360.0

SAMPLE NUMBER 50

TEMPERATURE = -12.0° C
STRAIN RATE = 5.33 x 10^{-3} min^{-1}
PERCENT SAND = 63.2
PERCENT ICE = 96.0
TOTAL VOLUME CHANGE = +0.745 cc
CONFINING PRESSURE = 690 psi

TIME (MIN.)	DEFL. (INS.)	LOAD (LBS.)
0.0	0.0000	0.0
1.0	0.0084	545.0
2.0	0.0171	1250.0
3.0	0.0265	1850.0
4.0	0.0373	2135.0
5.0	0.0487	2290.0
6.0	0.0601	2435.0
7.0	0.0716	2585.0
8.0	0.0833	2720.0
9.0	0.0951	2840.0
10.0	0.1062	2950.0
11.0	0.1177	3040.0
12.0	0.1290	3100.0
13.0	0.1409	3120.0
13.5	0.1470	3130.0
14.0	0.1016	360.0

SAMPLE NUMBER 51

TEMPERATURE = -12.0° C
STRAIN RATE = 2.66 x 10^{-3} min^{-1}
PERCENT SAND = 63.5 EST.
PERCENT ICE = 96.0 EST.
TOTAL VOLUME CHANGE = NA
CONFINING PRESSURE = 660 psi

TIME (MIN.)	DEFL. (INS.)	LOAD (LBS.)
1.0	0.0044	270.0
2.0	0.0087	535.0
3.0	0.0131	815.0
4.0	0.0177	1110.0
5.0	0.0226	1340.0
6.0	0.0277	1520.0
8.0	0.0355	1780.0
10.0	0.0500	1980.0
12.0	0.0613	2160.0
14.0	0.0726	2335.0
16.0	0.0840	2495.0
18.0	0.0955	2590.0
19.0	0.1014	2595.0

TABLE A-1.--Continued.

SAMPLE NUMBER 52

TEMPERATURE = -12.0° C
STRAIN RATE = 2.66 x 10^{-3} min^{-1}
PERCENT SAND = 63.2
PERCENT ICE = 96.5
TOTAL VOLUME CHANGE = +0.601 cc
CONFINING PRESSURE = 640 psi

TIME (MIN.)	DEFL. (INS.)	LOAD (LBS.)
0.0	0.0000	0.0
1.0	0.0046	190.0
2.0	0.0084	425.0
3.0	0.0126	700.0
4.0	0.0171	985.0
5.0	0.0219	1215.0
6.0	0.0269	1395.0
7.0	0.0321	1535.0
8.0	0.0375	1650.0
9.0	0.0429	1750.0
10.0	0.0484	1850.0
11.0	0.0538	1940.0
12.0	0.0594	2030.0
14.0	0.0705	2215.0
16.0	0.0816	2385.0
18.0	0.0922	2540.0
20.0	0.1036	2655.0
22.0	0.1148	2745.0
24.0	0.1264	2800.0
26.0	0.1378	2830.0
26.83	0.1426	2830.0
27.0	0.1020	260.0

SAMPLE NUMBER 72

TEMPERATURE = -12.0° C
STRAIN RATE = 4.42 x 10^{-3} min^{-1}
PERCENT SAND = 62.7
PERCENT ICE = 57.0
TOTAL VOLUME CHANGE = NA
CONFINING PRESSURE = 0 psi

TIME (MIN.)	DEFL. (INS.)	LOAD (LBS.)
0.0	0.0000	0.0
0.5	0.0033	67.0
1.0	0.0071	121.0
2.0	0.0142	264.0
3.0	0.0204	436.0
4.0	0.0271	616.0
5.0	0.0342	767.0
6.0	0.0419	873.0
7.0	0.0510	909.0
8.0	0.0610	865.0
9.0	0.0717	755.0
10.0	0.0833	631.0
11.0	0.0953	475.0
12.0	0.1083	298.0
13.0	0.1204	220.0
14.0	0.1308	188.0
15.0	0.1411	164.0
16.0	0.1510	155.0
17.0	0.1611	142.0
18.0	0.1713	132.0
19.0	0.1817	126.0
20.0	0.1920	121.0

TABLE A-1.--Continued.

SAMPLE NUMBER 73

TEMPERATURE = -12.0° C
STRAIN RATE = 2.66 x 10^{-3} min^{-1}
PERCENT SAND = 62.1
PERCENT ICE = 53.6
TOTAL VOLUME CHANGE = NA
CONFINING PRESSURE = 350 psi

TIME (MIN.)	DEFL. (INS.)	LOAD (LBS.)
0.0	0.0000	0.0
2.0	0.0073	325.0
3.0	0.0113	478.0
4.0	0.0152	620.0
5.0	0.0197	733.0
8.0	0.0338	1109.0
10.0	0.0440	1302.0
12.0	0.0546	1463.0
14.0	0.0656	1559.0
16.0	0.0770	1678.0
18.0	0.0892	1709.0
20.0	0.1040	1683.0
25.0	0.1352	1572.0
30.0	0.1691	1465.0
35.0	0.2038	1303.0
40.0	0.2373	1163.0
45.0	0.2697	1077.0

SAMPLE NUMBER 74

TEMPERATURE = -12.0° C
STRAIN RATE = 2.66 x 10^{-3} min^{-1}
PERCENT SAND = 62.5
PERCENT ICE = 55.8
TOTAL VOLUME CHANGE = NA
CONFINING PRESSURE = 1000 psi

TIME (MIN.)	DEFL. (INS.)	LOAD (LBS.)
0.0	0.0	0.0
1.0	0.0059	214.0
2.0	0.0104	487.0
4.0	0.0208	975.0
6.0	0.0318	1307.0
8.0	0.0428	1607.0
10.0	0.0542	1880.0
12.0	0.0658	2135.0
14.0	0.0774	2365.0
16.0	0.0895	2551.0
18.0	0.1013	2653.0
20.0	0.1131	2715.0
22.0	0.1251	2744.0
24.0	0.1377	2737.0
26.0	0.1496	2684.0
28.0	0.1609	2660.0

SAMPLE NUMBER 76

TEMPERATURE = -12.0° C
STRAIN RATE = 2.66 x 10^{-3} min^{-1}
PERCENT SAND = 63.4
PERCENT ICE = 58.2
TOTAL VOLUME CHANGE = NA
CONFINING PRESSURE = 700 psi

TIME (MIN.)	DEFL. (INS.)	LOAD (LBS.)
0.0	0.0000	0.0
2.0	0.0097	500.0
5.0	0.0270	1161.0
7.0	0.0389	1438.0
10.0	0.0565	1797.0
12.0	0.0676	1992.0
15.0	0.0845	2252.0
17.0	0.0964	2372.0
20.0	0.1164	2459.0
22.0	0.1266	2405.0
25.0	0.1428	2377.0
30.0	0.1696	2313.0
33.0	0.1859	2260.0
35.0	0.1963	2230.0
40.0	0.2232	2136.0
45.0	0.2499	2055.0

SAMPLE NUMBER 77

TEMPERATURE = -12.0° C
STRAIN RATE = 2.66 x 10^{-3} min^{-1}
PERCENT SAND = 62.3
PERCENT ICE = 95.0
TOTAL VOLUME CHANGE = +0.890 cc
CONFINING PRESSURE = 1000 psi

TIME (MIN.)	DEFL. (INS.)	LOAD (LBS.)
0.0	0.0000	0.0
2.0	0.0082	464.0
5.0	0.0229	1451.0
7.0	0.0356	1940.0
10.0	0.0568	2160.0
12.0	0.0693	2314.0
15.0	0.0877	2548.0
17.0	0.0998	2689.0
20.0	0.1182	2873.0
22.0	0.1291	2961.0
24.7	0.1471	3040.0
26.0	0.1551	3012.0
28.0	0.1652	2945.0
30.0	0.1745	2938.0

TABLE A-1.--Continued.

SAMPLE NUMBER 78

TEMPERATURE = -12.0° C
STRAIN RATE = 2.66 x 10^{-3} min^{-1}
PERCENT SAND = 62.9
PERCENT ICE = 55.0
TOTAL VOLUME CHANGE = NA
CONFINING PRESSURE = 100 psi

TIME (MIN.)	DEFL. (INS.)	LOAD (LBS.)
0.0	0.0000	0.0
1.0	0.0042	125.0
2.0	0.0086	259.0
4.0	0.0190	572.0
6.0	0.0313	809.0
8.0	0.0431	964.0
10.0	0.0558	1055.0
10.3	0.0581	1060.0
12.0	0.0689	1045.0
15.0	0.0875	988.0
20.0	0.1199	848.0
25.0	0.1537	702.0
30.0	0.1883	576.0
35.0	0.2214	499.0
39.0	0.2474	485.0

SAMPLE NUMBER 79

TEMPERATURE = -12.0° C
STRAIN RATE = 2.66 x 10^{-3} min^{-1}
PERCENT SAND = 63.7
PERCENT ICE = 59.4
TOTAL VOLUME CHANGE = NA
CONFINING PRESSURE = 0 psi

TIME (MIN.)	DEFL. (INS.)	LOAD (LBS.)
0.0	0.0000	0.0
1.0	0.0049	183.0
2.0	0.0109	369.0
3.0	0.0179	558.0
4.0	0.0254	696.0
5.0	0.0324	801.0
6.0	0.0405	837.0
7.0	0.0485	855.0
8.0	0.0559	852.0
10.0	0.0714	786.0
12.5	0.0902	542.0
15.0	0.1022	384.0
20.0	0.1317	255.0
25.0	0.1559	201.0

SAMPLE NUMBER 80

TEMPERATURE = -12.0° C
STRAIN RATE = 2.66 x 10^{-3} min^{-1}
PERCENT SAND = 63.4
PERCENT ICE = 95.5
TOTAL VOLUME CHANGE = +1.184 cc
CONFINING PRESSURE = 200 psi

TIME (MIN.)	DEFL. (INS.)	LOAD (LBS.)
0.0	0.0000	0.0
1.0	0.0036	208.0
2.0	0.0074	495.0
3.0	0.0111	820.0
4.0	0.0159	1172.0
5.0	0.0198	1467.0
6.0	0.0248	1665.0
7.0	0.0311	1732.0
8.0	0.0375	1793.0
9.0	0.0445	1852.0
10.0	0.0508	1810.0
11.0	0.0579	1725.0
12.0	0.0639	1664.0

SAMPLE NUMBER 81

TEMPERATURE = -12.0° C
STRAIN RATE = 2.66 x 10^{-3} min^{-1}
PERCENT SAND = 62.6
PERCENT ICE = 96.0
TOTAL VOLUME CHANGE = +1.178 cc
CONFINING PRESSURE = 1000 psi

TIME (MIN.)	DEFL. (INS.)	LOAD (LBS.)
2.0	0.0115	742.0
3.0	0.0170	1090.0
4.0	0.0228	1413.0
5.0	0.0293	1694.0
6.0	0.0363	1888.0
7.0	0.0436	2035.0
8.0	0.0511	2144.0
9.0	0.0588	2247.0
10.0	0.0662	2362.0
12.0	0.0807	2552.0
14.0	0.0950	2758.0
16.0	0.1093	2907.0
18.0	0.1236	3022.0
20.0	0.1382	3083.0
22.0	0.1527	3121.0
24.0	0.1676	3013.0
26.0	0.1824	3086.0
30.0	0.2135	3000.0

TABLE A-1.--Continued.

SAMPLE NUMBER 82

TEMPERATURE = -12.0° C
STRAIN RATE = 2.66 x 10^{-3} min^{-1}
PERCENT SAND = 62.8
PERCENT ICE = 97.0
TOTAL VOLUME CHANGE = NA
CONFINING PRESSURE = 200 psi

TIME (MIN.)	DEFL. (INS.)	LOAD (LBS.)
0.0	2.264	0.0
1.0	0.0059	131.0
2.0	0.0111	281.0
3.0	0.0149	510.0
4.0	0.0186	791.0
5.0	0.0222	1087.0
6.0	0.0264	1371.0
7.0	0.0313	1637.0
8.0	0.0371	1805.0
9.0	0.0437	1894.0
10.0	0.0505	1943.0
11.0	0.0576	1984.0
13.0	0.0705	2025.0
16.0	0.0877	1973.0
20.0	0.1112	1906.0
25.0	0.1387	1786.0
28.0	0.1544	1728.0

SAMPLE NUMBER 83

TEMPERATURE = -12.0° C
STRAIN RATE = 2.66 x 10^{-3} min^{-1}
PERCENT SAND = 63.5
PERCENT ICE = 96.0
TOTAL VOLUME CHANGE = NA
CONFINING PRESSURE = 0 psi

TIME (MIN.)	DEFL. (INS.)	LOAD (LBS.)
1.0	0.0037	173.0
2.0	0.0078	378.0
3.0	0.0111	613.0
4.0	0.0145	870.0
5.0	0.0184	1139.0
6.0	0.0230	1358.0
7.0	0.0288	1502.0
8.0	0.0348	1564.0
9.0	0.0416	1597.0
11.0	0.0546	1537.0
13.0	0.0671	1496.0
15.0	0.0801	1438.0
20.0	0.1127	1215.0
25.0	0.1499	840.0
30.0	0.1892	322.0
35.0	0.2251	170.0

SAMPLE NUMBER 84

TEMPERATURE = -12.0° C
STRAIN RATE = 2.66 x 10^{-3} min^{-1}
PERCENT SAND = 63.7
PERCENT ICE = 95.5
TOTAL VOLUME CHANGE = NA
CONFINING PRESSURE = 100 psi

TIME (MIN.)	DEFL. (INS.)	LOAD (LBS.)
1.0030.5	0.0031	80.0
1.0	0.0068	168.0
2.0	0.0123	450.0
3.0	0.0174	794.0
4.0	0.0226	1184.0
5.0	0.0284	1546.0
6.1	0.0362	1680.0
7.0	0.0424	1657.0
10.0	0.0607	1555.0
15.0	0.0882	1532.0
20.0	0.1258	1500.0
25.0	0.1555	1409.0

SAMPLE NUMBER 87

TEMPERATURE = -12.0° C
STRAIN RATE = 2.66 x 10^{-3} min^{-1}
PERCENT SAND = 63.2
PERCENT ICE = 32.9
TOTAL VOLUME CHANGE = NA
CONFINING PRESSURE = 100 psi

TIME (MIN.)	DEFL. (INS.)	LOAD (LBS.)
1.0	0.0055	168.0
2.0	0.0110	322.0
2.5	0.0138	400.0
3.0	0.0168	471.0
4.0	0.0234	600.0
5.0	0.0303	705.0
6.0	0.0377	782.0
7.0	0.0455	824.0
7.5	0.0495	838.0
8.0	0.0533	828.0
10.0	0.0677	799.0
15.0	0.0983	695.0
20.0	0.1286	575.0

TABLE A-1.--Continued.

SAMPLE NUMBER 88

TEMPERATURE = -12.0° C
STRAIN RATE = 2.66 x 10^{-3}
PERCENT SAND = 64.3
PERCENT ICE = 98.0
TOTAL VOLUME CHANGE = NA
CONFINING PRESSURE = 100 psi

TIME (MIN.)	DEFL. (INS.)	LOAD (LBS.)
0.5	0.0020	105.0
1.0	0.0042	206.0
2.0	0.0093	474.0
3.0	0.0143	798.0
4.0	0.0199	1188.0
4.7	0.0239	1451.0
5.0	0.0263	1553.0
5.7	0.0315	1640.0
6.0	0.0330	1620.0
7.0	0.0406	1574.0
9.0	0.0523	1495.0
11.0	0.0636	1432.0
13.0	0.0753	1343.0
15.0	0.0870	1257.0

SAMPLE NUMBER 89

TEMPERATURE = -12.0° C
STRAIN RATE = 2.66 x $10^{-3}min^{-1}$
PERCENT SAND = 63.0
PERCENT ICE = 99.0
TOTAL VOLUME CHANGE = NA
CONFINING PRESSURE = 100 psi

TIME (MIN.)	DEFL. (INS.)	LOAD (LBS.)
0.5	0.0027	107.0
1.0	0.0060	222.0
1.5	0.0083	355.0
2.0	0.0111	506.0
3.0	0.0167	857.0
4.0	0.0228	1227.0
4.5	0.0273	1412.0
5.0	0.0313	1500.0
5.5	0.0358	1534.0
6.0	0.0406	1532.0
8.0	0.0560	1330.0
10.0	0.0659	1203.0

SAMPLE NUMBER S-1 UNFROZEN SAND

TEMPERATURE = 20° C
STRAIN RATE = 2.66 x $10^{-3}min^{-1}$
PERCENT SAND = 64.0
PERCENT ICE = 0

CONFINING PRESSURE = 110 psi

TIME (MIN.)	DEFL. (INS.)	LOAD (LBS.)	ΔV (CC)
1.0	0.0059	64.0	+0.10
3.0	0.0179	182.0	+0.15
5.0	0.0298	244.0	+0.05
10.0	0.0625	310.0	+0.20
15.0	0.0935	335.0	+0.40
20.0	0.1254	346.0	+0.60
25.0	0.1574	341.0	+0.95
30.0	0.1896	332.0	+1.15
35.0	0.2216	313.0	+1.30
40.0	0.2540	297.0	+1.40
45.0	0.2870	277.0	+1.50
50.0	0.3195	255.0	+1.50
55.0	0.3516	250.0	+1.55
60.0	0.3833	243.0	+1.50
65.0	0.4151	243.0	+1.50

SAMPLE NUMBER S-2 UNFROZEN SAND

TEMPERATURE = 20° C
STRAIN RATE = 2.66 x $10^{-3}min^{-1}$
PERCENT SAND = 64.0
PERCENT ICE = 0

CONFINING PRESSURE = 48 psi

TIME (MIN.)	DEFL. (INS.)	LOAD (LBS.)	ΔV (CC)
0.0	0.0000	0.0	0.0
1.0	0.0060	52.0	-0.05
3.0	0.0184	104.0	-0.10
5.0	0.0307	122.0	-0.05
10.0	0.0626	144.0	+0.25
15.0	0.0951	152.0	+0.55
20.0	0.1267	156.0	+0.85
25.0	0.1593	148.0	+1.05
30.0	0.1913	136.0	+1.30
35.0	0.2237	126.0	+1.40
40.0	0.2542	118.0	LEAK
45.0	0.2881	115.0	
48.0	0.3073	114.0	

TABLE A-1.--Continued.

SAMPLE NUMBER S-3 UNFROZEN SAND

TEMPERATURE = 20° C
STRAIN RATE = 2.66 x 10^{-3} min^{-1}
PERCENT SAND = 64.0
PERCENT ICE = 0

CONFINING PRESSURE = 21.5 psi

TIME (MIN.)	DEFL. (INS.)	LOAD (LBS.)	ΔV (CC)
1.0	0.0400	6.0	-0.01
2.0	0.0040	24.0	-0.03
3.0	0.0090	42.0	-0.07
4.0	0.0180	56.0	-0.09
5.0	0.0260	67.0	-0.07
6.0	0.0360	75.0	+0.0
7.0	0.0460	89.0	+0.09
8.0	0.0570	100.0	+0.17
9.0	0.0670	111.0	+0.38
10.0	0.0800	115.0	+0.48
11.0	0.0930	116.0	+0.72
12.0	0.1050	116.0	+0.89
13.0	0.1160	117.0	+1.10
16.0	0.1280	128.0	+1.28
17.0	0.1400	120.0	+1.49
18.0	0.1520	120.0	+1.70
19.0	0.1640	121.0	+1.88
20.0	0.1820	117.0	+2.14
21.0	0.2020	116.0	+2.40
22.0	0.2130	116.0	+2.57
23.0	0.2290	116.0	+2.74
24.0	0.2510	116.0	
25.0	0.2630	115.0	
26.0	0.2770	115.0	
27.0	0.3010	112.0	
28.0	0.3170	112.0	
29.0	0.3350	112.0	
30.0	0.3410	112.0	
31.0	0.3420	100.0	

SAMPLE NUMBER S-4 UNFROZEN SAND

TEMPERATURE = 20° C
STRAIN RATE = 2.66 x 10^{-3} min^{-1}
PERCENT SAND = 64.0
PERCENT ICE = 0

CONFINING PRESSURE = 14.3 psi

TIME (MIN.)	DEFL. (INS.)	LOAD (LBS.)	ΔV (CC)
0.0	0.0000	0.0	+0.0
0.5	0.0050	3.0	-0.03
1.0	0.0080	5.0	-0.04
2.0	0.0110	10.0	-0.09
3.0	0.0190	23.0	-0.20
4.0	0.0280	32.0	-0.27
5.0	0.0380	39.0	-0.32
6.0	0.0490	44.0	-0.32
7.0	0.0590	48.0	-0.32
8.0	0.0700	52.0	-0.26
9.0	0.0810	55.0	-0.14
10.0	0.0930	56.0	+0.03
11.0	0.1040	58.0	+0.09
12.0	0.1160	60.0	+0.20
13.0	0.1280	62.0	+0.29
14.0	0.1410	63.0	+0.42
15.0	0.1520	64.0	+0.55
16.0	0.1640	65.0	+0.67
17.0	0.1760	65.0	+0.85
18.0	0.1880	65.0	+1.00
19.0	0.2000	65.0	+1.16
20.0	0.2110	66.0	+1.26
21.0	0.2250	66.0	+1.46
22.0	0.2350	66.0	+1.61
23.0	0.2500	66.0	+1.71
24.0	0.2620	66.0	+1.85
25.0	0.2740	66.0	+1.99
26.0	0.2860	66.0	+2.09
27.0	0.2980	65.0	+2.21

TABLE A-1.--Continued.

SAMPLE NUMBER S-5 UNFROZEN SAND

TEMPERATURE = 20° C
STRAIN RATE = 2.66 x 10^{-3} min^{-1}
PERCENT SAND = 64.0
PERCENT ICE = 0

CONFINING PRESSURE = 28.6 psi

TIME (MIN.)	DEFL. (INS.)	LOAD (LBS.)	ΔV (CC)
0.0	0.0000	0.0	0.0
1.0	0.0020	27.0	-0.03
2.0	0.0020	37.0	-0.03
3.0	0.0120	54.0	-0.05
4.0	0.0200	67.0	-0.08
5.0	0.0300	89.0	-0.08
6.0	0.0400	109.0	-0.02
7.0	0.0510	123.0	+0.02
8.0	0.0640	131.0	+0.14
9.0	0.0770	136.0	+0.30
10.0	0.0900	140.0	+0.45
11.0	0.1020	144.0	+0.60
12.0	0.1120	147.0	+0.76
13.0	0.1260	149.0	+0.91
14.0	0.1380	152.0	+1.21
15.0	0.1510	155.0	+1.41
16.0	0.1620	158.0	+1.61
17.0	0.1760	160.0	+1.82
18.0	0.1890	162.0	+2.03
19.0	0.2020	163.0	+2.27
20.0	0.2130	164.0	+2.45
21.0	0.2270	164.0	+2.70
22.0	0.2400	165.0	+2.88
23.0	0.2520	165.0	+3.06
24.0	0.2650	166.0	+3.24
25.0	0.2770	166.0	+3.32
26.0	0.2920	164.0	+3.50
27.0	0.3050	162.0	+3.68
28.0	0.3180	156.0	+3.86

SAMPLE NUMBER S-6 UNFROZEN SAND

TEMPERATURE = 20° C
STRAIN RATE = 2.66 x 10^{-3} min^{-1}
PERCENT SAND = 64
PERCENT ICE = 0

CONFINING PRESSURE = 50 psi

TIME (MIN.)	DEFL. (INS.)	LOAD (LBS.)	ΔV (CC)
0.0	0.0000	0.0	0.0
1.0	.0055	60.0	0.0
3.0	0.0173	120.0	-0.01
5.0	0.0297	139.0	-0.20
10.0	0.0608	157.0	-0.10
15.0	0.0942	162.0	+0.10
20.0	0.1242	162.0	+0.30
25.0	0.1542	157.0	+0.40
30.0	0.1818	152.0	
35.0	0.2004	151.0	

TABLE A-2

CREEP TEST DATA

TABLE A-2.--Creep Test Data.

SAMPLE NUMBER 90 UNIAXIAL

TEMPERATURE = -12.0° C
CONSTANT AXIAL STRESS = 1070 psi
PERCENT SAND = 63.3
PERCENT ICE = 94.7
TOTAL VOLUME CHANGE = +0.228 cc

TIME (MIN.)	DEFL. (INS.)	LOAD (LBS.)
1.0	0.0176	1074.0
10.0	0.0265	1074.0
30.0	0.0361	1072.0
60.0	0.0444	1066.0
90.0	0.0501	1065.0
120.0	0.0544	1065.0
150.0	0.0580	1065.0
180.0	0.0613	1064.0
210.0	0.0639	1065.0
240.0	0.0663	1065.0
270.0	0.0686	1065.0
300.0	0.0706	1067.0
310.0	0.0712	1065.0
322.0	0.0720	1065.0
322.0	0.0644	0.0
330.0	0.0620	0.0

SAMPLE NUMBER 91 STEP-STRESS

TEMPERATURE = -12.0° C
CONSTANT AXIAL STRESS = 1070 psi
PERCENT SAND = 63.6
PERCENT ICE = 95.1
TOTAL VOLUME CHANGE = +0.108 cc

TIME (MIN.)	DEFL. (INS.)	LOAD (LBS.)	σ3 (PSI)
1.0	0.0181	1077.0	0
10.0	0.0262	1086.0	
20.0	0.0311	1087.0	
30.0	0.0348	1090.0	
60.0	0.0427	1095.0	
90.0	0.0482	1097.0	
120.0	0.0527	1104.0	
150.0	0.0563	1105.0	
180.0	0.0594	1104.0	
187.0	0.0600	1108.0	0
191.0	0.0663	1116.0	350
200.0	0.0672	1109.0	
210.0	0.0681	1119.0	
240.0	0.0700	1123.0	
270.0	0.0714	1124.0	
300.0	0.0724	1124.0	
330.0	0.0737	1123.0	
360.0	0.0749	1121.0	
380.0	0.0757	1121.0	350

TABLE A-2.--Continued.

SAMPLE NUMBER 93 UNIAXIAL

TEMPERATURE = -12.0° C
CONSTANT AXIAL STRESS = 400 psi
PERCENT SAND = 63.8
PERCENT ICE = 60.8
TOTAL VOLUME CHANGE = NA

TIME (MIN.)	DEFL. (INS.)	LOAD (LBS.)
1.0	0.0150	400.0
10.0	0.0201	403.0
30.0	0.0242	405.0
60.0	0.0275	405.0
90.0	0.0300	406.0
120.0	0.0316	409.0
150.0	0.0330	409.0
180.0	0.0340	408.0
210.0	0.0349	406.0
240.0	0.0357	408.0
270.0	0.0364	407.0
300.0	0.0371	406.0
330.0	0.0378	406.0
350.0	0.0382	407.0
351.0	0.0358	0.0
355.0	0.0352	0.0

SAMPLE NUMBER 94 STEP-STRESS

TEMPERATURE = -12.0° C
CONSTANT AXIAL STRESS = 400 psi
PERCENT SAND = 63.8
PERCENT ICE = 59.4
TOTAL VOLUME CHANGE = NA

TIME (MIN.)	DEFL. (INS.)	LOAD (LBS.)	σ_3 (PSI)
1.0	0.0152	422.0	0
5.0	0.0190	402.0	
10.0	0.0210	402.0	
20.0	0.0236	402.0	
30.0	0.0254	401.0	
40.0	0.0269	402.0	
50.0	0.0280	402.0	
60.0	0.0290	402.0	
62.0	0.0293	404.0	0
64.0	0.0327	405.0	100

SAMPLE NUMBER 94 Continued

TIME (MIN.)	DEFL. (INS.)	LOAD (LBS.)	σ_3 (PSI)
70.0	0.0338	407.0	
80.0	0.0347	406.0	
90.0	0.0355	406.0	
100.0	0.0363	406.0	
110.0	0.0369	406.0	
120.0	0.0375	407.0	
122.0	0.0376	407.0	100
124.0	0.0391	410.0	200
130.0	0.0398	411.0	
140.0	0.0406	413.0	
150.0	0.0412	413.0	
160.0	0.0419	406.0	
170.0	0.0423	417.0	
178.0	0.0426	417.0	200
181.0	0.0453	415.0	400
190.0	0.0462	414.0	
200.0	0.0467	411.0	
210.0	0.0472	412.0	
220.0	0.0476	402.0	
230.0	0.0479	402.0	
240.0	0.0482	412.0	
242.0	0.0483	412.0	400
245.0	0.0504	390.0	600
250.0	0.0508	392.0	
260.0	0.0514	393.0	
270.0	0.0519	411.0	
280.0	0.0522	411.0	
290.0	0.0525	411.0	
300.0	0.0528	411.0	
303.0	0.0530	411.0	600
307.0	0.0558	411.0	800
310.0	0.0560	410.0	
320.0	0.0565	411.0	
330.0	0.0569	412.0	
340.0	0.0572	412.0	
350.0	0.0575	412.0	
360.0	0.0577	412.0	
361.0	0.0577	412.0	800
365.0	0.0606	415.0	1000
370.0	0.0610	415.0	
380.0	0.0614	416.0	
390.0	0.0618	415.0	
400.0	0.0620	416.0	
409.0	0.0622	416.0	1000

TABLE A-2.--Continued.

SAMPLE NUMBER 96 UNIAXIAL

TEMPERATURE = -12.0° C
CONSTANT AXIAL STRESS = 400 psi
PERCENT SAND = 63.8
PERCENT ICE = 95.2
TOTAL VOLUME CHANGE = -0.078 cc

TIME (MIN.)	DEFL. (INS.)	LOAD (LBS.)
1.0	0.0066	405.0
10.0	0.0085	405.0
30.0	0.0098	402.0
60.0	0.0111	404.0
90.0	0.0120	403.0
120.0	0.0125	403.0
150.0	0.0131	402.0
180.0	0.0135	405.0
210.0	0.0140	404.0
240.0	0.0145	403.0
270.0	0.0148	403.0
300.0	0.0152	403.0
320.0	0.0154	402.0
320.0	0.0140	115.0
330.0	0.0135	115.0

SAMPLE NUMBER 97 UNIAXIAL

TEMPERATURE = -12.0° C
CONSTANT AXIAL STRESS = 640 psi
PERCENT SAND = 63.3
PERCENT ICE = 58.8
TOTAL VOLUME CHANGE = NA

TIME (MIN.)	DEFL. (INS.)	LOAD (LBS.)
1.0	0.0194	639.0
10.0	0.0329	648.0
30.0	0.0429	651.0
60.0	0.0514	656.0
90.0	0.0571	655.0
120.0	0.0619	659.0
150.0	0.0659	661.0
180.0	0.0697	663.0
150.0	0.0659	661.0
180.0	0.0697	663.0
210.0	0.0734	662.0
240.0	0.0766	663.0
270.0	0.0798	662.0
300.0	0.0829	662.0
330.0	0.0861	662.0
360.0	0.0891	662.0
365.0	0.0895	662.0
365.0	0.0865	120.0
380.0	0.0851	120.0

SAMPLE NUMBER 98 STEP-STRESS

TEMPERATURE = -12.0° C
CONSTANT AXIAL STRESS = 640 psi
PERCENT SAND = 63.6
PERCENT ICE = 60.0 EST.
TOTAL VOLUME CHANGE = NA

TIME (MIN.)	DEFL. (INS.)	LOAD (LBS.)	σ_3 (PSI)
1.0	0.0172	616.0	0
10.0	0.0307	650.0	
30.0	0.0403	651.0	
50.0	0.0458	653.0	
56.0	0.0470	653.0	0
58.0	0.0513	660.0	100
60.0	0.0518	660.0	
70.0	0.0535	659.0	
80.0	0.0548	660.0	
90.0	0.0560	660.0	
110.0	0.0579	660.0	
115.0	0.0585	660.0	100
118.0	0.0600	662.0	200
120.0	0.0602	658.0	
130.0	0.0610	663.0	
140.0	0.0616	665.0	
150.0	0.0622	670.0	
160.0	0.0629	670.0	200
163.0	0.0652	662.0	400
170.0	0.0663	660.0	
180.0	0.0679	662.0	
210.0	0.0726	664.0	
230.0	0.0757	664.0	
239.0	0.0774	663.0	400
243.0	0.0804	660.0	600
250.0	0.0809	664.0	
260.0	0.0816	663.0	
270.0	0.0835	665.0	
280.0	0.0914	665.0	

LEAK AT 180 MIN.

TABLE A-2.--Continued.

SAMPLE NUMBER 99 UNIAXIAL

TEMPERATURE = -12.0° C
CONSTANT AXIAL STRESS = 640 psi
PERCENT SAND = 63.9
PERCENT ICE = 95.1
TOTAL VOLUME CHANGE = -0.078 cc

TIME (MIN.)	DEFL. (INS.)	LOAD (LBS.)
1.0	0.0042	627.0
10.0	0.0062	642.0
30.0	0.0083	641.0
60.0	0.0107	645.0
90.0	0.0122	645.0
120.0	0.0136	644.0
150.0	0.0147	643.0
180.0	0.0156	643.0
210.0	0.0165	645.0
240.0	0.0174	645.0
244.0	0.0175	645.0
244.7	0.0150	135.0
250.0	0.0142	135.0
256.0	0.0138	133.0

SAMPLE NUMBER 100 STEP-STRESS

TEMPERATURE = -12.0° C
CONSTANT AXIAL STRESS = 640 psi
PERCENT SAND = 63.8
PERCENT ICE = 95.5
TOTAL VOLUME CHANGE = -0.078 cc

TIME (MIN.)	DEFL. (INS.)	LOAD (LBS.)	σ_3 (PSI)
1.0	0.0114	668.0	0
10.0	0.0146	644.0	
20.0	0.0160	650.0	
30.0	0.0171	648.0	
40.0	0.0181	650.0	
50.0	0.0187	645.0	
58.0	0.0194	645.0	0
60.0	0.0228	644.0	100
70.0	0.0236	650.0	
80.0	0.0242	649.0	
90.0	0.0249	650.0	
100.0	0.0253	650.0	
110.0	0.0259	649.0	
119.0	0.0264	649.0	100
121.0	0.0275	654.0	200

SAMPLE NUMBER 100 Continued.

TIME (MIN.)	DEFL. (INS.)	LOAD (LBS.)	σ_3 (PSI)
130.0	0.0281	656.0	
140.0	0.0285	651.0	
150.0	0.0289	650.0	
160.0	0.0293	650.0	
170.0	0.0296	654.0	
177.0	0.0299	651.0	200
181.0	0.0320	655.0	400
190.0	0.0325	648.0	
200.0	0.0328	653.0	
210.0	0.0330	650.0	
220.0	0.0333	653.0	
225.0	0.0335	653.0	
230.0	0.0336	653.0	
240.0	0.0339	653.0	400
243.0	0.0363	655.0	600
245.0	0.0364	651.0	
250.0	0.0367	651.0	
260.0	0.0370	651.0	
270.0	0.0373	651.0	
280.0	0.0374	651.0	
290.0	0.0377	653.0	
300.0	0.0379	653.0	
302.0	0.0380	653.0	600
305.0	0.0405	652.0	800
310.0	0.0408	653.0	
320.0	0.0410	653.0	
330.0	0.0413	655.0	
340.0	0.0416	655.0	
350.0	0.0417	655.0	
358.0	0.0420	655.0	800
361.0	0.0445	655.0	1000
365.0	0.0446	655.0	
370.0	0.0448	655.0	
380.0	0.0450	655.0	
390.0	0.0452	655.0	
400.0	0.0454	655.0	
405.0	0.0455	655.0	1000

TABLE A-2.--Continued.

SAMPLE NUMBER 101 UNIAXIAL

TEMPERATURE = -12.0° C
CONSTANT AXIAL STRESS = 640 psi
PERCENT SAND = 62.9
PERCENT ICE = 95.7
TOTAL VOLUME CHANGE = -0.012 cc

TIME (MIN.)	DEFL. (INS.)	LOAD (LBS.)
1.0	0.0108	650.0
10.0	0.0142	642.0
30.0	0.0169	644.0
60.0	0.0195	643.0
90.0	0.0214	646.0
120.0	0.0231	648.0
150.0	0.0246	650.0
180.0	0.0256	648.0
210.0	0.0266	649.0
240.0	0.0275	649.0
270.0	0.0283	647.0
300.0	0.0291	650.0
330.0	0.0298	650.0
350.0	0.0302	650.0
351.0	0.0302	650.0
352.0	0.0269	105.0
360.0	0.0259	105.0
370.0	0.0257	105.0

SAMPLE NUMBER 102 UNIAXIAL

TEMPERATURE = -12.0° C
CONSTANT AXIAL STRESS = 1070 psi
PERCENT SAND = 63.3
PERCENT ICE = 95.8
TOTAL VOLUME CHANGE = +0.144 cc

TIME (MIN.)	DEFL. (INS.)	LOAD (LBS.)
1.0	0.0183	1065.0
10.0	0.0264	1085.0
30.0	0.0348	1084.0
60.0	0.0421	1090.0
90.0	0.0471	1100.0
120.0	0.0509	1097.0
150.0	0.0541	1100.0
180.0	0.0568	1098.0
210.0	0.0591	1097.0
240.0	0.0609	1099.0
270.0	0.0626	1103.0
290.0	0.0637	1103.0

SAMPLE NUMBER 102 Continued.

TIME (MIN.)	DEFL. (INS.)	LOAD (LBS.)
290.7	0.0573	130.0
291.0	0.0548	130.0
300.0	0.0530	130.0
310	0.0526	130.0
320.0	0.0523	130.0

SAMPLE NUMBER 104 STEP-STRESS

TEMPERATURE = -12.0° C
CONSTANT AXIAL STRESS = 750 psi
PERCENT SAND = 64.0
PERCENT ICE = 60.0 EST.
TOTAL VOLUME CHANGE = NA

TIME (MIN.)	DEFL. (INS.)	LOAD (LBS.)	σ_3 (PSI)
1.0	0.0265	745.0	0
2.0	0.0324	763.0	
3.0	0.0361	763.0	
4.0	0.0398	766.0	
5.0	0.0413	766.0	
5.7	0.0427	766.0	0
8.0	0.0498	772.0	100
9.0	0.0510	777.0	
10.0	0.0519	777.0	
11.0	0.0527	778.0	
12.0	0.0535	778.0	
13.0	0.0541	778.0	
13.3	0.0543	778.0	100
15.0	0.0575	786.0	200
16.0	0.0582	786.0	
17.0	0.0588	786.0	
18.0	0.0592	786.0	
19.0	0.0597	786.0	
20.0	0.0603	786.0	
21.0	0.0610	786.0	200
23.0	0.0644	776.0	400
24.0	0.0651	780.0	
25.0	0.0656	776.0	
26.0	0.0661	776.0	
27.0	0.0669	776.0	
28.0	0.0686	775.0	400

LEAK

TABLE A-2.--Continued.

SAMPLE NUMBER 107 UNIAXIAL

TEMPERATURE = -12.0° C
CONSTANT AXIAL STRESS = 750.0 psi
PERCENT SAND = 63.5
PERCENT ICE = 59.6
TOTAL VOLUME CHANGE = NA

TIME (MIN.)	DEFL. (INS.)	LOAD (LBS.)
1.0	0.0269	760.0
2.0	0.0328	757.0
3.0	0.0377	762.0
4.0	0.0409	765.0
5.0	0.0437	765.0
10.0	0.0539	768.0
15.0	0.0614	772.0
20.0	0.0677	773.0
25.0	0.0733	776.0
30.0	0.0788	778.0
35.0	0.0843	780.0
40.0	0.0902	783.0
43.0	0.0945	790.0
44.0	0.0961	788.0
45.0	0.0978	788.0
46.0	0.0996	788.0
46.7	0.0932	80.0
47.0	0.0920	80.0
48.0	0.0916	80.0
50.0	0.0911	80.0
54.0	0.0908	80.0

SAMPLE NUMBER 108 UNIAXIAL

TEMPERATURE = -12.0° C
CONSTANT AXIAL STRESS = 750 psi
PERCENT SAND = 63.7
PERCENT ICE = 95.2
TOTAL VOLUME CHANGE = -0.054 cc

TIME (MIN.)	DEFL. (INS.)	LOAD (LBS.)
1.0	0.0211	752.0
10.0	0.0264	760.0
30.0	0.0308	760.0
60.0	0.0348	763.0
90.0	0.0376	764.0
20.0	0.0399	765.0
50.0	0.0418	765.0
80.0	0.0434	765.0
10.0	0.0449	768.0
40.0	0.0461	767.0
70.0	0.0470	767.0
90.0	0.0478	767.0
94.0	0.0479	767.0
96.0	0.0453	122.0
00.0	0.0446	115.0
10.0	0.0441	115.0
20.0	0.0438	115.0

TABLE A-2.--Continued.

SAMPLE NUMBER 109 STEP-STRESS SAMPLE NUMBER 109 Continued.

TEMPERATURE = -12° C
CONSTANT AXIAL STRESS = 400 psi
PERCENT SAND = 63.1
PERCENT ICE = 95.5
TOTAL VOLUME CHANGE = -0.072 cc

TIME (MIN.)	DEFL. (INS.)	LOAD (LBS.)	σ_3 (PSI)
1.0	0.0125	400.0	0
10.0	0.0147	404.0	
20.0	0.0155	400.0	
30.0	0.0161	405.0	
40.0	0.0165	405.0	
50.0	0.0169	406.0	
59.0	0.0171	404.0	0
61.0	0.0204	407.0	100
70.0	0.0207	404.0	
80.0	0.0210	405.0	
90.0	0.0214	406.0	
100.0	0.0227	405.0	
110.0	0.0219	405.0	
120.0	0.0221	405.0	100
122.0	0.0231	409.0	200
130.0	0.0234	409.0	
140.0	0.0238	405.0	
150.0	0.0240	406.0	
160.0	0.0242	405.0	
170.0	0.0243	405.0	
180.0	0.0245	409.0	
182.0	0.0246	409.0	200
185.0	0.0266	408.0	400
190.0	0.0268	410.0	
200.0	0.0270	405.0	
210.0	0.0273	411.0	
220.0	0.0274	405.0	
230.0	0.0276	405.0	
240.0	0.0277	410.0	
241.0	0.0277	410.0	400
243.0	0.0298	410.0	600
250.0	0.0302	408.0	
260.0	0.0304	405.0	
270.0	0.0305	410.0	
280.0	0.0307	405.0	
290.0	0.0309	405.0	
300.0	0.0311	410.0	
304.0	0.0312	410.0	600
307.0	0.0333	407.0	800
310.0	0.0334	407.0	
320.0	0.0337	405.0	
330.0	0.0339	411.0	
340.0	0.0340	405.0	
350.0	0.0341	410.0	
359.0	0.0343	410.0	800
362.0	0.0365	410.0	1000
370.0	0.0368	410.0	
380.0	0.0371	405.0	
390.0	0.0373	410.0	
400.0	0.0376	405.0	
410.0	0.0377	405.0	
413.0	0.0378	411.0	1000

SAMPLE NUMBER 111 UNIAXIAL

TEMPERATURE = -12.0° C
CONSTANT AXIAL STRESS = 750 psi
PERCENT SAND = 63.4
PERCENT ICE = 70.5
TOTAL VOLUME CHANGE = NA

TIME (MIN.)	DEFL. (INS.)	LOAD (LBS.)
1.0	0.0158	750.0
10.0	0.0250	756.0
30.0	0.0330	764.0
60.0	0.0391	767.0
90.0	0.0431	767.0
120.0	0.0459	767.0
150.0	0.0483	768.0
180.0	0.0502	767.0
210.0	0.0519	770.0
240.0	0.0534	770.0
270.0	0.0547	770.0
300.0	0.0559	770.0
330.0	0.0571	770.0
360.0	0.0584	772.0
390.0	0.0594	772.0
420.0	0.0602	772.0
450.0	0.0611	772.0
480.0	0.0621	773.0
510.0	0.0629	773.0
530.0	0.0634	772.0
530.7	0.0582	108.0
533.0	0.0566	108.0

TABLE A-2.--Continued.

SAMPLE NUMBER 112 STEP-STRESS

TEMPERATURE = -12.0° C
CONSTANT AXIAL STRESS = 640 ps
PERCENT SAND = 64.0
PERCENT ICE = 60.0 EST.
TOTAL VOLUME CHANGE = NA

TIME (MIN.)	DEFL. (INS.)	LOAD (LBS.)	σ_3 (PSI
1.0	0.0180	648.0	0
5.0	0.0255	650.0	|
10.0	0.0303	654.0	|
20.0	0.0357	655.0	|
30.0	0.0395	653.0	|
40.0	0.0423	655.0	|
50.0	0.0446	655.0	|
60.0	0.0464	652.0	0
62.0	0.0502	656.0	100
70.0	0.0515	654.0	|
80.0	0.0527	657.0	|
90.0	0.0538	657.0	|
100.0	0.0547	657.0	|
110.0	0.0556	660.0	|
120.0	0.0565	660.0	100
123.0	0.0581	663.0	200
130.0	0.0587	663.0	|
140.0	0.0593	660.0	|
150.0	0.0598	662.0	|
160.0	0.0603	665.0	|
170.0	0.0607	665.0	|
180.0	0.0611	661.0	200
183.0	0.0637	660.0	400
190.0	0.0643	662.0	|
200.0	0.0647	662.0	|
205.0	0.0650	663.0	|
LEAK			

SAMPLE NUMBER 113 STEP-STRESS

TEMPERATURE = -12.0° C
CONSTANT AXIAL STRESS = 400 psi
PERCENT SAND = 63.1
PERCENT ICE = 60.0 EST.
TOTAL VOLUME CHANGE = NA

TIME (MIN.)	DEFL. (INS.)	LOAD (LBS.)	σ_3 (PSI)
1.0	0.0124	407.0	0
10.0	0.0192	405.0	|
30.0	0.0243	406.0	|
60.0	0.0283	406.0	|
62.0	0.0286	406.0	0
64.0	0.0320	405.0	100
70.0	0.0330	407.0	|
90.0	0.0348	407.0	|
120.0	0.0365	410.0	|
122.0	0.0366	410.0	100
124.0	0.0382	414.0	200
130.0	0.0391	412.0	|
150.0	0.0424	411.0	|
180.0	0.0476	410.0	|
182.0	0.0478	410.0	|
LEAK			

TABLE A-2.--Continued.

SAMPLE NUMBER 114 UNIAXIAL

TEMPERATURE = -12.0° C
CONSTANT AXIAL STRESS = 750 psi
PERCENT SAND = 64.2
PERCENT ICE = 68.5
TOTAL VOLUME CHANGE = NA

TIME (MIN.)	DEFL. (INS.)	LOAD (LBS.)
1.0	0.0239	751.0
10.0	0.0393	762.0
30.0	0.0501	765.0
60.0	0.0583	770.0
90.0	0.0636	771.0
120.0	0.0677	774.0
150.0	0.0709	775.0
180.0	0.0740	775.0
210.0	0.0766	775.0
220.0	0.0775	780.0
230.0	0.0784	780.0
240.0	0.0793	780.0
240.5	0.0756	100.0
241.0	0.0741	100.0
245.0	0.0729	100.0
250.0	0.0723	100.0

SAMPLE NUMBER 115 CONFINED

TEMPERATURE = -12.0° C
CONSTANT AXIAL STRESS = 750 psi
PERCENT SAND = 63.2
PERCENT ICE = 95.9
TOTAL VOLUME CHANGE = -0.012 cc
CONFINING PRESSURE = 210 psi

TIME (MIN.)	DEFL. (INS.)	LOAD (LBS.)
1.0	0.0163	750.0
10.0	0.0209	758.0
30.0	0.0249	762.0
60.0	0.0283	762.0
90.0	0.0306	762.0
120.0	0.0324	762.0
150.0	0.0340	762.0
180.0	0.0353	767.0
210.0	0.0364	767.0
240.0	0.0374	767.0
270.0	0.0383	767.0
300.0	0.0391	767.0

SAMPLE NUMBER 117 STEP-STRESS

TEMPERATURE = -12.0° C
CONSTANT AXIAL STRESS = 750 psi
PERCENT SAND = 63.6
PERCENT ICE = 60.5
TOTAL VOLUME CHANGE = NA

TIME (MIN.)	DEFL. (INS.)	LOAD (LBS.)	σ_3 (PSI)
1.0	0.0344	750.0	0
2.0	0.0399	765.0	
3.0	0.0438	765.0	
4.0	0.0475	770.0	
5.0	0.0502	770.0	
6.0	0.0524	770.0	
7.0	0.0544	770.0	
8.0	0.0562	770.0	
9.0	0.0578	770.0	
10.0	0.0592	770.0	0
12.0	0.0644	775.0	100
13.0	0.0655	775.0	
14.0	0.0663	776.0	
15.0	0.0672	776.0	
16.0	0.0679	777.0	100
18.0	0.0704	776.0	200
19.0	0.0712	776.0	
20.0	0.0717	780.0	
21.0	0.0724	780.0	
22.0	0.0729	780.0	
23.0	0.0732	782.0	
24.0	0.0736	780.0	
25.0	0.0740	780.0	
26.0	0.0744	780.0	
27.0	0.0747	780.0	200
29.0	0.0770	780.0	400
30.0	0.0774	780.0	
31.0	0.0778	780.0	
32.0	0.0780	780.0	
33.0	0.0783	780.0	
34.0	0.0786	780.0	
35.0	0.0789	780.0	
36.0	0.0791	780.0	
37.0	0.0793	780.0	
38.0	0.0796	780.0	
39.0	0.0797	780.0	
40.0	0.0799	780.0	
41.0	0.0801	780.0	400
43.0	0.0825	780.0	600
45.0	0.0829	780.0	

TABLE A-2.--Continued.

SAMPLE NUMBER 117-Continued.

TIME (MIN.)	DEFL. (INS.)	LOAD (LBS.)	σ_3 (PSI)
47.0	0.0833	780.0	
49.0	0.0836	780.0	
51.0	0.0838	785.0	
53.0	0.0841	785.0	
55.0	0.0844	785.0	
57.0	0.0849	785.0	
59.0	0.0851	785.0	
61.0	0.0853	785.0	600
64.0	0.0877	780.0	800
67.0	0.0883	783.0	
70.0	0.0888	784.0	
75.0	0.0893	785.0	
80.0	0.0898	785.0	
85.0	0.0901	785.0	
90.0	0.0905	785.0	
95.0	0.0907	785.0	
100.0	0.0909	785.0	800
104.0	0.0896	775.0	600
105.0	0.0896	775.0	
115.0	0.0896	775.0	
120.0	0.0899	775.0	
130.0	0.0901	775.0	
135.0	0.0902	775.0	
137.0	0.0904	775.0	600
142.0	0.0883	775.0	400
145.0	0.0885	775.0	
150.0	0.0886	775.0	
155.0	0.0887	775.0	
160.0	0.0889	775.0	
165.0	0.0889	775.0	400
170.0	0.0862	775.0	200
180.0	0.0864	775.0	
190.0	0.0866	775.0	
195.0	0.0867	775.0	200
200.0	0.0842	775.0	0
210.0	0.0856	775.0	
220.0	0.0868	775.0	
230.0	0.0878	775.0	
240.0	0.0887	775.0	
250.0	0.0897	775.0	
253.0	0.0900	775.0	
254.0	0.0819	75.0	
255.0	0.0806	75.0	
260.0	0.0794	75.0	
265.0	0.0790	75.0	
270.0	0.0789	75.0	
274.0	0.0787	75.0	0

SAMPLE NUMBER 118 CONFINED

TEMPERATURE = -12.0° C
CONSTANT AXIAL STRESS = 750 psi
PERCENT SAND = 62.7
PERCENT ICE = 94.7
TOTAL VOLUME CHANGE = -0.216 cc
CONFINING PRESSURE = 600 psi

TIME (MIN.)	DEFL. (INS.)	LOAD (LBS.)	σ_3 (PSI)
2.0	0.0192	750.0	600
10.0	0.0227	760.0	800
30.0	0.0266	762.0	
60.0	0.0298	762.0	
90.0	0.0324	767.0	
120.0	0.0342	767.0	
150.0	0.0357	767.0	
180.0	0.0371	767.0	
210.0	0.0381	765.0	
240.0	0.0390	765.0	800
270.0	0.0398	764.0	600
276.0	0.0327	0.0	
280.0	0.0322	0.0	
290.0	0.0317	0.0	
300.0	0.0315	0.0	
310.0	0.0313	0.0	

SAMPLE NUMBER 119 CONFINED

TEMPERATURE = -12.0° C
CONSTANT AXIAL STRESS = 650 psi
PERCENT SAND = 63.6
PERCENT ICE = 60.5
TOTAL VOLUME CHANGE = NA
CONFINING PRESSURE = 205 psi

TIME (MIN.)	DEFL. (INS.)	LOAD (LBS.)	σ_3 (PSI)
1.0	0.0225	650.0	200
10.0	0.0309	650.0	0
20.0	0.0346	650.0	
30.0	0.0373	656.0	
40.0	0.0397	656.0	
50.0	0.0423	656.0	
60.0	0.0450	656.0	
70.0	0.0474	656.0	
80.0	0.0506	656.0	
90.0	0.0534	656.0	
100.0	0.0564	656.0	
110.0	0.0597	656.0	
120.0	0.0632	656.0	0
150.0	0.0757	656.0	

LEAK

TABLE A-2.--Continued.

SAMPLE NUMBER 120 CONFINED

TEMPERATURE = -12.0° C
CONSTANT AXIAL STRESS = 640 psi
PERCENT SAND = 63.9
PERCENT ICE = 64.6
TOTAL VOLUME CHANGE = NA
CONFINING PRESSURE = 600 psi

TIME (MIN.)	DEFL. (INS.)	LOAD (LBS.)
2.0	0.0394	655.0
5.0	0.0438	656.0
10.0	0.0473	656.0
20.0	0.0510	660.0
30.0	0.0531	662.0
60.0	0.0566	662.0
90.0	0.0585	660.0
120.0	0.0597	660.0
150.0	0.0606	660.0
180.0	0.0614	660.0
210.0	0.0619	660.0
240.0	0.0624	665.0
260.0	0.0628	665.0

SAMPLE NUMBER 121 STEP-STRESS

TEMPERATURE = -12.0° C
CONSTANT AXIAL STRESS = 750 psi
PERCENT SAND = 62.3
PERCENT ICE = 95.5
TOTAL VOLUME CHANGE = -0.048 cc

TIME (MIN.)	DEFL. (INS.)	LOAD (LBS.)	σ_3 (PSI)
1.0	0.0170	755.0	0
10.0	0.0216	760.0	
20.0	0.0237	760.0	
30.0	0.0252	757.0	
40.0	0.0266	757.0	
50.0	0.0278	760.0	
60.0	0.0288	757.0	
61.0	0.0288	757.0	0
63.0	0.0325	760.0	100
70.0	0.0332	759.0	
80.0	0.0341	763.0	
90.0	0.0347	761.0	
100.0	0.0354	761.0	
110.0	0.0361	757.0	

SAMPLE NUMBER 121-Continued.

TIME (MIN.)	DEFL. (INS.)	LOAD (LBS.)	σ_3 (PSI)
120.0	0.0367	762.0	
122.0	0.0368	762.0	100
124.0	0.0379	760.0	200
130.0	0.0383	760.0	
140.0	0.0389	761.0	
150.0	0.0394	763.0	
160.0	0.0399	765.0	
170.0	0.0403	765.0	
180.0	0.0407	765.0	
181.0	0.0408	765.0	200
183.0	0.0427	765.0	400
190.0	0.0433	767.0	
200.0	0.0437	767.0	
210.0	0.0441	767.0	
220.0	0.0445	767.0	
230.0	0.0449	767.0	
240.0	0.0451	767.0	
243.0	0.0452	767.0	400
245.0	0.0482	767.0	600
250.0	0.0485	767.0	
260.0	0.0488	767.0	
270.0	0.0490	767.0	
280.0	0.0493	767.0	
290.0	0.0497	767.0	
300.0	0.0500	767.0	
304.0	0.0501	767.0	600
306.0	0.0515	770.0	800
310.0	0.0517	770.0	
320.0	0.0521	770.0	
330.0	0.0524	770.0	
340.0	0.0526	770.0	
350.0	0.0529	770.0	
360.0	0.0530	770.0	
365.0	0.0532	770.0	800